GPS MEASUREMENTS IN THE AUSTRALIAN AND INDONESIAN REGIONS (1989 - 1993)

PAUL TREGONING

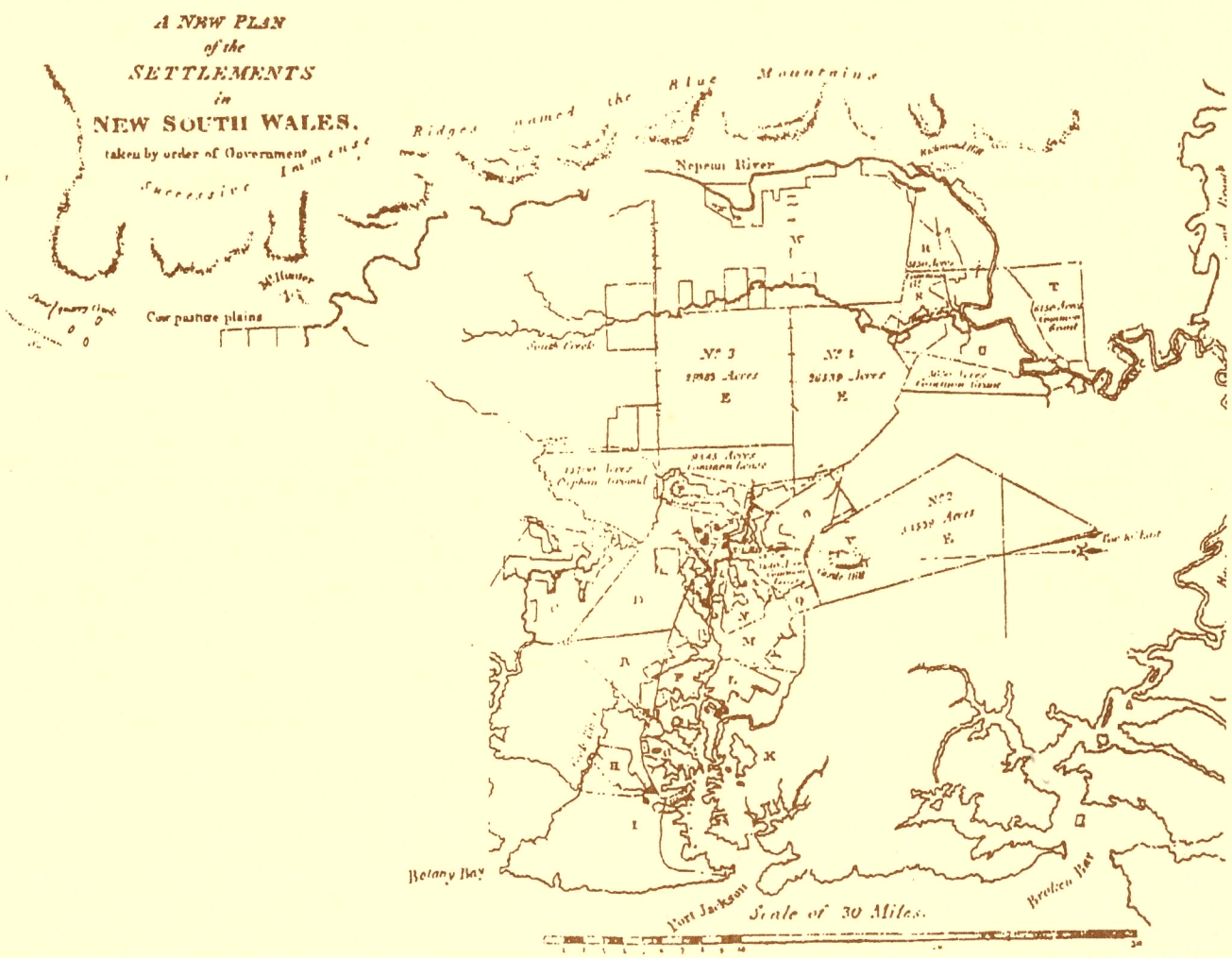

UNISURV S-44, 1996

Reports from

SCHOOL OF GEOMATIC ENGINEERING

THE UNIVERSITY OF NEW SOUTH WALES SYDNEY NSW 2052 AUSTRALIA

UNISURV REPORT S-44, 1996

GPS MEASUREMENTS IN THE AUSTRALIAN AND INDONESIAN REGIONS (1989 - 1993)

Studies of the Java Trench Subduction Zone, the Sunda Strait and the Australian Plate

Paul Tregoning

Completed, January, 1995
Received: April, 1996

SCHOOL OF GEOMATIC ENGINEERING
UNIVERSITY OF NEW SOUTH WALES
SYDNEY NSW 2052
AUSTRALIA

National Library of Australia

Card No. and ISBN 0 85839 068 X

ABSTRACT

The Australian plate is migrating Northwards from Antarctica, and the Northern edge of the plate is subducting beneath Indonesia. The subduction is frontal beneath Java and becomes more oblique Westwards beneath Sumatra. The obliquity of the collision is accommodated in Sumatra by a right lateral fault, the Central Sumatra Fault. This strike slip system is thought to be responsible for the formation of the Sunda Strait between Java and Sumatra.

This thesis investigated the tectonic activity of this collision zone by geodetically measuring motions across tectonic boundaries. There is an island, Christmas Island, located on the Australian plate about 150 km South of the subduction zone. Global Positioning System (GPS) measurements across the Java Trench were made between Christmas Island and West Java during five annual surveys commencing in 1989. This single baseline study was expanded in 1992 to include the Cocos Islands, located about 900 km Westsouthwest of Christmas Island, and a five station network spanning the Sunda Strait and the Southeastern end of the Central Sumatra Fault.

The data processed in this thesis is a subset of a much larger crustal deformation study encompassing most of Indonesia. In addition, the deformation surveys were supported by GPS measurements from a global fiducial tracking network which included some stations on the Australian plate. The GPS data was processed using GAMIT/GLOBK software to determine GPS derived station velocities and relative motions across the plate boundaries. Daily GPS solutions were computed, with global orbits being estimated using the available fiducial tracking data. The global data was quite sparse prior to 1992 and hence was incorporated in the regional solutions. With the introduction of the International GPS Service for Geodynamics (IGS) in 1992 the number of fiducial tracking stations increased significantly. It was decided to use a combination approach whereby the regional and global data was processed separately in GAMIT and then combined in GLOBK.

Inherent in any velocity field estimation is the definition of a reference frame. This is generally realised by the definition of coordinates of tracking stations. Any coordinate errors introduced into a campaign solution due to errors in the reference frame definition will be incorrectly interpreted as station velocities relative to the reference frame when all campaigns are simultaneously processed. Therefore, it is imperative that the reference frame be defined as consistently as possible in all daily solutions. However, due to the dramatic changes in the fiducial tracking networks from 1989 to 1993, it was not

possible to fix the coordinates of a set of stations without introducing biases into one or more of the annual campaigns. A simulation study was performed in order to determine how to constrain the coordinates of the fiducial tracking stations in a manner which best defined a reference frame whilst minimising campaign dependent coordinate biases. This study showed that the most consistent definition was obtained by constraining the coordinates of the thirteen core IGS stations to 0.2 m in all components, and further constraining the latitude of Hawaii to 0.1 mm.

Convergence across the Java Trench was estimated at 64±2 mm/yr in a direction of 15°± 4° and is in agreement with the convergence predicted by NNR-NUVEL-1A (71±2 mm/yr in a direction of 20°±4°). A spreading rate of 58±8 mm/yr was determined between Mawson, Antarctica and Yaragadee, Western Australia, from GPS measurements spanning 1991-1994. This is not significantly different from the NNR-NUVEL-1A prediction of 66 mm/yr. This indicates that relative motion at the boundaries of the Australian plate determined by GPS measurements agree with the plate motion model.

Velocities were estimated for stations located on the Australian plate and on West Java. The velocities of two stations on the Australian plate needed to be fixed in order to stabilise the GLOBK solution and obtain geophysically meaningful velocities. The GPS derived motions of six stations in the Australia/Indonesia region generally agree with the No-Net-Rotation NUVEL-1A (NNR NUVEL-1A) plate motion model predictions. However, the velocities of two stations (Darwin and Karratha) are significantly different from the plate motion model. It is not fully understood why this occurred, as there is no geophysical evidence to support internal deformation of the Australian plate to the levels that the GPS velocities indicate. However, the GPS data only spans twelve months on these stations, and it is believed that the velocity estimates are erroneous artefacts of the short span of processed data. It is thought that the velocity estimates of these stations will significantly change as more data is added to the current solution.

Extension of 25±10 mm/yr was measured across the Southern end of the Sunda Strait between Java and Sumatra. Motion was not detected between Java and Northeastern Sumatra, indicating that strike slip motion on the Central Sumatra Fault is occurring. The geodetic results of this network are limited by the small number of simultaneous observations on these stations. The inclusion of the 1994 GPS data will improve the geodetic understanding of this region.

ACKNOWLEDGEMENTS

There are many people who have been involved in teaching me about geodesy and GPS. I wish to thank Bruce Harvey, Art Stoltz, Bill Kearsley, Brian Donnelly and other staff members at the School of Geomatic Engineering for many discussions on a whole range of topics. Without the backup of a learned group the task of submitting a thesis would be much more difficult.

I wish to thank my supervisor, Professor Fritz Brunner, who instigated the Java Trench subduction project. His enthusiasm was never ending and he was always willing to listen to my problems and offer a different opinion on how to proceed. I approached this project in a slightly different manner to that which Fritz had intended but he allowed me the freedom to find my own way - only dragging me back to the correct path when I was digressing too far. Fritz moved to Graz, Austria, about four months prior to the submission of my thesis. He graciously offered to read a final draft of it which improved the final document significantly. I thank John Pollard for taking on the task of supervising me for the remaining time. He told me in my first year as an undergraduate that I should do a PhD, and his foresight turned out to be very good!

I received much technical advice from Peter Morgan and his staff at the University of Canberra (UC). Peter's group are the only other people in Australia who are processing GPS data with GAMIT/GLOBK software, and I had many fruitful discussions on how to operate the software, and how to interpret the results. I am thankful for the use of computing facilities at UC, and for the 1992 Antarctic solutions which Peter made available for me to incorporate into my solutions. I also received confirmation from UC that some of my strange results were being seen by others and were not as a result of my mistakes. This was at times invaluable, for my sanity if nothing else!

I made three visits to the Institution of Geophysics and Planetary Physics, Scripps Institution of Oceanography (SIO) during my study. Yehuda Bock, Peng Fang, Toto Puntodewo, Keith Stark, Jeff Genrich and Eric Calais helped me in many ways: Yehuda was a principal investigator and fundamental in getting the Indonesian project functioning, and taught me how to use GAMIT; Peng and Keith deserve countless thanks for producing the global orbits on a daily basis and Toto processed much of the 1989 and 1990 data before I started on the project. Tom Herring, Bob King and Simon McClusky (MIT) also provided advise on the operation of the GAMIT/GLOBK software.

I wish to thank Professor Jacub Rais and the staff at Bakosurtanal, Rob McCaffrey (principal geophysisict for the Indonesia project), Martin Hendy and all the field operators (there are too many to name) who were involved in the collection of the GPS data. There is a huge amount of time and organisation involved in collecting the dataset for a project such as this. The collection of data on Australian sites was organised by staff at the University of New South Wales (UNSW), Australian Surveying and Land Information Group and the Department of Lands Administration, Western Australia. I was not involved in the gathering of data on the Indonesian sites. I thank all those people who were involved in collecting data at the many sites used in this analysis.

Rob McCaffrey deserves a special mention for his contribution to my understanding of the geophysics involved in the subduction process. Martin Hendy was very helpful in organising the logistics of running GPS projects on a shoestring budget and I'm sure I must owe him yet another weekend rock climbing in Canberra! I thank David Lemon, Kim Mobbs and Merrin Pearce for proof reading my thesis and for arguing against me whenever my text didn't make sense.

Finally I would like to thank my family and friends who have supported me through the last four years. This research was done whilst receiving an Australian Postgraduate Research Award, and an Engineering Scholarship from the Faculty of Engineering, UNSW. Funding for this project was provided by an Australian Research Council small grant. Most of the figures plotted in this thesis were created using GMT software [Wessel & Smith, 1991].

CONTENTS

LIST OF FIGURES

LIST OF TABLES

CHAPTER 1

INTRODUCTION

The Australian plate is undergoing tectonic motion of the order of 50-70 mm/yr in a North-northeast direction. The Australian plate borders the Antarctic plate to the South, the Pacific plate to the East, the African and Indian plates to the West and the Southeast Asian plate to the North (Figure 1.1). There is a spreading zone separating the Australian and Antarctic plates, the Pacific plate subducts beneath the Australian plate and subduction is occurring where the Australian plate collides with Indonesia at the Java Trench. This thesis investigates the tectonic motion of the Australian plate, the subduction beneath Java and the tectonic activity in the Sunda Strait from geodetic measurements using the Global Positioning System (GPS).

The Java Trench region is one of the few subduction zones in the world where there is an island on the subducting plate close to the convergence zone. Christmas Island is about 150 km south of the subduction trench, and only 400 km from West Java. This has enabled excellent geodetic measurements of the convergence to be made across a relatively short baseline. Commencing in 1989, annual GPS observations were made at Christmas Island and Cibinong, West Java. There is another system of islands on the Australian plate, the Cocos Islands, which are situated about 900 km Southwest of Christmas Island and about 800 km from the subduction zone. GPS observations commenced at Cocos Islands in July 1992. A small survey network of four stations plus Cibinong was observed in Java and Sumatra in 1992 and 1993 to determine whether extension was occurring across the Sunda Strait between Java and Sumatra. GPS observations across the tectonic features in this area have allowed direct measurements to be compared with geological models of the region. GPS measurements between an Australian Antarctic base, Mawson, and stations on the Australian plate commenced in February 1991. This has enabled the spreading rate between the Australian and Antarctic plates to be estimated.

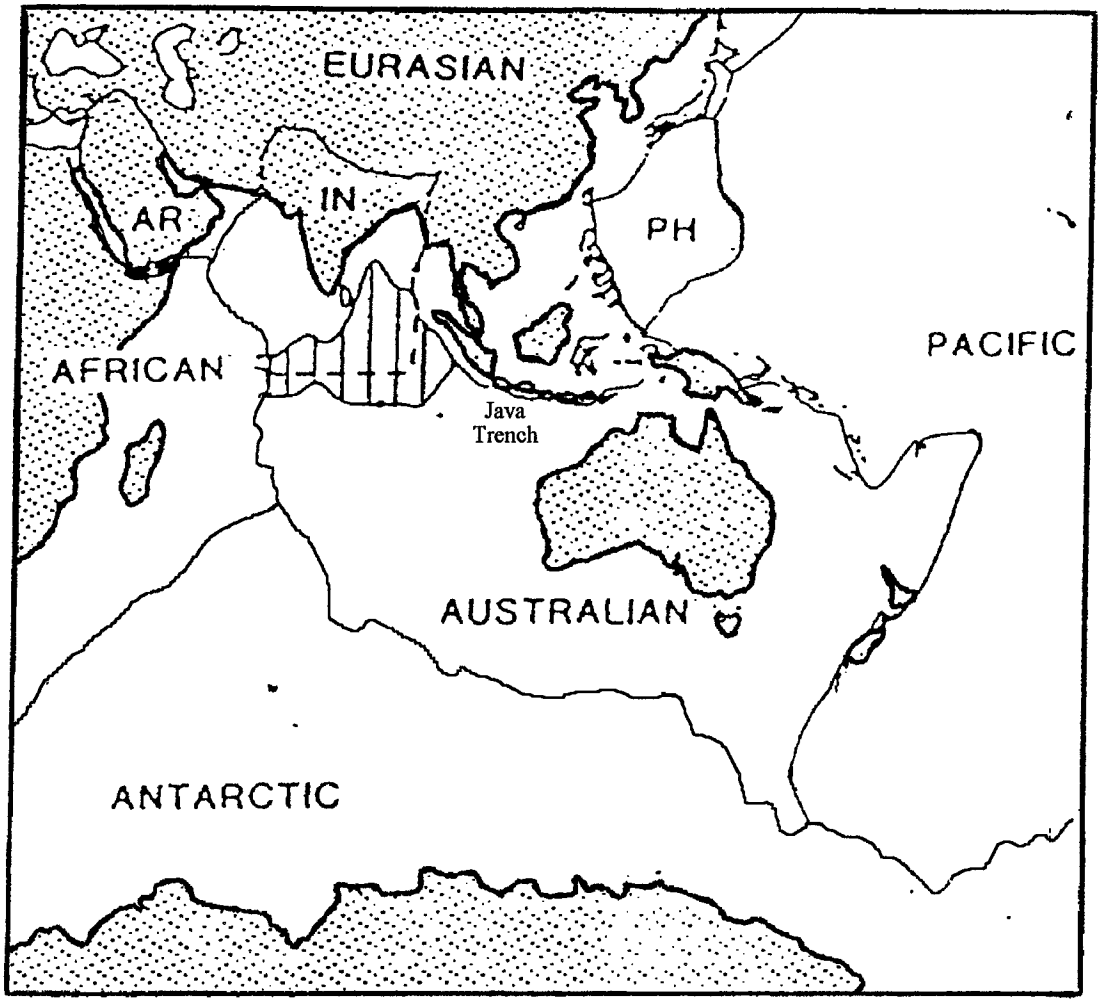

Figure 1.1 Tectonic plates in the Australian region. Plate abbreviations as follows: Indian (IN), Phillipine Sea Plate (PH), Arabian (AR). Hatched area indicates the diffuse deformation zone between the Indian and Australian plates.

The GPS surveys on these stations were part of extensive surveys throughout the whole Indonesian region (see e.g. Puntodewo et al. [1994]; Genrich et al. [1994]; Calais et al. [1994]) and were supported by a number of regional and global fiducial tracking stations. The GPS data was processed using the GAMIT software [King and Bock, 1993] and GLOBK [Herring, 1992], a Kalman filter program. The dataset was processed at Scripps Institution of Oceanography (SIO) and The University of New South Wales (UNSW) with some additional data from Massachusetts Institute of Technology (MIT) and the University of Canberra (UC). The project was a joint effort between UNSW, SIO, the National Coordination Agency for Surveying and Mapping, Indonesia (Bakosurtanal) and Rensselaer Polytechnic Institute (RPI).

The original concept of this project came from Professor Fritz K. Brunner (UNSW), Dr Yehuda Bock (SIO), Dr Rob McCaffrey (RPI) and Professor Jacub Rais (Bakosurtanal). Professor Brunner was aware of a paper by the Australian Geodesy subcommittee on a possible tectonic study involving Christmas Island and formulated a plan of a possible survey. At that time, the SIO and RPI groups instigated a crustal motion study of the Indonesian region and approached UNSW to cooperate by providing fiducial tracking data from Christmas Island. Professor Brunner saw this as an opportunity to investigate the convergence of the Australian and Southeast Asian plates, and formed a Memorandum of Understanding with Bakosurtanal to extend the studies of the American groups by monitoring the subduction between West Java and Christmas Island, and the possible extension across the Sunda Strait. The research at UNSW was funded by an Australian Research Council (ARC) small grant, with additional support from the Faculty of Engineering (UNSW), the Australian Army and the Australian Surveying and Land Information Group (AUSLIG).

1.1 OBJECTIVES OF THESIS

There are three main objectives of this thesis:

1. To compute the convergence of the Australian and Southeast Asian plates at the Java Trench.

2. To investigate whether the Sunda Strait is undergoing extension as a result of the oblique subduction at the Java trench.

3. To estimate a velocity field for the Australian plate.

To achieve these objectives, GPS data spanning up to five years was processed and analysed. Some results from the analysis have been published (see e.g. Genrich et al. [1994]; Puntodewo et al. [1994]; Calais et al. [1994]; Tregoning et al. [1994]).

1.2 GEODETIC ASPECTS

GPS was selected for the geodetic measurements of this project because of its low cost, ease of transportability and simplicity of field operation. GPS is a satellite navigation and time transfer system that has been adapted to geodetic positioning during the past 15

years by many geodesists. The system is operated and maintained by the United States Department of Defence (DoD). It is a system essentially based on timing, where the time delay between transmission of a signal from a satellite and the reception of the signal by a GPS receiver can be converted into a distance. Knowing the distance to a number of satellites and their location allows the position of the receiver to be determined. In geodesy, it is generally the relative position between two receivers that is computed in the processing. GPS is discussed in detail in Chapter 3.

Whilst Very Long Baseline Interferometry (VLBI) and Satellite Laser Ranging (SLR) are more precise geodetic measuring systems than GPS, there are very few observing stations in the Australian region. Installing new stations was beyond the scope of this project, and GPS provided a viable alternative. Today, GPS receivers are quite small and readily transportable, can typically operate from either an AC power source or battery power, and are relatively simple to operate. The quality of GPS results being obtained today are in the order of parts in 10^8 in position differences and 10-30 mm in height differences (see e.g. Dixon [1991]; Feigl et al. [1993] and Larson and Agnew [1991]). GPS is a much less expensive and more portable alternative to VLBI and SLR and, although not as precise, provides a very useful tool for geodynamic studies.

The determination of relative motion between two sites, or the motion of one site relative to the mantle of the Earth requires the definition of a reference frame. In this project, the GPS observations have been computed relative to a terrestrial reference frame. This frame is essentially defined by the predetermined coordinates of a number of global GPS permanent tracking stations. The configuration of the tracking network changed considerably throughout the project which created distortions in the satellite geometry influences during the evolution of GPS. It is critical that the stability of the GPS solutions are fully understood before the geodetic measurements can be interpreted geophysically. Thus, the definition of the reference frame is an important issue in this thesis.

1.3 OVERVIEW OF THESIS

Geodetic measurements with GPS have become an accepted tool for precise positioning. GPS has found applications in crustal motion studies, geophysical exploration and standard land surveying. The purpose of this thesis is to use GPS as a measuring tool in a crustal motion study of the Java Trench subduction zone, the Sunda Strait and the Australian plate.

An overview of plate tectonics is given in *Chapter 2*, with an explanation of the main features of the theory. A brief explanation of the main geophysical terms in the literature is given. Various global plate motion models derived from geological information are discussed followed by a brief summary of the geophysical studies that have been made in the Indonesian region. This includes seismic studies, gravimetric surveys and geological interpretations. Finally, the major GPS sites used in this analysis are briefly described.

Chapter 3 contains a brief description of GPS and the field campaigns of this project are documented. The theory and rationale behind the processing strategy is also outlined as well as possible error sources in the processing of the data.

The definition of a reference frame is discussed in *Chapter 4*, and illustrations are given as to how terrestrial and inertial reference frames are theoretically and practically defined for geodetic space systems. There is also a discussion of a simulation study investigating how changes in a global fiducial network affect GPS solutions in the Indonesian and Australian regions. A determination is made of the most appropriate definition of the terrestrial reference frame for the Australian and Indonesian region for all campaigns in this analysis. This determination includes the number of constraints that must be applied to both position and velocity parameters in order to stabilise the solutions.

The results of the GPS data analysis are presented in *Chapter 5*. Long and short term precisions are computed and the stability of the velocity estimates for a number of stations on the Australian and Southeast Asian plates are investigated. The convergence across the Java trench and the spreading rate between the Australian and Antarctic plates are estimated. Preliminary results of strike slip motion along the Central Sumatra fault are presented.

Chapter 6 contains conclusions and recommendations for future analyses of GPS data in the Australian region.

CHAPTER 2

GEOPHYSICS OF THE REGION

The Australian plate is colliding with the Southeast Asian plate as it moves North-Northeast away from Antarctica. This has created an interesting tectonic plate boundary. Global plate motion models can be used to predict the convergence at this subduction zone but no geophysical data from the region has been used in the computation of the plate motion models. Plate tectonic models make an important contribution to geophysics as they provide geologically based information against which other data can be compared. Motion at plate boundaries can be predicted and then compared with other measurements such as geodetic measurements and seismic information to determine whether plate collisions or separations are behaving according to the global plate motion model predictions. In this chapter I will discuss the theory of plate tectonics and plate tectonic models, describe the major geophysical processes occurring on the Earth, provide a brief description of the elements that provide geophysical information, outline the tectonic setting of the Australian/Indonesian region and give brief site descriptions of the GPS stations.

2.1 PLATE TECTONICS

The theory of continental drift was first presented by Alfred Wegener in 1912 and his book *Die Enstehung der Kontinente und Ozeane* was first published in 1915. His ideas met with much hostility from the geological community. He subsequently released many revised editions as his work and knowledge expanded. However, with his death in 1930 his ideas were largely forgotten (or deliberately ignored!) despite the efforts of a few scientists whose works supported Wegener (see e.g. Du Toit, [1937]; Holmes, [1945]). Palaeomagnetic studies in the 1950s revived Wegener's theory by showing that continental drift provided a means of resolving apparent magnetic polar migration. This was also met with scepticism and hostility by the scientific community of the time.

H. H. Hess [1962] introduced the idea that the ocean floor is spreading. Robert Dietz received a preprint of the paper and actually published a similar article [Dietz, 1961] prior to Hess but credit for the idea is given to Hess. The scientific community was still sceptical - the strongest argument against sea floor spreading was that there was no explanation of the forces required to initiate the process. The next major discovery adding weight to the plate tectonic argument was the discovery of the pattern of magnetic reversals in rocks near mid-oceanic ridges [Vine and Mathews, 1963] (see 2.2.2 for an explanation of magnetic reversals). Wilson [1965] introduced the idea of transform faults (see section 2.1.1) which explained the irregular pattern of magnetic reversals. Vine and Wilson [1965] used reversals of the terrestrial magnetic field to substantiate the sea floor spreading theories of Hess and Dietz. They compared the chart of magnetic reversals determined from rocks on the continents with the patterns seen either side of the Juan De Fuca spreading zones to date the sea floor and hence determine spreading rates. If the theory of sea floor spreading was true then the age of the sediments deposited on the sea floor should increase away from the ridge. Experiments were conducted in the Deep Sea Drilling Project (DSDP) during the late 1960s and 1970s which confirmed this (a brief history of the DSDP is given in Nierenberg [1978]). The case for plate tectonic motion and sea floor spreading was becoming harder to refute.

In April 1967, Jason W. Morgan presented a talk at the American Geophysical Union Meeting (AGU) in which he suggested that the Earth is composed of rigid portions of a sphere called plates. These plates are formed at spreading ridges, move rigidly across the surface of the Earth and disappear into the mantle at oceanic trenches. Thus, ridges are regions that create sea floor and trenches are regions where it is destroyed. He showed that the relative motion of the plates could be modelled using Eulerian mathematics. His paper outlining the theory was published in March 1968 [Morgan, 1968]. Le Pichon further developed the ideas of Morgan's paper and presented the first global plate tectonic model in March 1968 [Le Pichon, 1968]. By this time, the plate tectonic theory was becoming established, although the theory was not fully accepted throughout the world.[1]

Plate tectonics provides explanations for the formation of features on the Earth, such as the presence of deep oceanic trenches, slabs of the Earth's crust which are sinking into the Earth, mountain ranges, spreading centres etc. The Earth is comprised of three principal layers - the extremely dense *core*, the *mantle* and the surface skin called the

[1] This historical trail of developments of plate tectonics was adapted from Allègre [1988].

crust. Each layer has a distinct chemical composition. Plate tectonics introduced two new layers based on the rheological (deformational) properties of the Earth. The *lithosphere* or surface layer of the Earth is highly resistant to deformation and is comprised of the upper layer of the mantle and the rigid crust. The *aesthenosphere* lies beneath the lithosphere and is a soft, easily deformed layer of the mantle. The crust of the Earth consists of both continental and oceanic regions. Oceanic lithosphere is more dense and significantly thinner than continental lithosphere.

Plate tectonics assumes that the lithosphere of the Earth can be divided into a number of rigid plates which slide across the aesthenosphere. The theory of plate tectonics provides explanations for continental drift, collision zones and spreading centres, the concentration of earthquakes in certain regions and many other features that had puzzled geologists and geophysicists until the 1960s.

2.1.1 Plate Boundaries

There are three different types of plate boundaries which are briefly described below. The descriptions are by no means comprehensive - they are presented merely to illustrate the major aspects of the present-day plate tectonic theory:-

Trenches

Trenches are found where two plates are converging. At least one of the plates is comprised of oceanic lithosphere which bends downwards and sinks into the aesthenosphere beneath the overriding plate (which can be continental or oceanic lithosphere) [Cox and Hart, 1986]. This process is called *subduction.* The subducting slab is colder and more dense than the surrounding aesthenosphere and warms slowly as it sinks. This creates a temperature difference between the slab and the neighbouring rocks. The slab is brittle owing to its colder state, and earthquakes occur as it sinks into the aesthenosphere. The outer regions of the slab increase in temperature more quickly than the interior and becomes more deformable. Hence, earthquakes occur at the surface of the descending plate near the bend, and within the plate at greater depths where the brittle conflict occurs [Spence, 1987].

Earthquakes occurring in arc-trench regions can be classified as shallow, intermediate or deep focus earthquakes. When the positions of these are plotted in cross section they form a zone, a *Benioff zone*, which follows the direction of the descending slab. This distribution was first recognised by K. Wadati in the 1930s but was rediscovered 15

years later by the seismologist Benioff after whom the zone is named. If the slab was separated from the horizontal plate and considered as a single entity then the upper section of it would be under tension as the mass below pulled it into the mantle. Partway down the slab, the force of the mass of slab above pushing down would equal the pulling force from the mass below and there would be relatively little stress in the slab. Below this point, the slab would be under compression, as the mass of the slab above forced downwards whilst the downward motion of the leading edge of the slab is resisted by the aesthenosphere.

This is evident in the nature of the earthquakes associated with a descending slab. Downdip of the bend there is generally tensional stress in the slab to depths of about 200 km whilst the deeper earthquakes (about 400-650 km) are caused by compression. The transitional region generally displays little seismicity as the tension and compression forces caused by the mass of the slab above and below are in equilibrium (see e.g. Isacks and Molnar, [1971]; Spence, [1987]). This is a simplified explanation as there are many more forces acting on a subducting slab which create stresses (see section 2.1.2).

Subduction zones generally lie along a small circle and have many common tectonic features. Figure 2.1 shows a typical subduction zone. The major features of a subduction zone (trench, subducting slab, outer-arc ridge, fore-arc ridge and basin, back-arc region and accretionary wedge) are discussed in detail in Hamilton [1979].

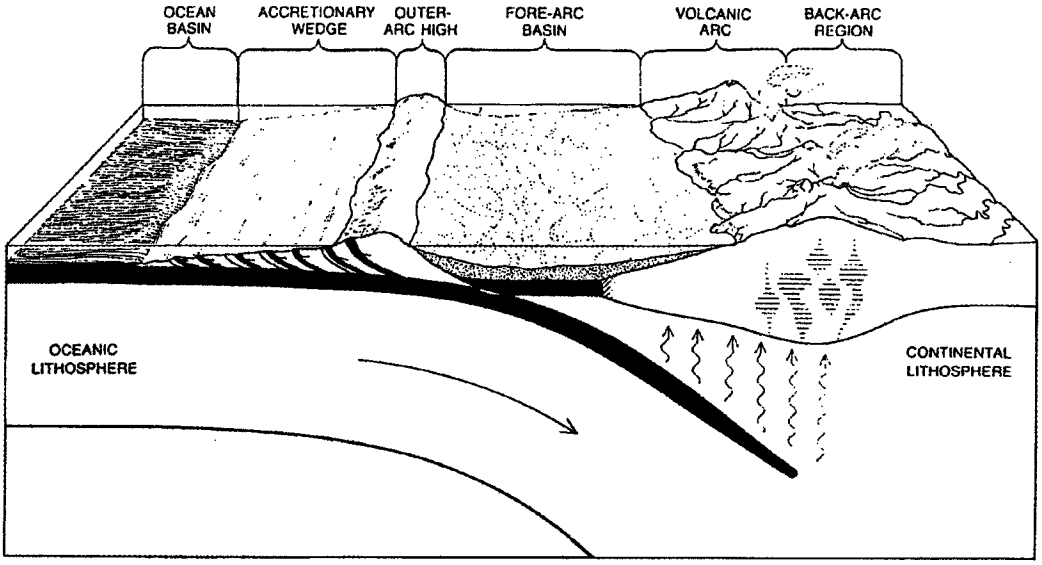

Figure 2.1 Subduction zone showing descending slab, accretionary wedge, outer-arc ridge, fore-arc ridge and basin and back-arc. Diagram from Burchfiel [1983].

Spreading Ridges

Spreading ridges (or rises) form where two plates are diverging, that is, the oceanic lithosphere of the plates is separating. Ridges are typically several thousands of kilometres wide at their bases, and ridge crests can be several kilometres above the flat abyssal plains that make up the oceanic lithosphere. At the boundary where the two plates are separating is a rift valley (or crack in the lithosphere). Deep rift valleys (ie. up to 1 km deep) are usually only found in spreading ridges with spreading rates less than 50 mm/yr [Menard, 1969]. Such valleys are usually only a few kilometres wide. Magma flows up through a rift and solidifies forming new sea floor. The rocks in the centre of the rift valley are typically bare of sediments as they are too young to have accumulated sedimentary deposits. As new sea floor is formed, the existing sea floor spreads bilaterally away from the ridge crest. The age of the rocks and the amount of sedimentary deposits increases as the distance from the rift valley increases.

The density of the rocks also increases away from the ridge crest. The lithosphere is hot and has a low density at the ridge crest. As the sea floor moves away from the rift, it cools and becomes more dense. This causes subsidence, resulting in the sea floor becoming deeper further from the rift: the depth of the ocean floor increases with the square root of the age of the crust [Bonatti and Crane, 1984]. Thus, the amount of subsidence of an ocean floor is dependent on age of the lithosphere rather than its distance away from the rift. Hence the shape of the ridge depends on the rate of spreading with fast spreading ridges being less steep than slower spreading ridges. Figure 2.2 shows cross sections of fast and slow rate spreading ridges. The spreading rate at a ridge can be estimated by dividing the distance from any point near the rift valley by the age of the volcanic rocks at that point. The age of the rocks can be estimated from the magnetic pattern of polarity reversals (see section 2.2.2 for an explanation of the Earth's magnetism and palaeomagnetism).

Fracture Zones and Transform Faults

Fracture zones are long, narrow mountain ranges which can cut across both abyssal plains and rises. Wilson [1965] introduced the concept of fracture zones into the hypothesis of sea floor spreading. They are usually about 60 km long but can be any length - some in the Pacific Ocean are thousands of kilometres long. They consist of many ridges and valleys which are aligned with the general trends of the zones. The rough topography is typical of that produced by strike slip faulting.

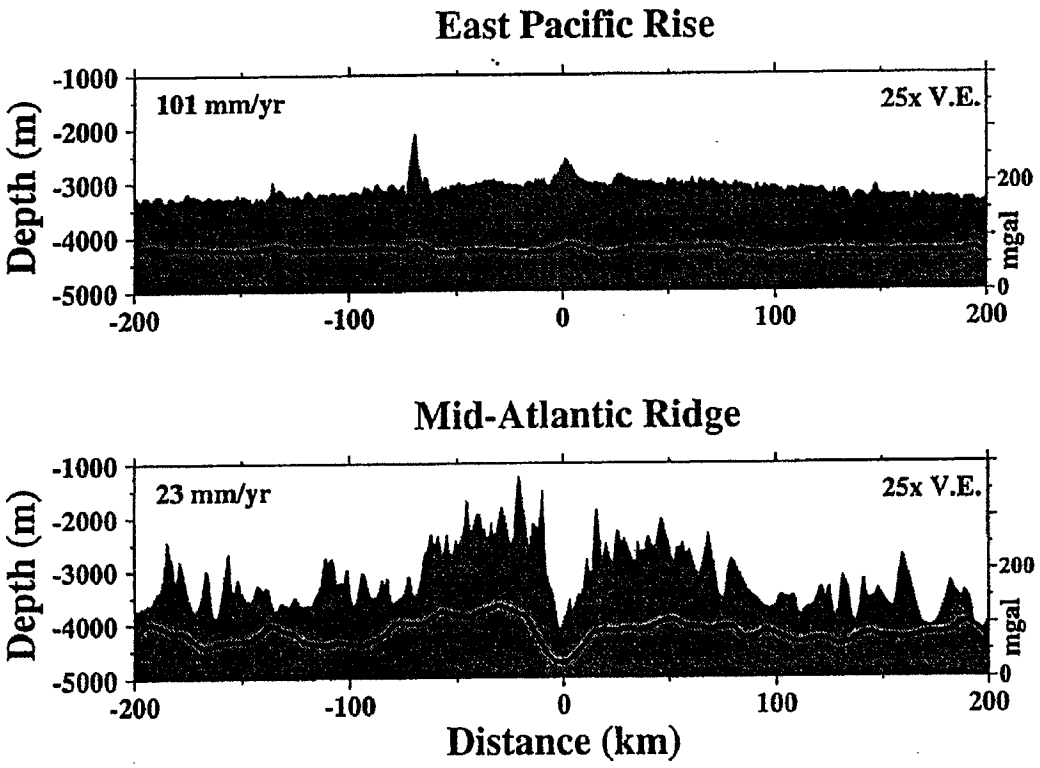

Figure 2.2 Cross section of a fast rate spreading ridge (East-Pacific rise) and a slow rate spreading ridge (Mid-Atlantic Ridge) [Small and Sandwell, 1994]. Gravity anomalies across ridges shown in heavy line.

Figure 2.3 shows a typical section of ridge between two separating plates. The crests of the ridges are offset and, according to plate tectonic theory, were offset at the time of formation [Cox and Hart, 1986]. The region between the crests of the ridges are called *transform faults*. These are the only sections where shearing between the two plates occurs. Other regions of the fracture zone are inactive as the lithosphere on both sides of the zone is part of the same plate hence there is no relative motion across it. Fracture zones form as a result of the intense shearing between the crests of the ridges. Beyond the transform faults, they are the inactive remains of earlier faulting They form along small circles, which can be useful for determining the relative motion of the plates.

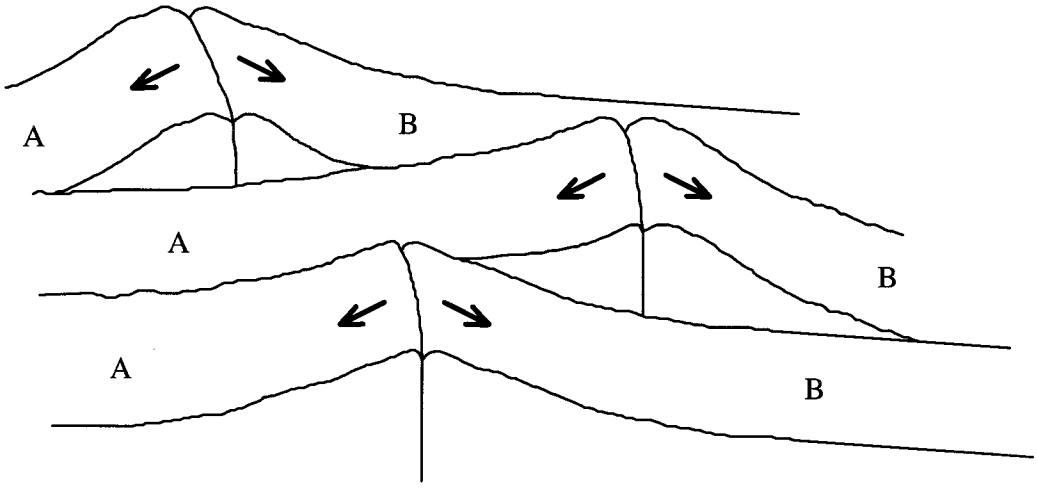

Figure 2.3 Separation of plates A and B at a ridge zone. Fracture zones form as a result of shear between ridges if the ridges are not collinear. Strike slip faulting occurs only along the transform faults (between the ridge crests). Arrows indicate the direction of motion of plates A and B. Figure adapted from Menard [1969].

2.1.2 Principal forces acting on lithospheric plates

There are many theories relating to the forces that initiate motion of the Earth's plates relative to the aesthenosphere, and it is an area that is still not fully understood. Many investigators have created both numerical and physical models of the driving mechanisms of tectonic motion (e.g. Molnar and Tapponier, [1977]; Ghose et al., [1990]; Carlson, [1983]; Shemenda, [1992]). It is generally accepted that the three main forces acting on the lithospheric plates are slab pull, ridge push and mantle drag, with slab pull being the principal force causing motion of the plates. There are minor forces (e.g. a suction force occurring between a descending slab and the overriding continental plate; frictional force opposing the motion of the descending slab) but these forces are considered more of a consequence of plate motion than the driving forces behind it and will not be discussed here. The three major forces will be briefly described:-

Slab Pull

The slab pull force results from the negative buoyancy of the descending slab. Once the slab has commenced sinking, the weight of the more dense slab causes it to continue sinking. The force is greatest at depths of 200-300 km where the difference in density is greatest, and dies out at about 700-1000 km [Cox and Hart, 1986]. As a result, the trailing plate is pulled after the slab into the aesthenosphere (this does not strictly mean that the plate is in tension, rather that the compressive force of the collision on the

horizontal portion of the subducting plate is less than if the subduction was not occurring). The slab pull force increases with the age of the subducting lithosphere (a consequence of the density of the lithosphere increasing with age) but appears to be independent of the velocity of the subduction [Cox and Hart, 1986].

Ridge Push

The ridge push force results from newly formed sea floor at a ridge pushing aside the adjacent plates. Since the ridges are often many kilometres above the abyssal plains, there is gravitational potential energy which forces the lithosphere to move, as if on a conveyor belt, away from the ridge. Forsyth and Uyeda [1975] calculated that the slab pull force was ten times more important than the ridge push force, and suggested that most of the force is balanced by viscous dissipation in the mantle. Carlson [1983] estimated that the slab pull force is three times more significant than the ridge push force in causing plates to slide over the aesthenosphere. Ridge push forces are generated over the width of the ridges, with the maximum force acting at the centre and decreasing to zero where the ridges meet the abyssal plains. Whilst ridge push is a lesser force to slab pull, it is nonetheless a significant force. Ridge push forces are almost always aligned in the same direction as slab pull forces, therefore their magnitudes simply add to create the velocity of the plates.

Mantle Drag

The importance of the mantle drag force depends on whether the driving force of plate tectonic motion is considered to be created by convection cells pushing the plates along, or the slab pull and ridge push forces. In the first instance, the frictional force between the aesthenosphere and the lithosphere is responsible for connecting the plates to the convection cells in the mantle and hence moving the plates across the surface of the Earth. In the second case, mantle drag is a resistive frictional force created as the lithosphere slides across the aesthenosphere.

2.2 PLATE MOTION MODELS

Plate tectonics can be modelled by dividing the lithosphere of the Earth into a number of sections or "plates" which are assumed to be rigid but moving relative to the stationary mantle of the Earth. Le Pichon [1968] proposed one of the first plate tectonic models of the Earth, based upon geological observations of sea floor spreading rates and azimuths

of fracture zones. This model divided the surface of the Earth into 6 rigid plates and allowed differential motion between the plates to be predicted. Using this information, it is possible to predict the relative motion between any two points on the Earth.

Plate motion models have continued to evolve, with many models being developed (e.g. Minster et al., [1974]; Chase, [1978]; Minster and Jordan, [1978]; DeMets et al., [1990]; Gripp and Gordan, [1990]; Argus and Gordon, [1991]; DeMets et al., [1994a]). The geological data used in creating a plate tectonic model of the Earth consists of transform fault azimuths, spreading rates and earthquake slip vectors (see section 2.2.2). Minster et al. [1974] proposed an absolute motion model comprised of 10 plates based on 68 spreading rates, the trends of 62 fracture zones and 106 slip vectors. The term "absolute" is used loosely here to describe motion relative to some predefined reference frame rather than relative to some arbitrarily fixed plate. Any motion cannot be truly absolute as it must be related to an origin and have a direction before the motion has any meaning at all (see Chapter 4 for an explanation of reference frames). Whether this underlying reference frame is the mantle of the Earth or some theoretical cartesian coordinate axes, the motion of an absolute model is assumed to be relative to a fixed terrestrial reference frame. The absolute model of Minster et al. [1974], AM1, used relative rates from their RM1 model and is based on the Wilson-Morgan fixed hotspot hypothesis. This provided one of the first global predictions of motion of sites anywhere on the Earth in an absolute sense.

Subsequent relative and absolute models have been derived. Minster and Jordan [1978] refined the RM1 and AM1 models to derive the RM2 relative model and AM0-2 absolute model. AM0-2 is the unique absolute motion model constructed by requiring that the lithosphere as a whole possesses no net rotation [Minster and Jordan, 1978]. The RM2 model divides the Earth into 11 plates, and was computed using 110 spreading rates, 78 transform fault azimuths and 142 earthquake slip vectors. DeMets et al. [1990] computed the NUVEL-1 relative motion model. This model is based upon the inversion of 277 spreading rates, 121 transform fault azimuths and 724 earthquake slip vectors to compute the Euler vectors of 11 assumed rigid plates relative to a fixed Pacific plate. They show that their NUVEL-1 model made significant improvements over the RM2 model in particular in fitting transform azimuths and spreading rates, and attribute much of the changes to additional data incorporated in their solution and the detection of errors in the input data of RM2.

Argus and Gordan [1991] took the relative rates of the NUVEL-1 model and derived an absolute model, No-Net-Rotation NUVEL-1 (NNR NUVEL-1). The NNR NUVEL-1 model is essentially the NUVEL-1 relative model but with an additional constraint that there is zero net torque applied to the lithosphere of the Earth. Baksi [1994] showed that the age of the magnetic anomaly used in NUVEL-1 to calculate spreading rates was in error, resulting in instantaneous velocities being overestimated by about 5%. The NNR NUVEL-1 model was subsequently modified to create NNR-NUVEL-1A [DeMets et al., 1994a]. This model is considered to be the most accurate global plate motion model currently available. Figure 2.4 shows the plate configurations of the models of Le Pichon, RM2 and NUVEL-1.

There was no data used from the Sunda Arc in the computation of any of these plate motion models. In many oceanic subduction zones, the earthquake slip vectors are neither normal to an oblique subduction trench nor parallel to the relative plate convergence directions [McCaffrey, 1992]. Therefore, the inclusion of such slip vectors may actually degrade the accuracy of a plate motion model. The available data for the Sunda Arc was deliberately omitted from the NUVEL-1 model as the authors chose to avoid using slip vectors from subduction regions where the seismicity in the overriding plate is widely dispersed. In addition, there is no geologic or geodetic measurement of the subduction rate across the Java Trench available to incorporate into any of the models.

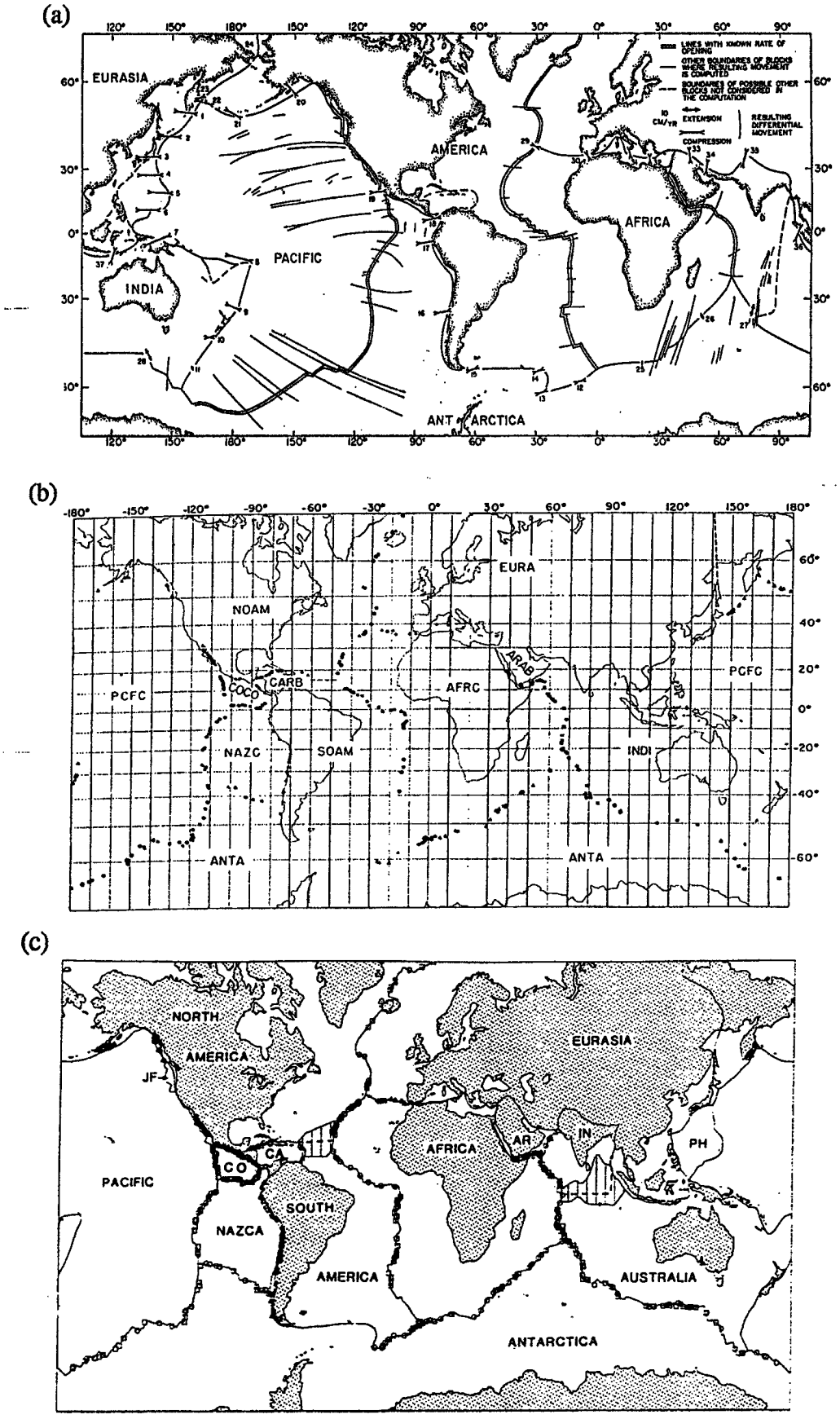

Figure 2.4 Division of the Earth into rigid plates in the models of a) Le Pichon [1968], b) Minster and Jordan [1978] and c) DeMets et al. [1990].

2.2.1 Euler Vectors

There are two terms which are used in the literature to describe motions of rotating plates - an Euler pole and an Euler vector. An Euler pole is a unit vector that defines a rotation axis about which a body rotates. If an Euler pole is considered on a sphere of unit radius with axes X, Y, Z, then the coordinates of the Euler pole can be expressed in terms of spherical coordinates, ϕ and λ (see Figure 2.5). This is analogous to latitude and longitude, respectively.

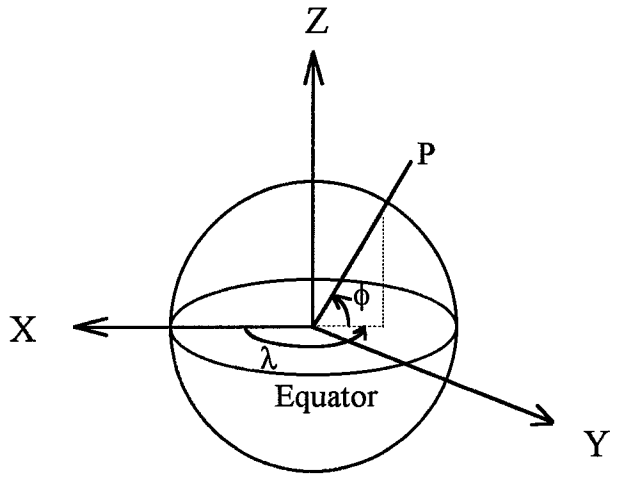

Figure 2.5 Location of Euler pole in terrestrial reference system. Euler pole (P) is defined by ϕ, λ of a rotation axis.

An Euler vector is simply an Euler pole and an angular velocity (ω) at which a plate on the Earth's surface rotates about the Euler pole [Chase, 1978]. If a site moves at a velocity of ω for a time t, then the motion of the site can be predicted relative to the reference frame by rotating the point about the Euler pole by amount ωt (Figure 2.6).

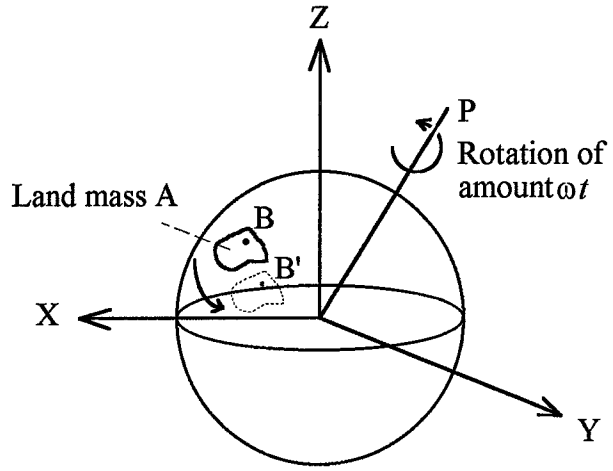

Figure 2.6 Land mass A is rotated about Euler Pole P by amount ωt. The motion of point B to B' on the land mass traces a small circle about the axis of the Euler Pole.

2.2.2 Data used in the computations of plate motion models

Information for the computation of plate motion models comes from three sources - transform fault azimuths, spreading rates and slip vector earthquake fault plane solutions. The observations required to provide this information are quite varied and are obtained using independent methods.

Transform fault azimuths

Transform faults have been described in section 2.1.1. The faults define small circles about an Euler pole which defines the relative motion of the two plates. Hence, a line perpendicular to the azimuth of a transform fault at a point on the fault will pass through the Euler pole which describes the plate motion. Transform fault azimuths are determined from analyses of the sea floor topography.

Spreading rates

Spreading rates across oceanic ridges provide a direct measure of tectonic motion. In simple terms, the age of the sea floor is determined and the distance to the centre of the ridge measured. The rate of spreading is computed by dividing the distance to the ridge centre by the age of the sea floor. However, it is not such a simple task to determine the age of the sea floor. There are two methods by which this can be achieved - radiometric dating of core samples and using palaeomagnetic observations.

Palaeomagnetism is the study of the magnetic properties of rocks. As rocks cool below a certain temperature the spin moment of electrons of the atoms in the minerals contained in rocks become aligned with the magnetic field of the Earth. This temperature is known as the *Curie temperature*, and is generally between 120°-600°C depending on the composition of the rock. However, the Curie temperature is always below the melting temperature of the rock, therefore the alignment of the magnetic particles of rocks occurs with the rocks in a solid state.

An analysis of the magnetism of a rock sample will indicate the direction of the magnetic pole at the time the temperature of the rock reached the Curie temperature. This can be useful in tracing the migration of a particular region relative to the magnetic pole. The primary importance of palaeomagnetism to plate tectonics was the discovery that throughout history the Earth's magnetic field has many periods when the polarity was reversed. Mercanton first proposed the theory of reversals of the Earth's magnetic field

in 1926. By comparing the magnetism in rocks of the same age from many geographical locations Cox et al. [1968] established a table of inversions for the last 4 million years. Vine and Mathews [1963] hypothesised that if sea floor was being continually created at a ridge, then the pattern of positive and reversed magnetism should be apparent in the sea floor either side of the ridge. They showed that this was in fact the case for the Juan De Fuca ridge.

Thus, if the pattern of magnetic reversals for a region of sea floor is known, the age of the sea floor can be determined from the inversion table of Cox et al. [1968] and hence the spreading rate at the ridge estimated [Vine and Wilson, 1965]. This is the standard approach for determining spreading rates at oceanic ridges.

Slip vectors

Slip vectors are determined from earthquake fault plane solutions and are estimates of the shear which occurs between two plates at a fault as a result of seismic activity. Cox and Hart [1986] provide an excellent description of how to calculate slip vectors (including how to draw and interpret the fault plane solutions used by geophysicists to represent earthquake solutions). The slip vector of an earthquake indicates the relative motion of the plates on the fault plane of the solution, and whether the earthquake has occurred on a normal fault (diverging plate boundary), thrust fault (converging boundary) or strike slip fault (plate boundary where the plates "slide" past each other).

Azimuths of slip vectors provide information on the direction of motion of the plates, whilst magnitudes of slip vectors indicate how much movement has occurred as a result of earthquakes. In the computation of plate motion models, it is the horizontal component of slip vectors that is of most interest as it is generally assumed that the plates of the Earth experience no vertical motion.

DeMets [1993] investigated the sensitivity of the NUVEL-1 model to the inclusion of slip vectors in the computation. He computed two further models, the first with slip vectors at subduction zones omitted, and the second with all slip vectors removed from the model. He found that using or not using earthquake slip vectors in deriving a global plate motion model had little effect on the ability to derive an accurate description of present-day plate velocities.

2.3 GEOPHYSICAL SETTING OF AUSTRALIA AND INDONESIA

The boundary between the Australian plate and the Indonesian Archipelago has many interesting tectonic features. The Java Trench is a part of the Sunda Arc, an Island arc which stretches from the Eastern Himalayas through Western Burma, the Andaman Sea, Sumatra and Java Eastward to the Banda Arc in Eastern Indonesia (see Figure 2.7). The Java Trench is an active collision zone between the Australian and Southeast Asian plates. The oceanic crust of the Australian plate is subducting beneath the Indonesian arc whilst it appears that the subduction in the Banda arc actually occurs behind the Banda islands [Calais et al., 1994].

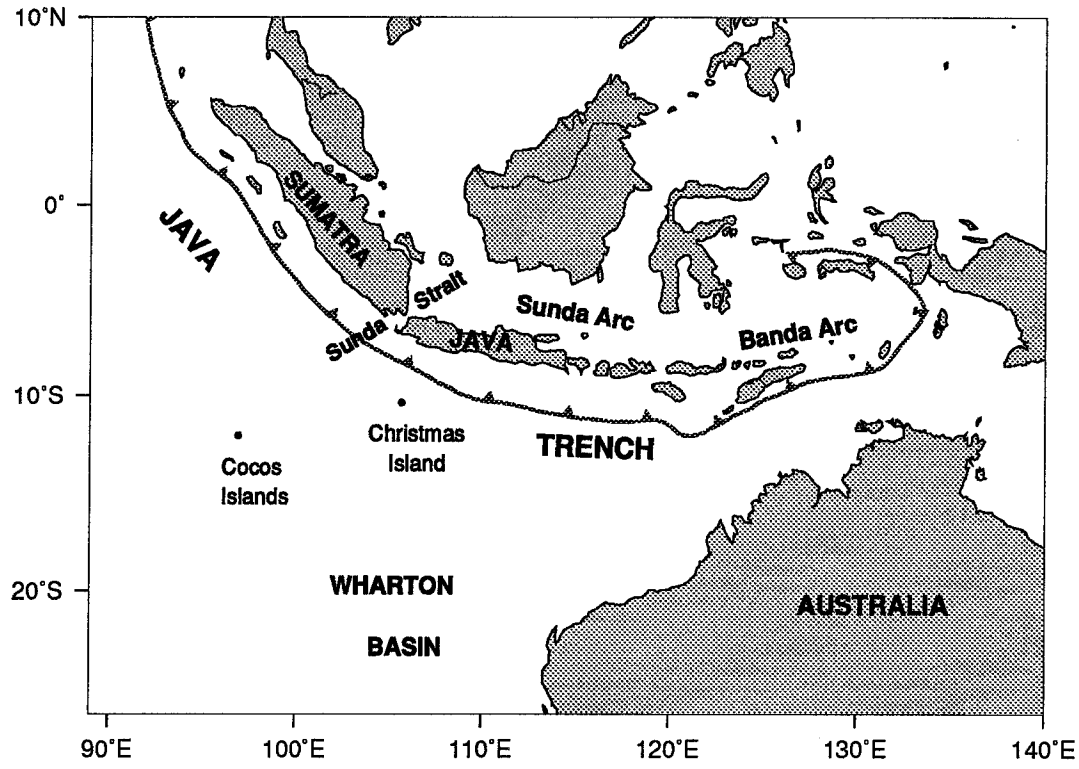

Figure 2.7 Geophysical setting of the boundary between the Australian and Southeast Asian plates.

2.3.1 Subduction Features

The Australian plate is subducting beneath the Sunda Arc, with frontal subduction occurring near Java and becoming oblique Westward along the trench. The age and thickness of the descending slab increases from Sumatra to Java. The Benioff zone below a depth of 100 km dips about 65° and extends to about 650 km beneath Java whilst dipping 30°-40° and extending to only 200 km beneath Sumatra. The length of the curving Benioff zone (measured from the trench downward along the slab) extends

about 800 km beneath Java and only about 400 km beneath Sumatra (or 550 km measured in the direction of subduction). In both regions, the slab extends about 500 km horizontally beyond the trench in the direction of subduction [Hamilton, 1979]. Beneath Java the age of the oldest crust is about 152 Ma whilst beneath Sumatra the crust is about 46 Ma.

Huchon and Le Pichon [1984] report that the outer-arc ridge is less developed off Java than off Sumatra, where the influx of sediments from the Bengal deep sea fan is larger. The morphological expressions of the outer-arc ridge and fore-arc basin have disappeared off the Sunda Strait. However, the morphology of the melange wedge (the sediment deposits that form above the oceanic plate and in front of the continental plate) remains constant along the trench from Sumatra to Java for a distance of 80-100 km away from the trench [Huchon and Le Pichon, 1984]. The subduction trench bends closer to land just near the Sunda Strait but then moves further away once South of Java.

A geodetic measurement of convergence across the subduction zone is important as it provides an independent comparison of crustal motion to that predicted by the plate motion models. Geophysical studies in the Indonesian region which consider the subduction process all use convergence estimates from global plate motion models, but to date there has not been any independent check on the accuracy of the models in the Indonesian region. A geodetic measure of convergence across the subduction zone will provide a measure of the sum of total plate convergence and any elastic resistance at the trench should the plate interface be locked. It is not possible to separate these two quantities from the determination of convergence from a single baseline, but it does provide another piece of geophysical information to aid in the understanding of the processes occurring in the region.

NUVEL-1 predicts convergence of 71 mm/yr in a direction of 20°. From geodetic measurements, Tregoning et al. [1994] estimated a convergence of 67±7 mm/yr in a direction of 11°±3° (see section 5.2.2 for a more detailed explanation of the geodetic measurement of convergence across the subduction zone). Using the mean estimates of 14 slip vectors between 105°E and 110°E [McCaffrey, 1994], Tregoning et al. [1994] estimated a convergence azimuth of 11°±9°. Figure 2.8 shows the direction of slip vectors from earthquakes between 100°E and 110°E.

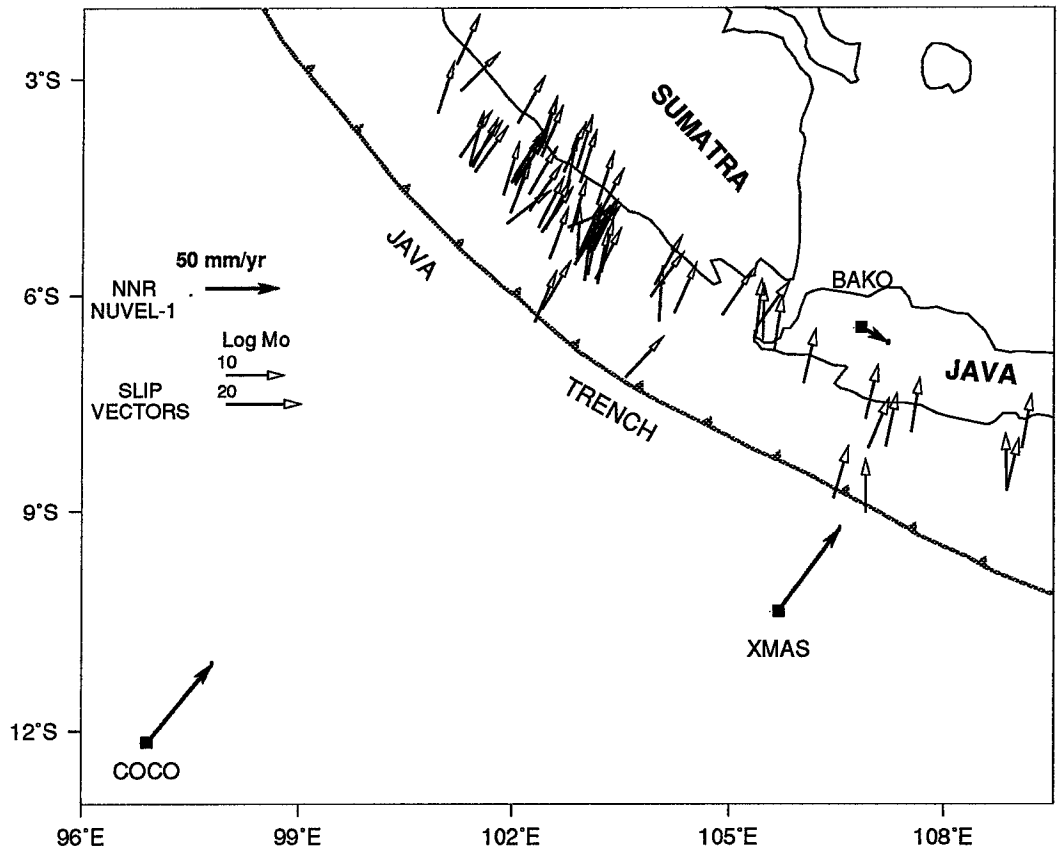

Figure 2.8 Direction of slip vectors from earthquake solutions between 100°E and 110°E. Slip vector data from McCaffrey [1994].

2.3.2 Sunda Strait

The Sunda Strait is important in the tectonic framework of the Indonesian area. Situated between Java and Sumatra, it is the transitional region between the oblique and shallow subduction beneath Sumatra and the frontal, deeper subduction beneath Java. The Sunda Strait lies at the intersection of two grabens (rift valleys), and an active N-S seismic and volcanic belt runs through its centre. The explosion of Krakatau volcano in 1883 occurred in the middle of the Sunda Strait, and today there is still an active volcano, Anak Krakatau, located in the Strait. The water depth varies from about 80 m in the North to about 1900 m at the Southwest entrance of the Strait.

Central Sumatra Fault

The oblique nature of the subduction in Sumatra is accommodated by the presence of a right lateral strike slip fault which runs from transform faults in the Andaman extensional

basin, along the Southern part of Sumatra and ends somewhere in the Sunda Strait (e.g. Molnar and Tapponnier, [1975]; Jarrard, [1986]; Huchon and Le Pichon, [1984]; McCaffrey, [1991]). The slip rate on this fault is not well known. Jarrard [1986] estimated from an analysis of slip vectors that the right lateral slip rate will not exceed 36 mm/yr. McCaffrey [1991] concluded from an analysis of slip vectors that the Northwestward motion of the fore arc in Sumatra relative to the upper plate (Southeast Asia) will increase from near zero at the Sunda Strait to 45-60 mm/yr in Northwest Sumatra. This would result in variable slip on the Central Sumatran Fault. Reid [1913] reported 2 m of right lateral strike slip which occurred as a result of the 1892 earthquake. Earthquakes between 1920 and 1960 resulted in slips of about 0.5m [Katili and Hehuwat, 1967]. Pramumijoyo and Sebrier [1991] measured structural striations observed on fault planes in the Sunda Strait region and conclude that two fault kinematics have occurred: firstly dextral strike slip faulting (found only in Miocene or older formations) and secondly normal faulting which probably began in Pliocene to Quaternary times. They suggest that the change from strike slip faulting to normal faulting 5 million years ago (Ma) may have reactivated two major fault systems within the area - the Semengka and Lampung Bays fault zones (see Figure 2.9).

Huchon and Le Pichon [1984] assumed that the Central Sumatra fault ends in the Sunda Strait, which probably explains why there is little sedimentation in the Southwest region of the Sunda Strait. Nishimura et al. [1986] state that there is no evidence that the Central Sumatra fault extends into West Java but rather ends within the Strait on a North-South fracture zone. Harjono et al. [1991] confirmed from seismic studies that the fault does not cross the Sunda Strait but seems to terminate in a N-S graben.

Bathymetry

A joint French-Indonesian study of the geology and geophysics of the Sunda Strait was conducted between 1983 and 1985 [Harjono et al., 1991]. Part of the study included bathymetric studies of the Sunda Strait. The main feature of the bathymetry is a North-South graben located at the Southern entrance of the Strait. The sea bottom depth in this graben is greater than 1500 m with 500 m of Plio-Quaternary sediments being deposited [Renard et al., 1985].

The bathymetry of the Sunda Strait is shown in Figure 2.9. The sea depth in the Sunda Strait is generally less than 100 m to the East of Krakatau with about 2000 m of sediment deposits [Huchon and Le Pichon, 1984]. West of Krakatau, the Southeast part of the Semengka Bay is up to 500 m deep and provides the Northern bound of the N-S

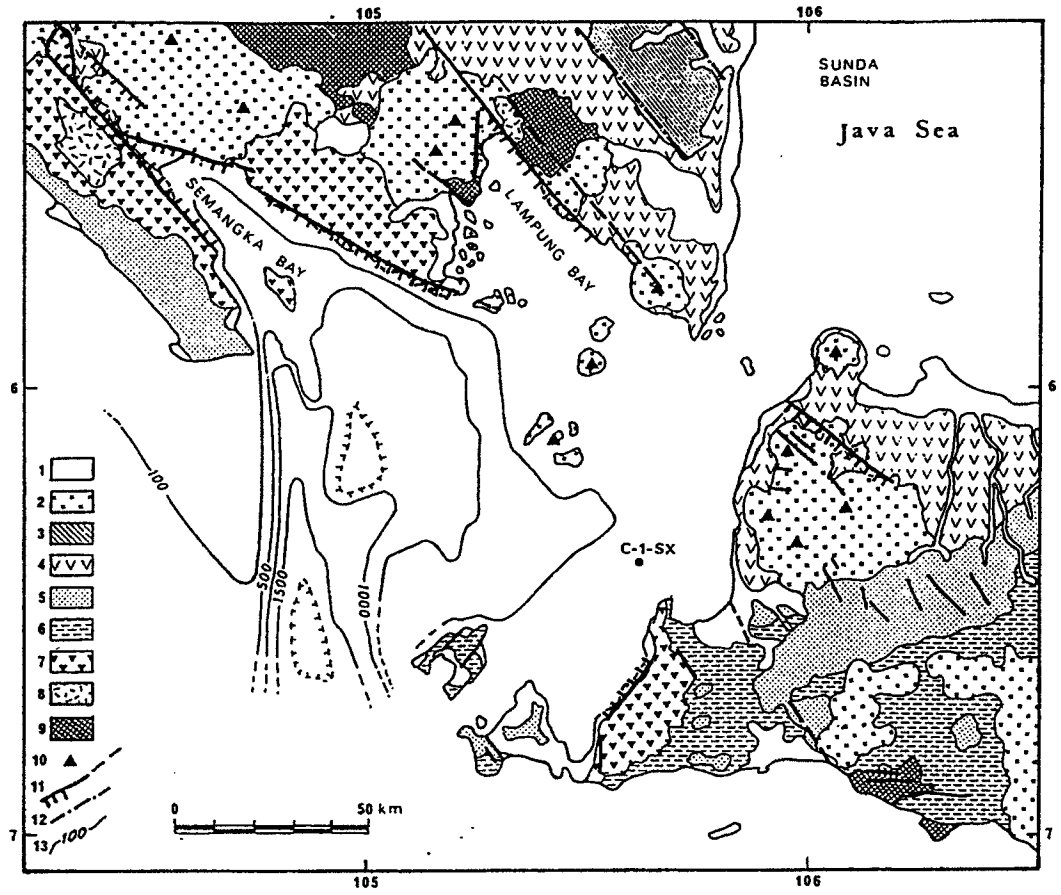

Figure 2.9 Faults in the Semengka Bay region. 1. Holocene deposits; 2. Plio-Quaternary volcanic products; 3. Sukadana Quaternary basalt; 4. Plio-Quaternary tuffs; 5. Pliocene marine sediments; 6. Miocene marine sediments; 7. Oligo-Miocene to Upper Miocene volcanic products; 8. Cretaceous granite; 9. Pre-Tertiary basement; 10. Quaternary volcanoes; 11. Faults with normal component; 12 fissural direction; 13. Bathymetric contour lines (in metres). (Figure from Pramumijoyo and Sebrier,[1991])

graben in the Western part of the Sunda Strait. The centre of this graben is about 1500 m deep, covered by about 500 m of sediments [Pramumijoyo and Sebrier, 1991].

Huchon and Le Pichon [1984] calculated extension coefficients for the Northeast and Southwest regions of the Sunda Strait (using the formulation of Le Pichon et al. [1982]) using subsidence estimates of 800 m and 2795 m respectively. This indicated that there is a definite increase in tectonic subsidence to the South, and that the extensional coefficient is 2.3 times greater than in the North. This has implications regarding the extensional regime that is operating in the Sunda Strait and will be discussed later.

Formation of the Sunda Strait

There are two theories as to how the Sunda Strait was formed. The first suggests that the Strait opened as a result of Sumatra rotating away from Java. Based on a geometric analyses of the changing depth of the Benioff zone and ages of volcanic activity, Ninkovich [1976] concluded that Sumatra underwent a clockwise rotation of about 20° in the last 10 million years. Nishimura et al. [1986] used palaeomagnetic studies to hypothesise that the Sunda Strait was formed by the clockwise rotation of Sumatra at a rate of 5-10°/Ma. Jarrard and Sassajima [1980] infer from palaeomagnetic data that during the late Mesozoic Sumatra drifted Northward accompanied by a clockwise rotation of about 30°, and was situated near its current position by the early Tertiary period.

The second and currently accepted theory is that the Strait formed as a result of oblique subduction. Oblique subduction usually creates a strike slip fault on the continental side of the subduction zone (see e.g. Jarrard, [1986]). The small sliver of land between the strike slip fault and the subduction trench accommodates the oblique nature of the subduction by shearing laterally along the fault (Figure 2.10). In so doing, the trailing edge of the fore-arc sliver has moved away from Java and the Southern end of the Sunda Strait has opened. Huchon and Le Pichon [1984] proposed that the Strait is caused by extension due to the Northwest lateral motion of the Southwest Sumatra block along the Central Sumatra Fault. They use the result of Jarrard and Sassajima [1980] to state that there is no strong evidence to substantiate a rotation of Sumatra relative to Java during the Neogene and so rule out the opening of the Strait by rotation as suggested by Ninkovich. They propose that a combination of compression from the subduction and extension from strike slip faulting moves the location of the trench slightly Northward immediately South of the Sunda Strait. This maintains the consistency of the morphology near the trench. Seismic studies by Lassal et al. [1989] and Harjono et al. [1991] have confirmed that the Sunda Strait is undergoing extension. Geodetic measurements across the Sunda Strait will be used to determine the strain pattern in this region.

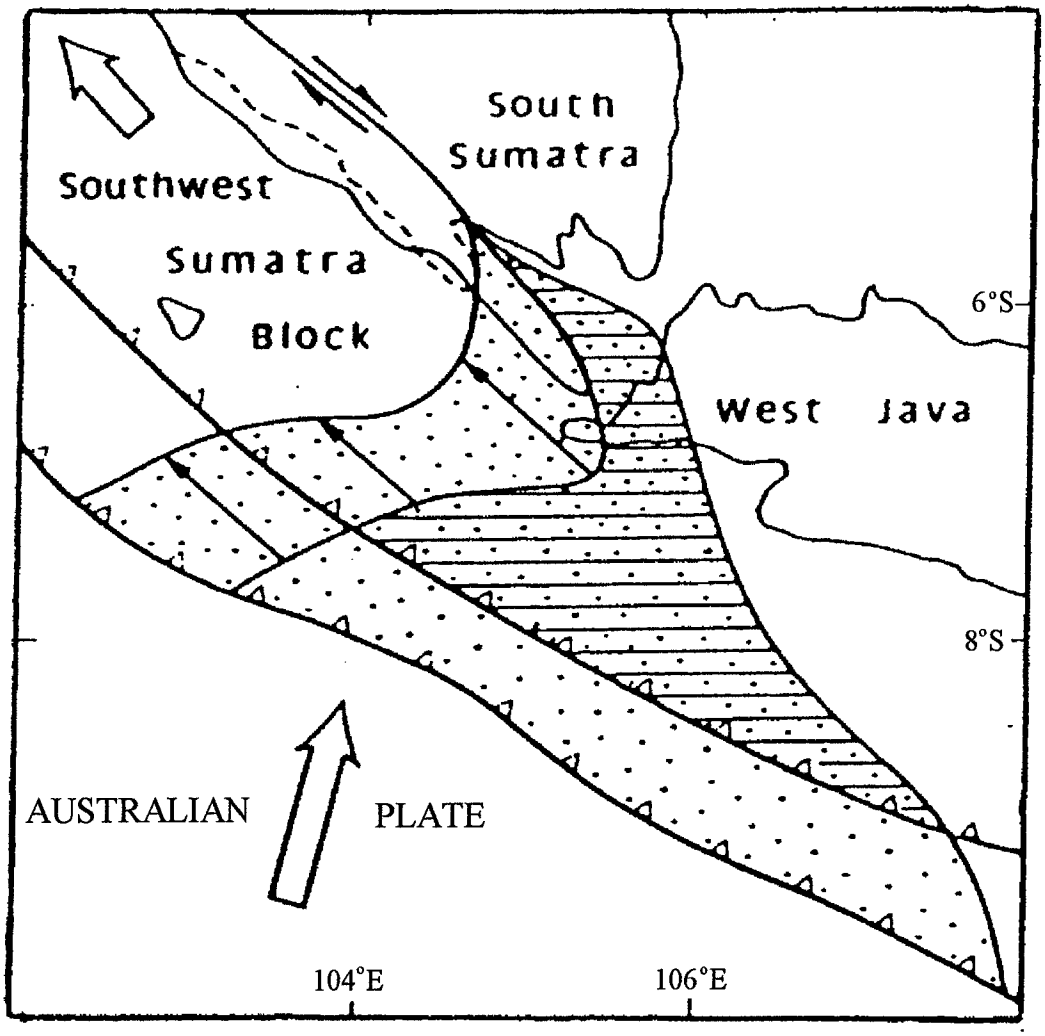

Figure 2.10 Mechanism of the formation of the Sunda Strait as a result of oblique convergence of the Australian and Southeast Asian plates. Dashed line represents the present position of the Southwestern coast of Sumatra. Arrows indicate total displacement of the Southwest Sumatra block. Hachured area indicates the region of future stretching, stippled area indicates the region already stretched [Huchon and Le Pichon, 1984].

2.3.3 Indian Ocean

The Indian Ocean lies to the South of the Indonesian Archipelago. The Ocean floor is quite deep, around 5000 m in most areas. Immediately South of Java is the Wharton Basin, an area of Late Jurassic and Early Cretaceous age near Australia but becoming younger Northward and Westward. The floor of the basin is mostly a rough oceanic basement covered by a thin layer of sediments [Hamilton, 1979]. There are a number of major features in the Indian Ocean near the Indonesian region - a Palaeogene volcanic island (Christmas Island), an island which has formed from coralline deposits on a

volcanic base (Cocos Islands), a 200 km wide ridge which stands about 2000-4000 m above the surrounding sea floor (Ninetyeast Ridge) and a wide plate boundary between the Indian and Australian plates which is located to the Southwest of Sumatra at the Western side of the Wharton Basin [DeMets et al., 1994b].

The tectonic understanding of the Indian Ocean has changed considerably in the past 15 years. Originally it was thought that India and Australia were part of the same plate (see e.g. plate motion models by Le Pichon, [1968]; Minster et al., [1974]; Chase, [1978]). Minster and Jordan, [1978] hypothesised that India and Australia were either not part of the same rigid plate, or there was a large amount of intraplate deformation occurring. Weins et al. [1985] proposed that India and Australia lay on distinct, rigid plates separated by a wide East-West striking plate boundary zone. DeMets et al. [1990] formulated a plate motion model which separated the Indian and Australian plates. DeMets et al. [1994b] estimated the location of a wide, diffuse boundary between the two plates.

At the Southern edge of the Indian Ocean is a spreading ridge which separates the Australian and Antarctic plates. This provides a ridge push force on the Australian plate, which will influence the subduction process occurring at the Northern end of the plate. The NNR-NUVEL-1A model predicts a spreading rate of 66 mm/yr between Mawson (Antarctica) and Yaragadee (Western Australia).

2.4 GEOLOGY OF THE GPS SITES

Any crustal motion survey requires reoccupation of monumented sites. Therefore, it is essential that the monuments are stable relative to the surrounding topography, or that their motions are known. This allows any motion detected in the geodetic measurements to be attributed to crustal motion rather than localised deformation. The ground location of sites used in this research project have not been selected and constructed by the author, and many have not been visited by the author. Thus the degree of connectivity of the marks to the underlying region is unknown at some key sites. The organisations involved in this project decided that fieldwork North of the Java Trench would be the responsibility of Bakosurtanal, with assistance from SIO and RPI, and sites South of the Java Trench were the responsibility of UNSW.

In this thesis I have defined a station to be the actual monument to which the geodetic observations are related, and a site to be the region surrounding a station. Some of the stations on the Australian continent used in this project are part of the Australian Fiducial

Network (AFN), installed and operated by the Australian Surveying and Land Information Group (AUSLIG) [Manning and Harvey, 1992], whilst others have been selected and operated by other organisations such as Jet Propulsion Laboratory (JPL) and Cooperative International GPS Network (CIGNET). A brief geological and site description will be given for the stations of most interest to this thesis, namely the Cocos Islands, Christmas Island, Cibinong and the Sunda Strait stations. A more comprehensive description of some sites is given in Appendix 1. Figures 3.1 and 3.2 show the location of stations at the sites mentioned below.

2.4.1 Christmas Island

Christmas Island (S10°30', E105°40') is an isolated pinnacle in the Eastern Indian Ocean. It is thought that Christmas Island emerged during the Eocene Era (about 50 Ma) as one of a chain of sub-marine volcanoes caused by a spreading ridge in the Earth's crust off the Northwest coast of Australia. Molten lava erupting through the sea bed would have gradually built up until the Island was created. Most of the island is composed of Tertiary limestones [Woodroffe, 1988]. Christmas Island is located on the Australian plate, and the NNR NUVEL-1A model predicts that it has a velocity of 71 mm/year at a true bearing of 37°. The Island is about 150 km South of the Java Trench and Woodroffe [1988] estimated that the rate of uplift of the Island relative to sea level is between 0.05 and 0.25 mm/year. This is probably due to a slight bulging in the oceanic plate as it subducts.

The GPS station located on Christmas Island is a brass plaque set in concrete at ground level. The mark is part of the survey network of Christmas Island which is administered by the Department of Lands Administration, Western Australia (DOLA). The mark is regularly occupied by DOLA using terrestrial methods as part of ongoing developments of the Island. No relative deformation of the Christmas Island network has been detected at the 5 mm level (Ken Alexander, DOLA, pers. comm., 1993). The GPS surveys were conducted by setting a tripod over the brass plaque.

2.4.2 Cocos Islands

The Cocos Islands (S12°10', E96°50') in the Eastern Indian Ocean are a small group of coral reef islands. There are two main sections - the South Keeling Islands which are a group of islands surrounding a coral lagoon, and North Keeling Island which is a single island about 40 km North of the main group. The islands vary in size from about 11 km long to only a few hundred metres in diameter. The islands have emerged from the

ocean through deposition of coralline limestone upon volcanic basements. Studies of Microatolls on Cocos Island have been made to monitor changes in sea level (Woodroffe et al. [1990a]; Woodroffe et al. [1990b]) which indicate that at least 0.5 m of emergence has occurred on the Islands in the last 3000 years. The NNR NUVEL-1A model predicts that the Cocos Islands are moving 71 mm/yr in a direction of 37°. DeMets et al. [1994b] hypothesised that the Cocos Islands lie very close to a diffuse deformation zone between the Indian and Australian plates. If the Islands happen to lie within this deformation zone then the motion of the Cocos Islands may not be that which would be expected if the Islands were a part of the Australian plate.

The GPS station at the Cocos Islands is located on West Island, and forms part of the AFN. West Island is comprised of coralline limestone, and has a highest point of about 5 m above sea level. The mark is the centre of a steel screw thread on a concrete pillar set into the compacted coral remains that form the soil of the island. The station was installed in June 1992 by the Australian Construction Service under the direction of AUSLIG. I made the first occupation of the station in July 1992 for the Indonesia 1992 survey. I observed a terrestrial survey to connect the pillar into a local survey network, and to allow future resections to be observed in order to monitor the stability of the pillar relative to West Island. Subsequent resections in January 1993 and August 1993 have found that no relative horizontal motion is detectable at the 4 mm level.

2.4.3 Indonesian Sites

The primary station in Indonesia for this project, called Bakosurtanal, is at Cibinong, West Java. It is a brass plaque set in a concrete pillar located within the grounds of Bakosurtanal (Indonesian National Agency for Surveying and Mapping), Cibinong, West Java. This mark is a principal station in the Indonesian National Geodetic Network. The station has been observed in all Indonesian surveys since 1989.

The Sunda Strait sites (see Figure 3.1) were selected during a reconnaissance in October 1991 in which I participated. The stations of Dempo, Bukit Pillar and Krakatau were existing pillars observed during Doppler surveys in the 1980s using the Transit system. Tanjung Cina was an existing mark observed as part of a joint Indonesian/French GPS survey in the 1980s. New stations were selected at Krui and Benkayang, and were constructed subsequent to the reconnaissance of 1991. All antennas were mounted on tripods set over ground marks. As mentioned in section 2.3, the fieldwork for these stations was performed by staff members of Bakosurtanal, and personnel from SIO and RPI. The station at Krakatau was not reobserved in the 1993 campaign as the field party

were not permitted on the island due to the danger of an eruption. Consequently, there has only been one occupation on this station and hence it has not been included in the analysis of the data presented in this thesis.

2.4.4 Australian Fiducial Network Sites

In June 1992, AUSLIG installed the AFN to be observed during the two week Epoch92 period [Manning and Harvey, [1992]; Morgan and Manning, [1992]]. Epoch92 was a two week period in 1992 (26th July - 8th August) when about one hundred GPS stations were observed by many organisations as part of a pilot project by the International GPS Service for Geodynamics (IGS). The fieldwork for the Indonesian survey of 1992 was combined with the AFN survey, resulting in the AFN stations of Darwin and Karratha being incorporated into the regional stations of this project. These stations were installed and operated by AUSLIG. The monumentation consists of a concrete pillar set into bedrock, with the actual mark being the centre of a screw thread on a pillar plate located on the pillar. Local terrestrial surveys to reference marks were made at each station in order to check local stability. These local surveys will be repeated to check for any local deformation (M. Hendy, AUSLIG, pers. comm., 1994). Rogue SNR-8 receivers have since been permanently installed by AUSLIG at Darwin (April 1994), Karratha (June 1994) and Cocos Islands (August 1994). Resurveys of recovery marks at Darwin and Karratha have confirmed that there is no localised motion of the pillar at the 2 mm level.

CHAPTER 3

GPS, FIELD CAMPAIGNS AND PROCESSING METHODS

GPS was initiated in 1973 by the United States of America Department of Defence (DoD) as a military navigation system. The system consists of space, control and user segments which have been explained in detail elsewhere (see e.g. Parkinson & Gilbert, [1983]). This Chapter will give a short explanation of certain pertinent aspects of GPS to illustrate how specific benefits and problems have resulted from using GPS for crustal motion studies. More comprehensive explanations of GPS can be found elsewhere (e.g. Dixon, [1991]; Parkinson & Gilbert, [1983]; Milliken & Zoller, [1980]; Spilker, [1980]; King et al., [1985]).

3.1 WHAT IS GPS?

The Global Positioning System currently consists of 24 satellites operating in three orbital planes. The orbital parameters of the satellites have been selected such that each satellite will pass over the same point on the ground once every sidereal day. There are three versions of satellites - Block I satellites, which were the pilot satellites designed to test the operation of the system, and Block II and Block IIa satellites which would replace the Block I satellites, and form the operational system. The satellites are equipped with atomic frequency standards, which are used to create carriers to transmit on two L-band frequencies - L1 at 1575.42 MHz and L2 at 1227.6 MHz. Codes are modulated onto the carrier signals in order to transfer GPS time and one-way ranging signals from the satellites to a receiver. The L1 signal is modulated with two pseudo-random noise codes - the Clear Acquisition code (C/A code) and the Precise code (P-code). The L2 signal is modulated with only the P-code. Both L-band frequencies are also modulated with a 50 Hz navigation message which contains information regarding the health of the satellites, clock parameters, an ephemeris (known as the broadcast ephemeris) and other information. The C/A code has a repeat time of 1 millisecond and a modulated chip rate of about 300 m. The P-code with a modulated chip rate of about

30 m repeats every 37 weeks. However, each satellite is assigned a unique seven day section of the code which repeats every week [Parkinson & Gilbert, 1983].

GPS measurements can be made in two modes - navigation and geodetic modes. The whole system essentially operates by deducing the transmission time of the satellite signal and using this to compute a distance from the satellite to the receiver. The following is adapted from Dixon [1991]. A GPS receiver operates by cross-correlating the incoming satellite signals modulated by codes with exactly the same codes generated within the receiver. The internal codes are shifted until in phase with the incoming codes, thus determining the time delay necessary to match the two signals. The time delay is a measure of the time of transmission of the satellite signal from the satellite to the receiver. However, this time delay contains effects such as the offset of the receiver clock to GPS time and atmospheric delay of the signal. The time delay can be converted into a distance or range between the receiver and satellite but, due to these effects, the range will be biased and is therefore known as a pseudorange. By combining pseudorange measurements to a number of satellites and the satellite locations provided by the broadcast ephemerides, the receiver position can be determined. This is essentially the procedure used in the GPS navigation mode.

It is also possible to obtain range information through measuring the phase and Doppler shift of the carrier signal itself. Since the wavelength of the carrier phase is significantly shorter than the lower frequency code modulations, phase measurements of the carrier signal are more precise than pseudorange measurements. In addition, phase measurements can be made to 1/1000 of a cycle without any need to cross correlate signals. For a signal with a wavelength of 0.19 m, this corresponds to a precision of 0.19 mm. If the initial integer number of cycles between the receiver and satellite at the time of signal acquisition can be determined then a very accurate range measurement is known. In many receivers, it is not actually the carrier phase but the lower frequency carrier beat phase that is measured. The carrier beat phase is generated by mixing the satellite signal with a local oscillator signal. This forms the basis of geodetic GPS observations.

The higher frequency of modulation of the P-code signal allows for more precise measurements of P-code pseudoranges than C/A code pseudoranges. The C/A code is readily available to the civilian community but the DoD reserve the right to encrypt the P-code to a secret Y-code, decipherable only by military receivers. If the P-code is encrypted to the Y-code, and if this Y-code is not known, then the basic code correlating techniques cannot be used on the L2 frequency, and only C/A code correlation can be

applied to L1. This results in only C/A pseudoranges being determined within the receiver. Other partial correlation techniques can be implemented to recover phase information from the L2 signal which do not require knowledge of the Y-code but do recover full wavelength L2. The encryption process from P-code to Y-code is known as Anti Spoofing (AS), and can be implemented by the DoD on only Block II and IIa satellites to deliberately downgrade the ability of the user to accurately determine real time positions on the Earth.

The other method implemented by the DoD to degrade the accuracy of the system is called Selective Availability (SA) which again can only be applied to Block II and IIa satellites. Under SA, the accuracy of the broadcast ephemeris and broadcast satellite clock offsets are degraded, and the satellite oscillator frequency is "dithered" or altered slightly from its correct frequency. This affects the accuracy of a receiver solution in navigation mode which is totally dependent on the broadcast ephemeris, satellite clock offset and the assumption that the satellite frequency is constant. The effect on geodetic positioning with SA can be lessened to some extent. Degradation of the ephemeris can be overcome by estimating the motion of the satellites from phase measurements. The error in the satellite clock offset is also limited as it is only of importance in estimating the receiver clock offset. With the use of long term averaging and modelling of SA, an accuracy of 1μs in the receiver clock offset is sufficient.

The formation of double differences also reduces the effect of satellite and receiver clock offsets from GPS time (see Section 3.3.1). However, the dithering of the satellite frequency can produce significant phase errors, in particular when receivers do not observe simultaneously. The effect is greatest on long lines. As the distances between stations is generally greater in the Southern hemisphere than the Northern hemisphere, the consequences of SA can be larger in the Southern than the Northern hemisphere. Feigl et al. [1991] demonstrate how the effects of SA dithering can be overcome by modelling the frequency deviations.

There are essentially three types of geodetic receivers available - P-code receivers which have knowledge of both the P and C/A codes, cross correlating receivers which recover the L2 phase without using the P-code and squaring receivers which can only decode the C/A code on the L1 frequency. The electronic design of the geodetic receiver will determine how phase measurements are performed. A by-product of code correlation processes is the ability to reconstruct the phase observables, but this requires knowledge of the code modulation. However, the phase of the carrier signal can be recovered without knowledge of the code modulation by multiplying the signal with itself. This

results in the second harmonic of the original carrier phase without any code modulation, but the wavelength is halved [Dixon, 1991]. Receivers using this technique are known as squaring type receivers. The obvious advantage of this procedure is that the high precision information of the carrier phase can be obtained without any information of the code modulation, but in the process the signal to noise ratio is significantly reduced. This can lead to poorer tracking of L2 in squaring type receivers, in particular during periods of high ionospheric activity. In addition, halving of the wavelength makes resolution of the initial number of integer wavelengths at the time of acquisition more difficult.

Observations on both the L1 and L2 frequencies allow the ionospheric delay of the incoming signals to be removed by combining the two signals into an ionospheric free Lc combination at a one-way level. This is essential when observing long baselines where the incoming signals will pass through different sections of the ionosphere. The Lc combination (see e.g. King et al., [1985]) is calculated as:

$$\phi_{Lc} = \frac{f_1^2}{f_1^2 - f_2^2}\phi_{L1} - \frac{f_2^2}{f_1^2 - f_2^2}\phi_{L2} \qquad (3.1)$$

where ϕ_{Lc} = phase of ionospheric free combination
ϕ_{L1} = phase of L1 frequency
ϕ_{L2} = phase of L2 frequency
f_1 = frequency of L1
f_2 = frequency of L2

Prior to the introduction of AS, cross correlating P-code receivers could provide full wavelength L1 and L2 phase measurements which can be combined to form the widelane combination, L5, with a longer wavelength (0.86 m) than either the L1 (0.19 m) or L2 (0.24 m) frequencies. The widelane combination (see e.g. King et al., [1985]) can be expressed as:

$$\phi_{WL} = \frac{f_1}{f_1 - f_2}\phi_{L1} - \frac{f_2}{f_1 - f_2}\phi_{L2} \qquad (3.2)$$

It is easier to solve for initial phase ambiguities of the widelane combination than to solve for the L1 and L2 ambiguities due to the longer wavelength of the widelane combination. It is also useful in cycle slip detection in the preprocessing of GPS data [Blewitt, 1990].

For this reason, it is beneficial to observe large scale static geodetic measurements with P-code receivers. When AS is operating, the P-code receivers must resort to either squaring techniques or other methods to once again recover the phase observable of L2. Some manufacturers have developed cross correlation techniques which allow the full wavelength of the L2 signal to be recovered without knowledge of the modulated codes. AS has been turned on continuously since February 1994.

3.2 FIELD CAMPAIGNS

There have been seven field campaigns which have provided GPS data from the Indonesian and Australian stations. The dataset used in the analysis of this thesis is a subset of a larger geodynamics project encompassing most of Indonesia. The stations of interest to this thesis located in Indonesia are Cibinong (BAKO) and Bukit Pillar (BPIL) in West Java, Tanjung Cina (CINA), Dempo (DEMP) and Krui (KRUI) in Sumatra (Figure 3.1) and Benkayang (KAYA) in Kalimantan (Figure 3.2). The stations on the Australian plate are Christmas Island (XMAS) and Cocos Islands (COCO) in the Indian Ocean, Yaragadee (YAR1), Caversham (CAVE), Karratha (KARR), Darwin (DARW), Townsville (TOWN), Canberra (DS40 and DS42), Hobart (TAS1, HOB1 and HOBA) and Smithfield (AUSA and AUSB) in Australia (Figure 3.2). In addition, Antarctic stations at Mawson (MAW1 and MAWS), Casey (CAS1), Davis (DAV1), Macquarie Island (MAC1) and a distribution of global tracking stations have been used to compute the GPS orbits (fiducial network used was subject to data availability)(Figure 3.3). A complete listing of station occupations, days observed and receiver types as used in this thesis can be found in Appendix 1.

The GPS campaigns commenced in 1989 (days of year 254-263) with the BAKO-XMAS baseline being observed along with some stations along the Sumatra transect [Puntodewo, 1994]. The survey in 1990 reobserved the BAKO-XMAS baseline along with additional stations in Indonesia. Data was available for the stations of DS40, TAS1 and TOWN in addition to BAKO and XMAS during the Indonesian campaign of 1991. All of the Indonesian campaigns prior to 1992 were processed by combining the regional data with the available global tracking data. The amount and distribution of global tracking data varies greatly with each campaign, and hence the quality of the global orbits in the first three years is quite variable. Also, the number of GPS satellites has steadily increased from 8 satellites in 1989 to 25 satellites in 1993, which has resulted in the more recent solutions being stronger than the earlier solutions. Figure 3.4 shows the global tracking scenarios used from 1989 through to the present configuration. The weakness of the reference frame in the Southern hemisphere is investigated in detail in Chapter 4.

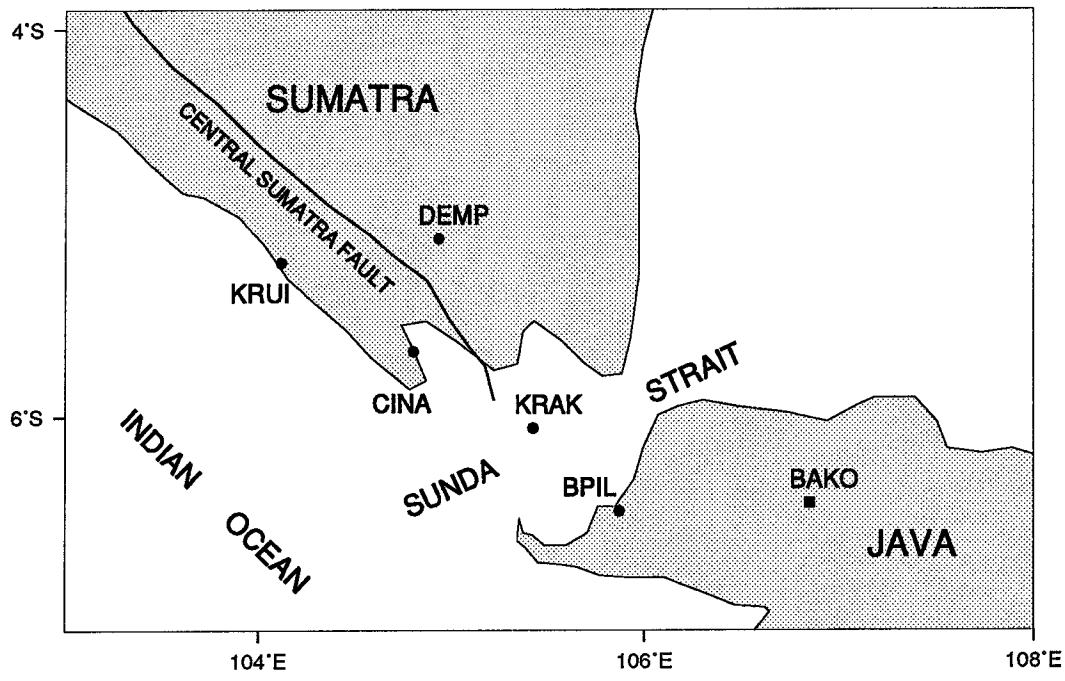

Figure 3.1 The GPS network of the Sunda Strait. BAKO station not observed simultaneously with other stations in the 1993 survey.

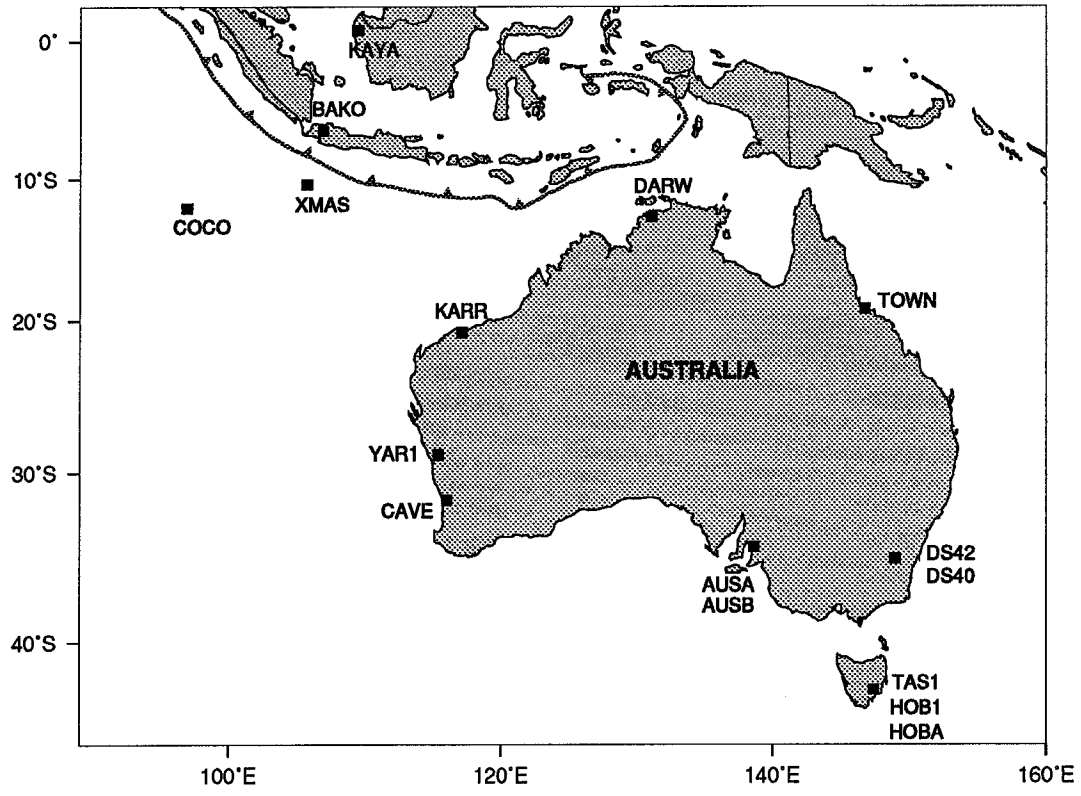

Figure 3.2 GPS stations located in the Australian region used in the processing.

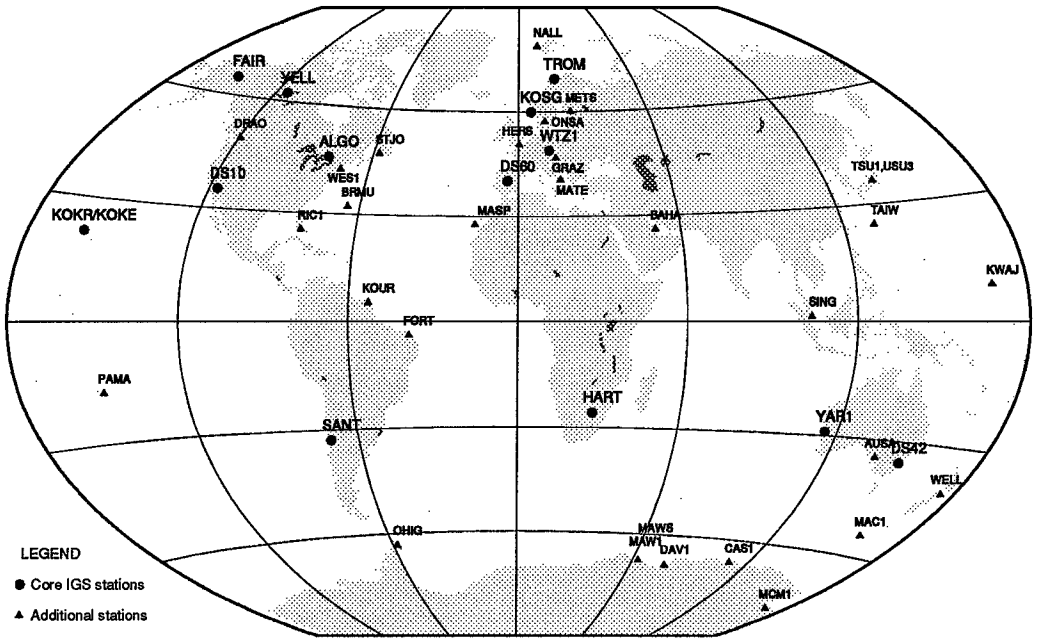

Figure 3.3 Location of global fiducial stations.

The fiducial network improved considerably in 1992 with the introduction of the International GPS Service for Geodynamics (IGS) [Mueller and Beutler, 1992]. IGS instigated a number of processing centres in Europe and North America which began processing global orbits using GPS data from a set of core GPS stations distributed throughout the world (see e.g. Bock et al., [1993a]; Dow et al., [1993]; Kouba et al., [1993]; Rothacher et al., [1993]; Schutz et al., [1993a]; Zhu et al., [1993]; Zumberge et al., [1993]). In addition, analysts involved in this project had become more aware of the rather poor quality of the GPS solutions in the Southern hemisphere and realised the importance of regional tracking stations in obtaining the highest quality solutions. Hence more regional stations were added to the campaign plan. Table 3.1 lists the regional (non global fiducial) stations that were observed in Australia and Indonesia that have been used in the analysis.

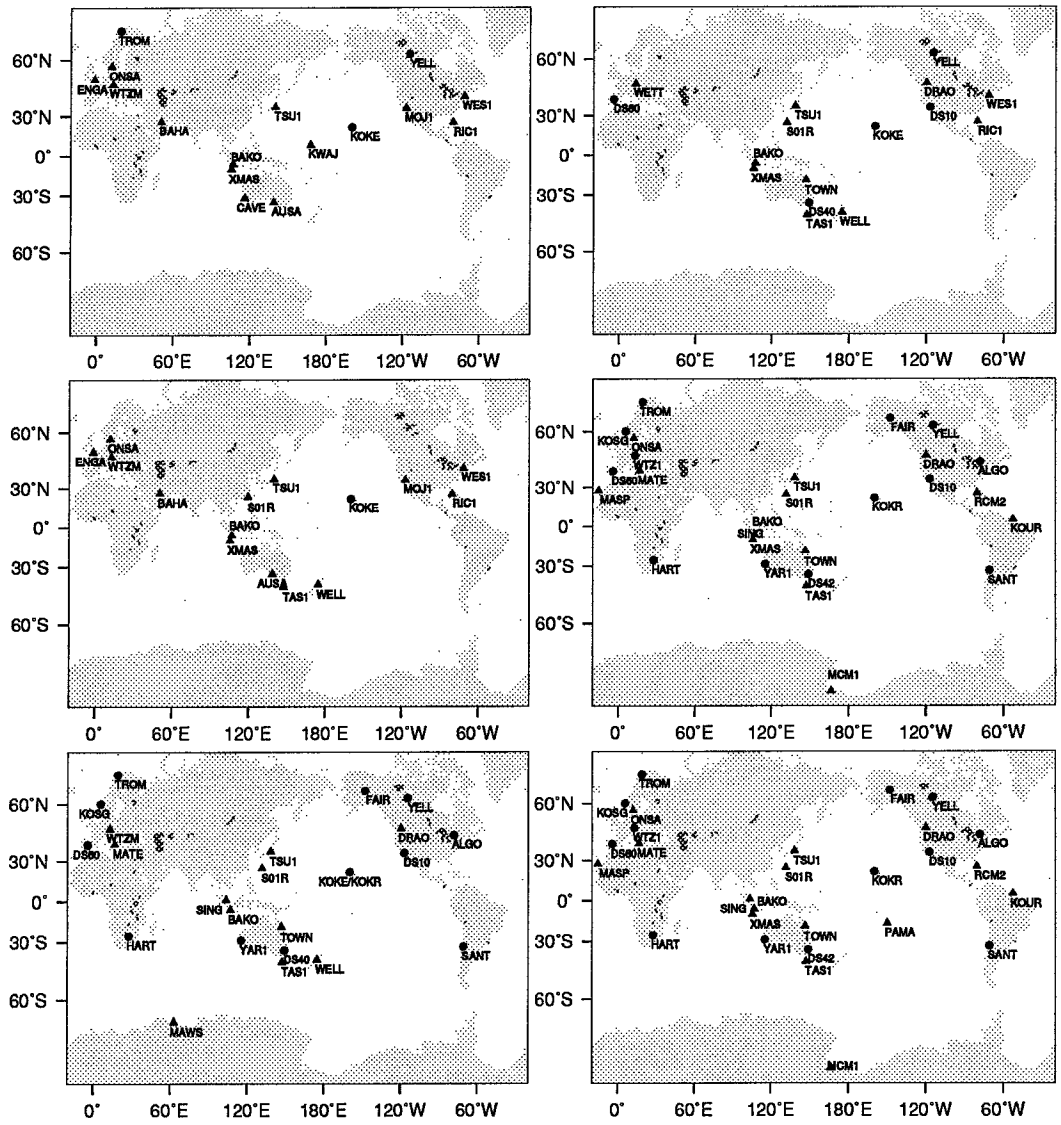

Figure 3.4 fiducial tracking networks used in Indonesian campaigns: a) 1989; b) 1990; c) GIG'91; d) 1991; e) 1992 and f) 1993.

The BAKO station was observed during the GPS IERS and Geodynamics Experiment - 1991 (GIG'91) experiment [Blewitt, 1993], by a commercial company, Racal Surveys, who generously provided the GPS data and field notes from this period. GIG'91 was a 22 day experiment in January and February 1991 when a tracking network of Rogue SNR-8 P-code receivers, similar to the 1992 IGS network, was operational. At the same time there were about 100 receivers of various types operating for a number of campaigns (see e.g. Melbourne et al., [1991], Rothacher et al., [1992]). Stations observed at this time in the Australian region include YAR1, DS40, TAS1, TOWN and MAWS. Of the 21 Rogue stations observed during GIG'91, 10 were still operational in August 1993 and form the basis of the core IGS global GPS network. GIG'91 was the first high quality GPS campaign in the Southern hemisphere, and having observations on

these regional stations during this period improves their position and velocity solutions immensely.

Table 3.1 Station occupations 1989-1993.

Australian Stations			Indonesian Stations		
Station	Year	Days of Year	Station	Year	Days of Year
XMAS	1989	254-263	BAKO	1989	254-263
	1990	200-223		1990	200-223
	1991	170-181		1991	030-042,170-181
	1992	207-230		1992	207-233, 244-247
	1993	227-239		1993	017-024,227-229,235-245
COCO	1992	207-227	BPIL	1992	224-231
	1993	017-022,227-245		1993	230-234
DARW	1992	207-220	KAYA	1992	213-224
	1993	017-024,227-245		1993	230-235
KARR	1992	207-233	CINA	1992	231-233
	1993	227-245		1993	231-234
DS40	1991	030-042,175-181	KRUI	1992	231-233
				1993	231-234
TAS1	1990	200-233			
	1991	030-042,175-181	DEMP	1992	224-231
	1992	207-233		1993	231-234
	1993	017-024			
TOWN	1991	030-042, 175-181			
	1992	207-245			
	1993	227-245			
CAVE	1989	260-263			
	1992	244-247			
	1993	242-245			

3.3 GPS DATA PROCESSING

The GPS observations for this project have been processed using the GAMIT software [King and Bock, 1993] and GLOBK, a network adjustment Kalman filter program [Herring, 1992]. As the dataset for this thesis is a subset of a larger Indonesian project, the data processing has been a cooperative effort. The majority of the 1989 and 1990 data was processed at SIO by Puntodewo [1994]. Global orbit solutions from August 1991 processed at SIO [Bock et al., [1993b]; Fang et al., [1992]] have been included to provide better quality GPS orbits. Global solutions for the GIG'91 data were generously provided by Bob King, DaNan Dong (MIT) and Peter Morgan (UC), and Antarctic solutions for January 1991 and January 1992 as processed at UC were incorporated into the final solutions. I processed the remaining Indonesian data (part of 1989 dataset, regional GIG'91 stations, 1991, 1992, January 1993 and August 1993 datasets) at UNSW. The processing was performed as a two step procedure - firstly as daily GAMIT solutions, and secondly the combining of daily solutions in GLOBK to give an overall solution. Both steps will now be explained in detail.

3.3.1 GAMIT solutions

The GPS phase observations were analysed in single day least squares solutions (0000-2400 UT). The parameters estimated in the GAMIT solutions are all station coordinates, 9 initial conditions of each satellite state vector (X, Y, Z cartesian position, three cartesian velocities, one solar radiation pressure parameter and a Y and Z bias), a residual tropospheric delay parameter at each station and phase ambiguities (e.g., Dong and Bock, [1989]; Feigl et al., [1993]). It is possible to estimate the parameters in four different ways: applying loose or tight constraints to parameters, and either estimating the initial phase ambiguities as real values or resolving the estimates to integers. Loose constraints are typically 100 m for station coordinates and 5000 m for satellite initial conditions. A simple first order earth tide model with constant Love and Shida numbers was used (ie. no K_1 term, ocean tide or pole tide models).

The phase data must be preprocessed to remove any cycle slips or outliers. Cycle slips are integral jumps or steps in the phase data, usually caused by a loss of lock of the phase tracking loop within the receiver. There are a number of different algorithms which have been developed to efficiently remove cycle slips (see e.g. Blewitt, [1990]). In practice, the process of cleaning the data and estimating the orbit is an iterative one. If a precise

orbit is unavailable then the coordinates of well known stations are generally tightly constrained to assist in accurately estimating the orbit. The "unclean" data of stations are checked for cycle slips against the data of stations which are known to produce reliable and mostly "clean" data. When the data is free of cycle slips the solution is rerun and the "loosely" constrained solution is produced.

The GAMIT solutions produce an output file for each day which contains the loosely constrained least squares estimates for the station coordinates, satellite parameters, ambiguities and the corresponding full variance-covariance matrix. Owing to the intercontinental distance of the baselines, no attempt was made to resolve the phase ambiguities to integer values. In the second stage of the data processing these solution files are entered as "quasi-observations" into the Kalman filter (GLOBK), and a combined solution for all the GPS daily solutions can be estimated.

Phase measurements can be differenced between two receivers and two satellites to create a double differenced phase observable. This reduces the adverse effects of drifts in both receiver and satellite clocks, and is the fundamental observable in the GAMIT weighted least squares solution. The observation equation for a double differenced phase is:

$$\phi_{1,2}^{i,j} = (\phi_1^i - \phi_2^i) - (\phi_1^j - \phi_2^j) + \Delta N + \Delta T + \Delta C + noise \qquad (3.3)$$

where subscripts *1,2* refer to stations *1* and *2*
superscripts *i,j* refer to satellites *i* and *j*
ΔT = residual difference of propagation delay
ΔN = residual difference of ambiguities of the four one way ambiguities
ΔC = residual clock errors. This includes both receiver and satellite clock errors
noise = random and unmodelled noise contained in the measurements

At the time of processing the data for this project, the GAMIT software only allowed a single residual tropospheric delay parameter per site per day to be estimated, and there was no facility for antenna phase centre variation modelling or ocean tide loading effects (see section 3.4). The software has since been further developed to incorporate some of these features (Bob King, pers. comm., 1994). However, the software developments occurred too late for all of the data included in this thesis to be reprocessed and reanalysed.

The vast majority of the observation sessions for this project were between 18 and 24 hours in duration. It was decided that the data would be processed in daily solutions. The Indonesian campaigns of 1989-1991 were processed incorporating the regional data with the global fiducial station data to produce a single global solution. When the number of fiducial stations increased, it became logistically difficult to process all the fiducial and regional data in a single solution. As a result, the regional data was processed independently of the global data, with the nearest global fiducial station data being added to the regional data in order to provide a link between the two solutions. The fiducial network for each campaign is shown in Figure 3.4 and the processing of each campaign is described briefly below.

1989

The processing of the 1989 data was relatively straightforward - the DoD had not deliberately degraded the system at this time. The Indonesian stations were incorporated into the available global fiducial network, and daily least squares solutions were computed. There were only 8 satellites available in 1989, and just 10 fiducial stations. Figure 3.4a clearly shows how limited the fiducial tracking data was in the Indonesian region, with only one fiducial station (AUSA) in the Southern hemisphere.

There was data available from CAVE, observed as part of the 1989 Asia-Pacific Experiment (APEX) [CSTG Bulletin, 1989] which was incorporated in the solutions, overlapping with the BAKO-XMAS survey on the final four of nine days observed. Puntodewo [1994] had originally excluded this station from the 1989 processing but I incorporated it to add regional strength to the solutions. The weak solutions of the 1989 data could be improved by constraining the CAVE coordinates, provided accurate coordinates of this station could be determined. CAVE was reobserved for four days during the 1992 and 1993 campaigns, and I estimated coordinates of the station from these observations. These coordinates were back rotated to 1989 using a NNR NUVEL-1A velocity estimate for CAVE and then constrained in the solutions of the 1989 data.

1990

The data of the 1990 campaign was processed at SIO and has been documented by Puntodewo [1994]. The major problems associated with this data were due to the fact that Selective Availability (SA) was operating, and under SA conditions a mixture of Trimble 4000SST, Rogue SNR-8 and TI4100 receivers created timing difficulties. The

TI4100 receivers observed 92 milliseconds before the GPS second whereas the other receivers were observing on the GPS second (plus a drift of the receiver internal oscillator away from GPS time). With the satellite clocks being dithered, the difference in simultaneity of the phase measurements was significant, and the TI4100 data could not be combined with the other data. The global fiducial data was cleaned of cycle slips and then used to estimate the satellite clock parameters (using a program written by Kurt Feigl based on the theory described in Feigl et al. [1991]). Tight constraints were then applied to fiducial stations in order to compute a global orbit. The regional network of stations was broken into smaller sub-networks so that simultaneous observations were grouped together. This helped to reduce the effects of SA (see Puntodewo [1994] for a full explanation). These multiple solutions were later combined in the Kalman filter, GLOBK. The fiducial network is shown in Figure 3.4b

GIG'91

The GIG'91 Rogue SNR-8 data was initially processed at Massachusetts Institute of Technology (MIT) using the GAMIT software but by a slightly different method. Instead of solving for a daily set of state vectors for the satellites, the data was processed using weekly state vectors for each satellite and then daily orbits were stochastically estimated in the Kalman filter. This essentially allowed daily variation of the orbits about a common initial condition. The fact that all the daily orbital estimations are related to the same state vectors adds strength to each of the daily solutions. However, stochastic and deterministic orbital solutions cannot be combined in GLOBK. As all the Indonesian data had been processed using deterministic satellite orbits, I decided to reprocess the existing GIG'91 solutions into daily orbital solutions.

I processed the regional data observed during the GIG'91 period in daily solutions, incorporating the nearby Rogue stations to provide a connection between the regional and global solutions. The regional and global solutions could then be combined in the Kalman filter stage of the processing. This is essentially the processing strategy used by many people (see e.g. Feigl et al., [1993]; Bock et al., [1993b]; Puntodewo et al., [1994]; Burc Oral, [1994]) to pass information from global orbital solutions to regional GPS networks. The global and regional stations incorporated into the GIG'91 processing are shown in Figure 3.4c

1991

The 1991 Indonesian campaign spanned days 160 - 186 of 1991 with the BAKO-XMAS baseline being observed on days 170 - 181. The global fiducial network that operated during the GIG'91 campaign was not fully available and so the processing was performed by combining the Indonesian data with the available global tracking data in the GAMIT solution. Of the 12 days observed on the baseline, there were 5 days (170-174) where the number of stations available to form a global fiducial network was quite poor (see Figure 3.8). As such, I only used days 175-181 in the final solutions (Figure 3.4d). The effects of the additional fiducial tracking data was considerable and is discussed in section 3.4.5.

1992 and subsequent data

With the introduction of the IGS in June 1992, there was once again an excellent global tracking network in operation. The 1992 Indonesian data (days of year 207-233) was processed using the global and regional solution approach, with the nearest global tracking stations being incorporated into the regional solutions. The duplication of the data from these stations has a minimal effect when the two solutions are combined in GLOBK as it comprises less than 10% of the total double differences in the solutions. Burc Oral [1994] investigated the feasibility of a GPS data analysis where separate regional and global GAMIT solutions were combined in GLOBK. The investigation showed that daily repeatabilities from combination type analyses (ie. combining regional and global solutions) were similar to those of a simultaneous analysis of all the data. For a network with baseline lengths of the order of 100 km, the number of global tracking stations incorporated into the regional analysis had little effect on the repeatability of the network solutions, whilst networks with longer baselines required several sites to be common in the regional and global solutions in order to obtain results similar to the simultaneous approach. This provides justification for splitting the data into regional and global solutions which are then combined in GLOBK. From July 1992 onwards, the regional GPS data has been processed with this regional/global strategy. At least five stations are common to both solutions to provide a tie between them.

During the Indonesian survey of 1992, Anti Spoofing (AS) was turned on by the DoD for the first time on the majority of satellites. A total of 9 of the 27 days observed were affected by AS. The firmware of many receivers was not capable of operating under AS at the time and many of the fiducial stations failed to record useful data. As such, the global orbit available from the processing centres for these days was of an inferior quality to the non AS days, with some centres simply providing broadcast orbits for the satellites

affected by AS. It was decided to ignore the AS days as the benefits of processing regional data without a high quality global orbit was questionable.

Sunda Strait Solutions

The Sunda Strait stations were observed in 1992 and again in 1993 (see Figure 3.1). In 1992, the stations were not all observed simultaneously and, due to lost data because of AS, there are only two and three days of useful observations at KRUI and CINA, respectively. There is insufficient data to compute a reliable daily repeatability of these measurements so the quality of the solutions must be inferred from surrounding stations. For the stations not observed simultaneously, baseline lengths must be inferred from coordinate solutions in either the GAMIT or GLOBK solutions.

The 1993 Sunda Strait survey again suffers from non simultaneous observations at key stations. The receiver at BAKO did not function during the survey, therefore the principal Indonesian station - common to all other stations in 1992 - was not available in 1993. The stations KRUI, DEMP, BPIL and CINA were observed with Trimble SSE receivers. The normalised root mean squared (nrms) of the GAMIT solutions increased from around 0.35 to 0.55-0.6 when the SSE data was added into the regional solution (acceptable levels are 0.3 - 0.4). To date, it is not fully understood why this occurs. I suspect that there may have been a hardware or firmware problem in the Trimble SSE receivers used in the Sunda Strait 1993 survey.

3.3.2 GLOBK solutions

The process of Kalman filtering was developed by Rudolph Kalman in 1960 and has since been utilised as a processing strategy (e.g. Gelb, [1974]). It is an estimation process where the initial state vectors of a number of parameters are predicted forward to estimate the value of the parameters at the next epoch. Herring et al., [1991a] describe in detail the mathematical formulation of GLOBK. Here, I will show only the principal formulas of the filter (extracted from Herring et al., [1991a]):

The GPS observables can be related to the parameters to be estimated by:

$$y_t = A_t x_t + v_t \tag{3.4}$$

where subscript t refers to epoch t, y is the vector of differences between the observations and the value as calculated from a priori information, x is the vector of

adjustments to the a priori values of the parameters, V is a vector of residuals (noise) and A is a matrix of partial derivatives relating changes in parameters to changes in the observables. The state transition equation provides the link between epoch t and epoch $t+1$:

$$x_{t+1} = S_t x_t + w_t \tag{3.5}$$

where S is the state transition matrix at time t and W is a vector containing information of random perturbations affecting the state between t and $t+1$ (ie. W represents the stochastic nature of the transition). S is the matrix which predicts the state (or the value) of a parameter at time t forward to time $t+1$.

The filter estimation is sequential. The filter moves from epoch t to epoch $t+1$ in a number of steps. Firstly, the state at t must be predicted forward to $t+1$:

$$x_{t+1}^{t} = S_t x_t^{t} \tag{3.6}$$

$$C_{t+1}^{t} = S_t C_t^{t} S_t^{\mathrm{T}} + W_t \tag{3.7}$$

where C_{t+1}^{t} is the covariance matrix of the parameters at time $t+1$, incorporating all information up to and including time t; W_t is defined to be $w_t w_t^{T}$. Next, the parameter estimates and covariance matrix are updated as follows:

$$x_{t+1}^{t+1} = x_{t+1}^{t} + K(y_{t+1} - A_{t+1} x_{t+1}^{t}) \tag{3.8}$$

$$C_{t+1}^{t+1} = C_{t+1}^{t} - K A_{t+1} C_{t+1}^{t} \tag{3.9}$$

where K, the Kalman Gain, is:

$$K = C_{t+1}^{t} A_{t+1}^{\mathrm{T}} (V_{t+1} + A_{t+1} C_{t+1}^{t} A_{t+1}^{\mathrm{T}})^{-1} \tag{3.10}$$

and V_t is defined to be $v_t v_t^{T}$. Equations 3.6 to 3.10 define the whole sequence of operations for processing the data. Once epoch $t+1$ has been updated, the filter continues using epochs $t+1$ and $t+2$ and so on until the last epoch is reached.

The parameters that can be estimated in GLOBK are cartesian coordinates and velocities of stations, 9 parameters of the satellite state vectors and Earth orientation parameters (UT1-UTC and polar motion). All of these parameters can be estimated either stochastically or deterministically. Stochastic estimation of a parameter allows daily variation of the value of the parameter (represented in the W_t matrix), whereas a deterministic estimation is essentially an estimate of a weighted mean value with no daily variation (ie. W_t is zero). A noise function needs to be assigned to the parameter functions (represented in the W matrix) if the parameters are to be estimated stochastically. In the case of GLOBK, it is assumed that the parameters behave according to a random walk process with the stochastic noise based on white noise theory [Herring, 1992].

The behaviour of the parameters are represented in the transitional S matrix by an affine transformation. The transformation parameters are estimated from the first two epochs where the station parameters occur, and are refined and improved with further occurrences. The predicted estimates of x^t_{t+1} are combined with the observation residuals (y_{t+1}) at that epoch to improve and update the S matrix. Figure 3.5 shows a basic flow chart of the filtering process employed in GLOBK.

It is possible to perform two types of solutions with GLOBK to analyse the GPS data - forward and back solutions. A forward solution is essentially the final estimate of the parameters after the last new data has been incorporated into the filter. This applies for all parameters whether they have been estimated stochastically or deterministically. In the case of the back filter solution, the parameter estimates and corresponding covariance matrices at each epoch from the forward run are smoothed going backwards in time. The estimates of parameters going forward in time incorporate all available information of the parameters prior to that epoch. Back smoothing allows all information from subsequent epochs to also be combined into the estimate of the parameters at a particular epoch. In other words, the back filter estimate at a single epoch includes the information of all other epochs whereas a forward estimate only includes information of epochs which have preceded it in time. This results in a back filter estimate at any epoch being more precise and more accurate than a forward estimate for the same epoch. Back filter solutions provide a means of obtaining daily estimates of stochastic parameters (e.g. station coordinates, Earth orientation parameters), which can be used to determine short and long term precisions of the filter solutions.

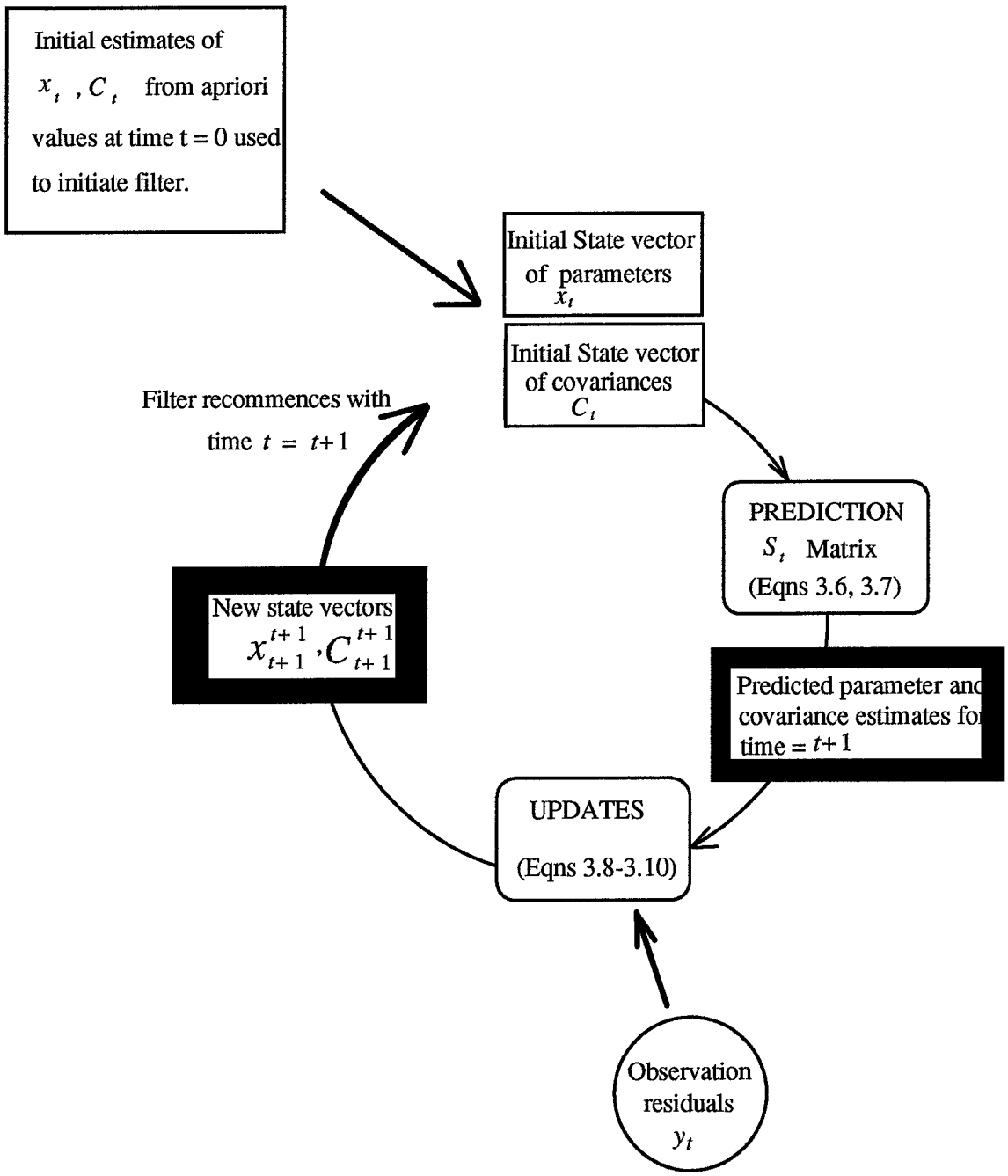

Figure 3.5 Flow chart of the filtering process in GLOBK. Diagram shows the cyclic nature of the filtering. The parameter state vector and covariance matrix at t are firstly predicted forward to t+1 using the transition matrix. The estimated state vector and covariance matrix for t+1 is then merged with the observations at t+1 and updated. The updated state vector and covariance matrix are then used as the starting values for the next epoch. Equation numbers at the relevant stages of the process are shown in parentheses, with the results of each step shown in black boxes. Thick arrows indicate the addition of new data to the filter.

The GAMIT solution files are used as pseudo observations in the Kalman filter. A priori information is required for both the satellite and station positions. The filter takes the initial estimate of the parameters and, combining both the pseudo observations of range from stations to satellites and the a priori weights, makes an updated estimate of the parameters. In the case of station coordinates, this estimate is predicted forward using the transitional matrix to create a priori information for the next set of pseudo observations. For satellite positions, the a priori values are the initial state vectors used in the GAMIT solution for that day. The quality of the estimates of the Kalman filter can be assessed by the χ^2 value resulting from the filtering of each file. As each new set of observations is added to the filter, the χ^2 value is computed as follows:-

$$\chi^2 = \frac{1}{f} (V^T * \text{cov} * V) \tag{3.11}$$

where V = vector of observed - predicted residuals scaled by the Kalman gain

cov = covariance matrix of the parameters at that epoch

f = degrees of freedom

The χ^2 value is a measure of how consistently the data fits together. Therefore, the smaller the amount of data contained in a solution file - such as the number of stations and satellites - the easier such data can be fitted and the lower will be the χ^2 value for that file. According to Herring [1992], a χ^2 value less than 10 indicates that the solution is acceptable. This value has been adopted based on GPS processing experience by the MIT GPS group, using GPS data prior to the IGS global fiducial tracking network. Global orbits produced by SIO show χ^2 values typically less than 5. From experience gained in the processing of this project, the χ^2 value is dependent on the amount of data, the distribution of stations comprising the dataset and the number of files observed on the same day that are combined in the filter. I think this value of less than 10 is too small as χ^2 values for data observed after 1992 are typically between 5 and 15. Similar values have been obtained at UC for similar analyses of GPS data in the Australian region [P. Morgan, pers. comm., 1994].

When any global GPS solutions are filtered, the χ^2 values should be below 10 if the solution is acceptable. However, if a regional file on the same day is added to the filter, the χ^2 value for the second file filtered will always be much larger than for the first file, and often above 10. This is caused by differences in the estimates of the orbital elements in the global and regional solutions which are being forced to a common value. This causes the data in the second file to differ from the a priori information more than the

first file filtered on that day. It does not matter whether the global or regional file is filtered first. The size of the χ^2 value for the second file is therefore variable as it depends to a large extent on how much the estimates of the regional and global orbits differ.

Theoretically, the χ^2 values should be one, providing the constraints on the parameters are correctly applied and all data is consistent. The fact that the χ^2 values are typically higher than one suggests that either the a priori constraints on some parameters have overestimated the precisions of the parameters or the regional and global data are inconsistent. A solution with 10 m a priori constraints on all station coordinates yields similar χ^2 values, indicating that the large χ^2 values are not caused by the incorrect levels of constraints on station coordinates. However, the GPS solutions do not have the internal stability to allow for a free adjustment hence constraints must be imposed. This introduces tension in the solutions (mainly in the orbits as indicated above) when regional and global solutions are combined and, as a result, the χ^2 values are higher than 1. Equation 3.11 shows that the χ^2 values are determined from the covariance matrix and the difference between predicted and observed parameter values. Providing that the larger χ^2 values are due solely to a regional/global orbit mismatch, there will not be any adverse effects on the stability of the filter as the orbital parameters for the next day are estimated independently of the previous day.

3.3.3 Constraints

As in any estimation process, the a priori constraints imposed on the parameters are fundamental in the determination of the GLOBK solution. This issue is of great importance in this project as most of the earlier solutions are quite weak in a global sense. In addition, the estimation of station velocities is particularly sensitive to the a priori weighting of the global velocity field. The constraining or fixing of station coordinates and velocities significantly influences the terrestrial reference frame of the GPS results from the Kalman filter (see Chapter 4).

3.3.3.1 Cartesian Coordinates

It is important that any stations which are tightly constrained in the filter solution have been coordinated in a consistent system (in this thesis "tight" constraints are considered to be 1 mm in a horizontal direction, 10 mm in the vertical). In the 1980s the

International Earth Rotation Service (IERS) defined an International Terrestrial Reference Frame (ITRF) by adjusting solution coordinates from a number of processing centres. The solutions were derived from GPS, SLR and VLBI datasets. There have been many readjustments of the ITRF, the most recent being known as ITRF 92 [Boucher et al., 1993]. A core of thirteen GPS stations co-located with either SLR or VLBI stations have been adopted by IGS as being a consistent set of coordinates which form the basis of the ITRF 92 terrestrial reference frame. Table 3.2 lists the core IGS stations which are also shown in Figure 3.3.

Table 3.2 Core IGS stations and station codes used in this analysis. The plate upon which the station is located is shown, and other space techniques co-located at the site are listed. Plate abbreviations are North American (noam), South American (soam), Australian (aus), Eurasian (eura), Pacific (pac) and African (afr).

STATION	CODE[1]	PLATE	CO-LOCATION
Algonquin	ALGO	noam	VLBI
Goldstone	DS10	noam	VLBI, SLR
Tidbinbilla	DS42	aus	VLBI, SLR
Madrid	DS60	eura	VLBI
Fairbanks	FAIR	naom	VLBI
Hartebeesthoek	HART	afr	VLBI
Kokee Park	KOKR	pac	VLBI, SLR
Kootwijk	KOSG	eura	SLR
Santiago	SANT	soam	VLBI, SLR
Tromso	TROM	eura	VLBI
Wettzell	WTZ1	eura	VLBI, SLR
Yaragadee	YAR1	aus	SLR
Yellowknife	YELL	noam	VLBI

Constraining these stations in the Kalman filter provides an excellent definition of a reference frame for the GPS solutions containing all these stations (1992 onwards). For the solutions prior to 1992 when only a subset of these core stations were observing, it is more difficult to define the same reference frame. In the 1989 solutions, only the stations of YELL (Canada) and TROM (Norway) were observed from the set of core stations.

[1] Some station codes shown in the table are not official IGS codes:- DS10 ↔ GOLD; DS42 ↔ TIDB; DS60 ↔ MADR; KOKR ↔ KOKB; WTZ1 ↔ WETT.

None of the core stations are included in the 1990 solutions and in 1991 only YELL, DS10 (California, USA), DS60 (Spain) and DS40 (an eccentric mark to DS42, Australia) were included. Thus, the number of constrained stations in these solutions is significantly less, and so the reference frame is more weakly defined. This can introduce biases in the solutions. This issue is investigated in detail in section 4.4.1.1.

3.3.3.2 Eccentric Stations

Continuity of a reference frame defined by fixing or tightly constraining coordinates is best obtained by using a consistent and unchanging set of stations. Unfortunately, history shows that "permanent" tracking stations may not be so permanent as the stations are often moved to new locations at the same site. To apply the same constraints without distorting the reference frame definition by introducing a coordinate error at the site, the coordinates of the "old" station must be transferred to the "new" station. This results in the need for ties between the old and new stations - and sometimes simultaneous GPS observations have not been made between the stations. In the dataset of this thesis, there have been tracking stations moved at the sites of Hawaii (KOKR and KOKE), Canberra (DS40, DS41 and DS42) and Mawson (MAW1 and MAWS). Transferring the coordinates of YAR1 to CAVE - two stations about 300 km apart - can be considered as a similar situation. I will discuss below how I have transferred the coordinates between "eccentric" stations.

KOKE

There was a station on Hawaii, KOKE, located about 50 m from the core IGS GPS station, KOKR, which was observed in all solutions from 1989 to 1991. It was replaced by the KOKR station in 1992. Data between the two stations was observed simultaneously during the GIG'91 campaign which allowed me to transfer the coordinates of KOKR to the KOKE station. The coordinate errors introduced in this transfer are less than 10 mm - the short term precisions of the baseline components are 1.9 mm, 1.8 mm and 8.6 mm for N, E and U, respectively. It has been assumed that the coordinates of KOKE are well known and are consistent with the other core IGS stations, hence I consider the station KOKE to be a core station. This is particularly important, as either KOKE or KOKR have been included in every solution of this analysis, thus providing a consistent core station in all solutions. Figure 3.6 shows the daily baseline components resulting from a GLOBK back solution of the GIG'91 data. The statistics shown in the figure are as follows: wmean is the weighted mean estimate,

nrms is the normalised root mean squared of the weighted mean, wrms is the weighted root mean square about the mean.

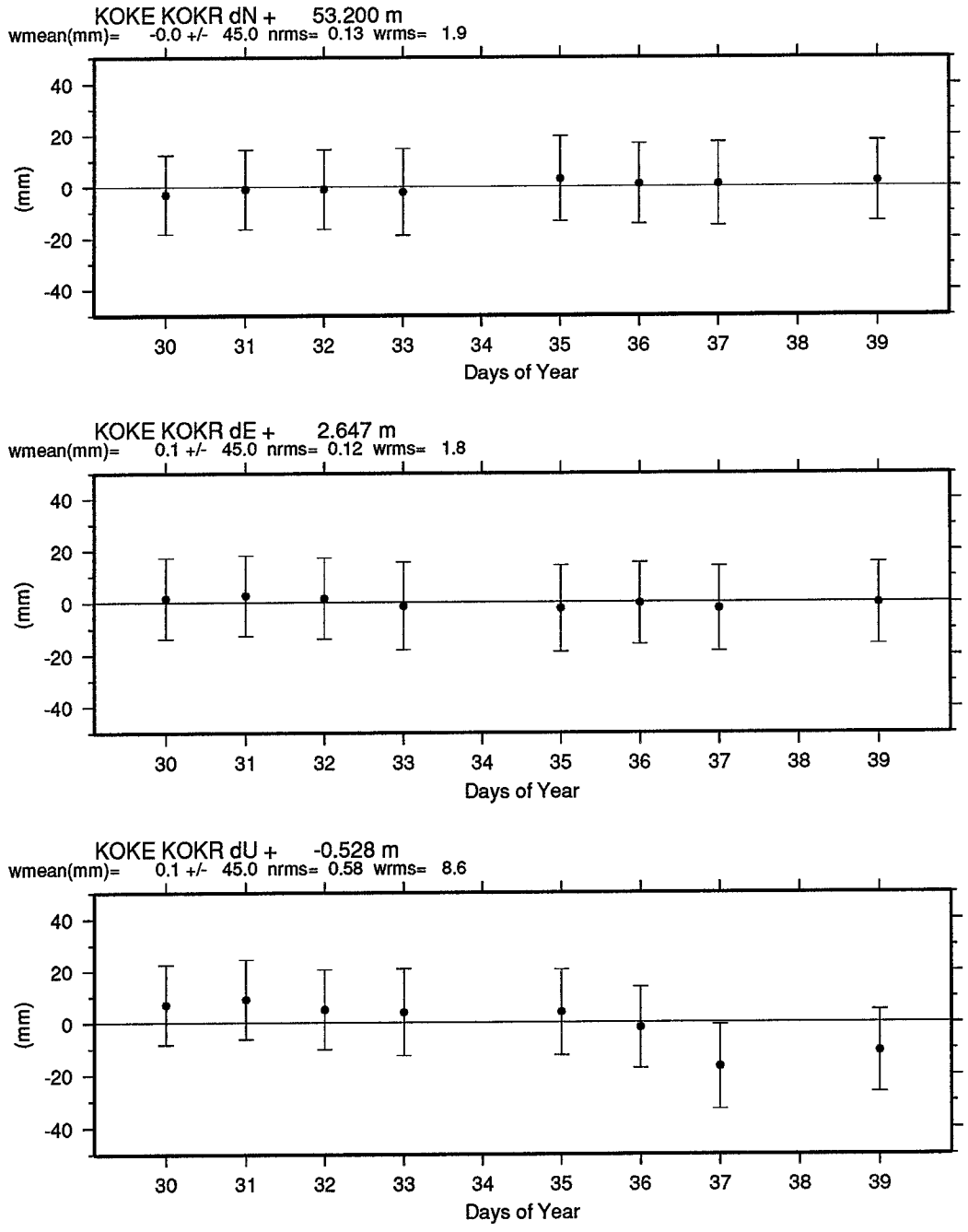

Figure 3.6 Daily solutions of baseline components between KOKE and KOKR during GIG'91.

DS40

The Deep Space Network station at Tidbinbilla, Canberra (DS40) was relocated in February 1992 to a temporary mark (DS41) and finally located at its current position (DS42) on 12th May 1992. No simultaneous GPS observations were made between

marks. DS42 is a core IGS station and hence is tightly constrained in my solutions. To transfer the coordinates of DS42 to DS40, I adopted the dX, dY, dZ between the marks computed in a three dimensional adjustment by AUSLIG in April 1994. There was a height error of 0.13 m made in the initial local survey connecting the final GPS mark (DS42) to the VLBI antenna. This was only detected in April 1994, hence any coordinate adjustments which may have used a local tie between the VLBI and GPS marks at Tidbinbilla (e.g ITRF 92) will be in error by 0.13 m in the local vertical component. DS40 is not constrained as tightly as the core IGS stations.

MAWS

Sporadic GPS observations have been made at Mawson (MAWS), an Australian Antarctic base, commencing in 1990. I have incorporated data from MAWS in the regional GIG'91 solutions and MAWS data observed in January 1992 has been processed at UC. In January 1992, a new pillar (MAW1) was constructed at Mawson for the installation of a permanently operational receiver. In January 1993, a receiver observed at MAW1 and in December 1993 AUSLIG installed a rogue SNR-8000 at MAW1. This receiver is still operational. Simultaneous GPS observations were made between MAWS and MAW1 on 15th and 16th February 1992. There were very few global tracking stations operating during these two days and so the "absolute" accuracy of the coordinates for MAWS and MAW1 is systematically biased. However, since the two stations are only about 200 m apart, the relative vector between the stations will be free of any bias. I computed the relative cartesian vector between MAWS and MAW1 - the difference in the vector from the two days was 0 mm, 2 mm and 25 mm in X, Y and Z, respectively. Table 3.3 shows the relative cartesian vector between MAWS and MAW1.

CAVE

Coordinates were transferred from YAR1 to CAVE, both located on the West coast of Western Australia. The stations are about 300 km apart, and have been simultaneously observed for four days in both 1992 and 1993. I determined the coordinates of CAVE from these eight days. Applying tighter constraints to this station forces information of the coordinates of YAR1 into the 1989 solution where CAVE was observed without YAR1. Figure 3.7 shows the daily baseline components resulting from a GLOBK back solution of the 1992 and 1993 observations of this baseline. Here the short term precisions are 10.1 mm, 10.2 mm and 12.8 mm for N, E and U, respectively. As the baseline between YAR1 and CAVE is about 300 km, there is the possibility that slight

errors have been introduced in the coordinates of CAVE, so the constraints applied to CAVE are not as tight as those applied to the core IGS stations.

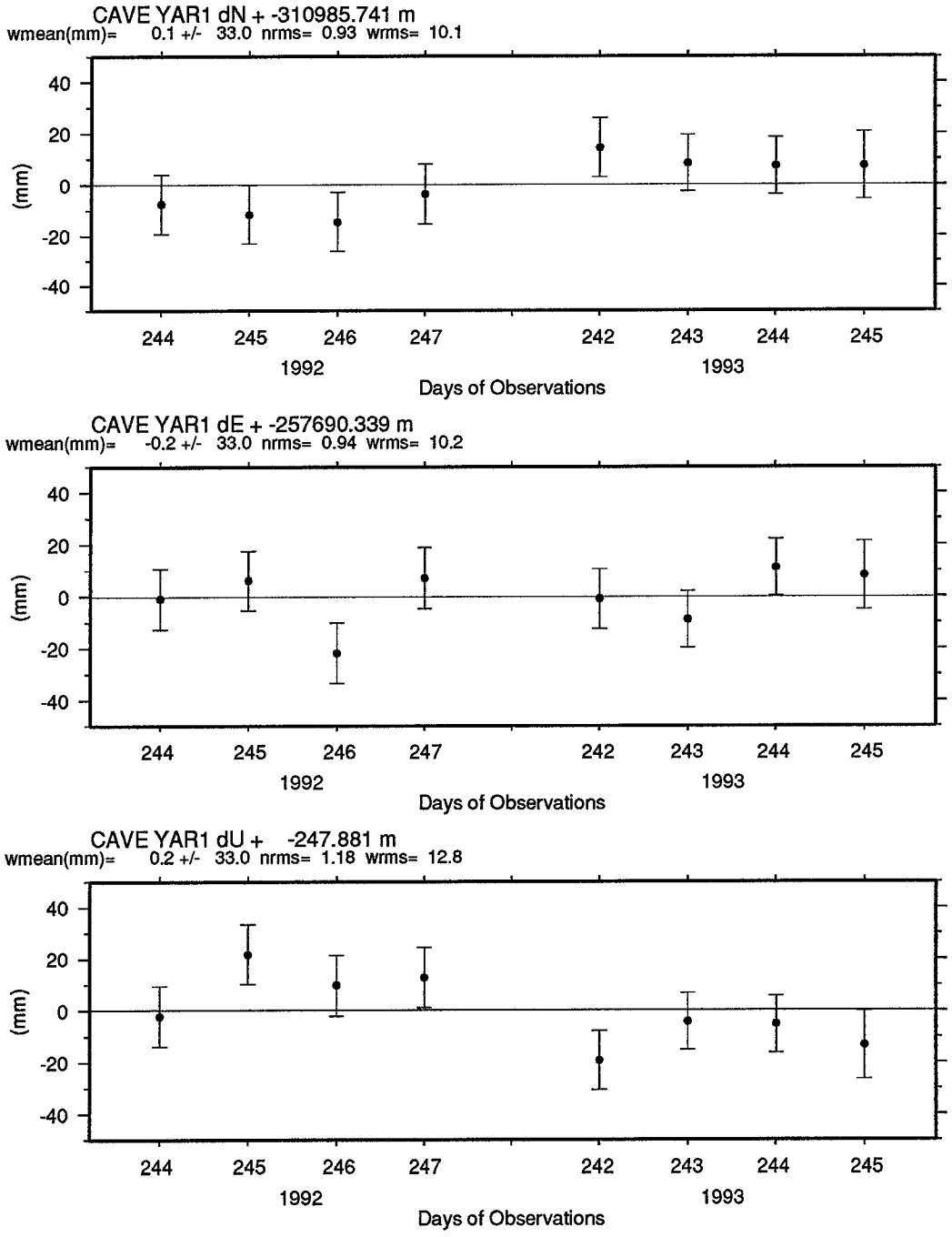

Figure 3.7 Daily solutions of baseline components between CAVE and YAR1: observed in 1992 on days of year 244-247, 1993 on days of year 242-245.

Table 3.3 shows the cartesian components of the vector between the principal and eccentric stations for the stations discussed above:

Table 3.3 Relative cartesian components of vectors between principal and eccentric stations. Values in table are to be added to coordinates of principal mark in order to coordinate eccentric marks.

BASELINE	BASELINE COMPONENTS		
	dX (m)	dY (m)	dZ (m)
KOKR-KOKE	20.082	4.160	48.829
DS42-DS40[2]	8.072	-194.860	-182.463
MAW1-MAWS	-40.175	259.867	100.097
YAR1-CAVE	13 634.816	-167 762.998	-266 856.350

3.3.3.3 Cartesian Velocities

According to the theory of plate tectonics, the Earth's plates are moving relative to some stationary terrestrial reference frame. The ramifications of this to geodesy are that not only must the terrestrial coordinates of tracking stations be determined, but their velocities relative to the terrestrial reference frame must be considered. Fixing station velocities at incorrect values will introduce errors into the reference frame definition which will propagate through to the positions of all the stations. There are a number of ways to approach this problem, and examples of individual processing strategies have been discussed in Section 4.3. In calculating the ITRF 92, Boucher et al. [1993] adjusted the velocity solutions of a number of processing centres, and superimposed on these adjustments the NNR NUVEL-1 model. GPS solutions alone do not yet have the strength to solve implicitly for a global velocity field as the high quality global GPS dataset presently only spans 3 years. The ITRF 92 velocity field has been used by Genrich et al. [1994], Puntodewo et al. [1994] and Tregoning et al. [1994] in calculating results from the Indonesia experiments.

3.4 ERROR SOURCES

As explained in section 3.3.1, the GPS data were processed resulting in a least squares estimate of daily orbital parameters, site coordinates, residual tropospheric delay

[2] Connection values are prior to the discovery of the 0.13 m height error. That is, the connection shown is compatible with the processing of DS42 data in this analysis.

parameters and phase ambiguities. The solutions involve estimating many parameters, and many physical effects are contained in the phase data. These effects must be either modelled or estimated to remove biases. The accuracy of such procedures is dependent on the accuracy of the mathematical models used. Incomplete modelling of effects will result in incorrect estimates of parameters, and any unmodelled effects which may behave similarly to other parameters will corrupt the estimates of those parameters. In such situations, there is always the possibility of introducing errors by either estimating the wrong value of a nuisance parameter (such as an initial phase ambiguity, or atmospheric parameters) or erroneously assuming that a certain effect has been modelled perfectly (such as the ocean loading due to the Earth tides, or the force model of a satellite orbit). There is also the possibility that corrupted data - due to either multipathing, cycle slips or receiver hardware problems - may have been used in the solutions. Systematic centring errors can also be introduced in setting up of instruments which will affect the accuracy of a campaign solution rather than the precision of that particular campaign.

The errors in GPS processing can affect either the estimate of the horizontal position, vertical position or a combination of both. In particular, there are many error sources which may have affected the vertical component of the analysis of the Indonesian dataset. As a result, it was decided to concentrate the analysis on the horizontal component of the solutions. This chapter will look at some errors pertinent to this project, where possible identifying whether the horizontal or vertical component will be most affected by the error. Other common error sources in GPS (e.g. multipathing, propagation delays, orbital errors) have been dealt with extensively elsewhere (see e.g. Dixon, [1991]; Feigl et al., [1991]; Beutler, [1992]; Gurtner et al., [1989]).

3.4.1 Antenna Phase Centre Variations

Errors of up to 0.1 m have been detected in the vertical component of baselines when data from mixed antennas are combined. This was first noticed by scientists at the University of Berne and subsequent testing has shown that it is partly caused by phase centre variations within different antennas. When residual tropospheric delay parameters are estimated, variations in the location of the electrical phase centre of the antenna can exhibit characteristics similar to a tropospheric delay. This results in an erroneous estimate of the residual tropospheric delay thereby introducing a height error, but there is no significant error introduced to the horizontal components. Rocken [1992] showed that the effect can be greatly reduced by applying elevation dependent phase corrections to the observations. Phase centre variation within antennas becomes more critical when a mixture of antenna types are used in a campaign. Unfortunately, nearly all the

Indonesian surveys used a mixture of Rogue, Trimble, Ashtech, Minimac and Texas Instrument antennas and often stations have been occupied by a variety of receiver and antenna types. This will almost certainly degrade the vertical repeatability of the results but the horizontal components should remain relatively unaffected by this error.

To illustrate this effect I will describe one instance where two receivers were used to observe on the same station. At the Mt Pleasant Observatory in Hobart, CIGNET installed a Minimac 2816 AT receiver to act as a permanent GPS tracking site. In March 1993 this receiver was replaced by a Rogue SNR8000 receiver with a Dorne Margolin-T antenna. In subsequent global GPS solutions, I found that the local Up value for the site had changed from 49.03 m to 49.11 m - a difference of 0.08 m, whereas the local horizontal position had changed by less than 4 mm. Similar results have been computed by Peter Morgan at UC and Simon McClusky at MIT. No explanation for this difference has yet been found but it has led to further investigations into the phase centre modelling of Minimac antennas.

Prior to 1994, the GAMIT software did not have the facility to apply elevation dependent phase corrections. The software has been modified at MIT to incorporate this but at present the modifications have only been tested for Trimble and Rogue (chokering) antennas (Bob King, pers. comm., 1994). A survey was conducted in Hobart in March 1994 using Rogue, Trimble, Ashtech and Minimac receivers and corresponding antennas observed on precisely levelled pillars. The aim was to obtain a comprehensive dataset in order to test the phase centre models on Ashtech and Minimac antennas. The phase centres of the Ashtech LMXII antennas were found to drift randomly with time, rendering phase centre modelling completely ineffective (Simon McClusky, pers. comm., 1994). The data from the Minimac receivers were inconclusive (Simon McClusky, pers. comm., 1994), and hence phase centre modelling of Minimac antennas has not yet been tested in the GAMIT software.

I have not reprocessed the Indonesian dataset using phase centre modelling as it is currently not possible using GAMIT to model phase centre variations for a significant number of antennas used in the surveys. This project is more interested in horizontal crustal motion than in the vertical component and hence, at this stage of the project, little can be gained by refining the height estimates of a subset of the sites in some of the surveys. As mentioned in Section 1.2, geological results show vertical motions on Cocos and Christmas Islands to be less than 1 mm/year which is currently too small to be detected by GPS.

3.4.2 Data Decimation

Most of the GPS data was collected at a 30 second sampling rate. However, in the analysis this data was decimated and all data processing in GAMIT was performed using one minute data for 1989 observations and two minute data for all other observations. The decision to decimate the data was driven by computer hardware and time constraints. Puntodewo [1994] processed the campaigns of 1989 and 1990 at 1 and 2 minute sampling intervals, respectively. In addition, data files cleaned at 2 minute intervals were available from SIO as a by-product of the IGS global orbit computations [Bock et al., 1993b]. I decided to process the remainder of the project at a 2 minute sampling interval. Morgan et al. [1993] showed that, for crustal motion studies, the decimation of a 24 hour dataset from 30 second to 2 minute observations has an insignificant effect on the horizontal coordinate estimates, but significantly increases the formal errors and significantly changes the value of the vertical coordinate. Again, I decided that the bias possibly introduced into the vertical component was not a major concern as horizontal components are more critical to this project.

3.4.3 Receiver Clock Drifts

Brunner and Tregoning [1994] have shown that mixing of receivers may introduce position errors. Zero-baseline experiments showed that a combination of Trimble SST and SSE receivers operating with a single Trimble SST antenna yielded errors of up to 9 mm horizontally and 40 mm vertically. This type of error will be inherent in most of the Indonesian solutions, as nearly all campaigns have a mixture of receivers. In addition, most of the receivers used on the Indonesian sites and Cocos and Christmas Islands were either Ashtech Ld XII's or Trimble 4000 SST receivers. From experience, these receivers had low quality oscillators, which typically lost or gained about 1 ms every 20 minutes.

The errors introduced by receiver clock errors will affect the height results much more than it will the horizontal positions. This provides further justification for not analysing the height results of this project.

3.4.4 Horizontal Position Errors due to Height Errors

Blewitt [1993] showed that errors in the vertical ΔU at one end of a baseline cause an error in length $\Delta L = \Delta U * L/2R$ where L is the baseline length and R is the radius of the Earth. To limit the introduced error to less than 10 mm on a baseline of 1000 km, the

maximum allowable error in vertical is 0.13 m. This should be attainable with GPS. However, if the height errors are greater than this value, or the baseline lengths are greater, position errors will be introduced as a result. For the longer baselines in the Indonesian regional network (e.g. COCO-TAS1 ~ 5500 km) a 0.1 m height error will introduce a 0.04 m error in baseline length.

3.4.5 Fiducial Networks

As mentioned in Section 3.2, the fiducial networks available during the campaigns varied greatly which in turn introduces biases into the solutions. This is particularly prevalent during the 1989 to 1991 surveys.

To illustrate the effects of a changing fiducial network on the BAKO, XMAS solutions, I will look at days 170-181 of the 1991 Indonesian solutions. The first five days (170-174) suffer from a lack of fiducial tracking data (only 7 global stations) whilst the remaining days (175-181) incorporate global fiducial tracking data from 16 stations (see Fig. 3.8a and 3.8b). Figure 3.9 shows the GAMIT solution corrections to a priori coordinates and formal one sigma error bars for latitude, longitude and radius (spherical coordinates) for BAKO and XMAS. The same a priori coordinates were used in all solutions, with the core IGS stations (plus KOKE) constrained to 5 mm horizontally, 10 mm vertically - all other stations were constrained to 10 m in all components. It is clear that the error bars are significantly reduced when a more comprehensive fiducial network is incorporated in the solutions. The spread of the daily solutions decreases with an increase in the number of tracking stations and there is a systematic difference in the mean values of days 170-174 and 175-181. The daily pattern of the adjustments to each station are similar. This indicates that regional biases are being introduced which are affecting the coordinates of both stations equally. Thus, the configuration of the fiducial network is critical to the precision of the solutions and can introduce biases affecting the accuracy of the solutions. The possible introduction of biases from different fiducial networks was analysed in a simulation study of all Indonesian campaigns. The results of the study are given in section 4.4.1.1

3.4.6 Ocean Tide Loading

Tidal deformations affect a number of geophysical and geodetic measurements [Lambeck, 1988]. The solid earth tides are well understood and are commonly incorporated into GPS processing software. The ocean tides are more problematic as the amplitude and phase relations of the ocean loading effects can be very localised.

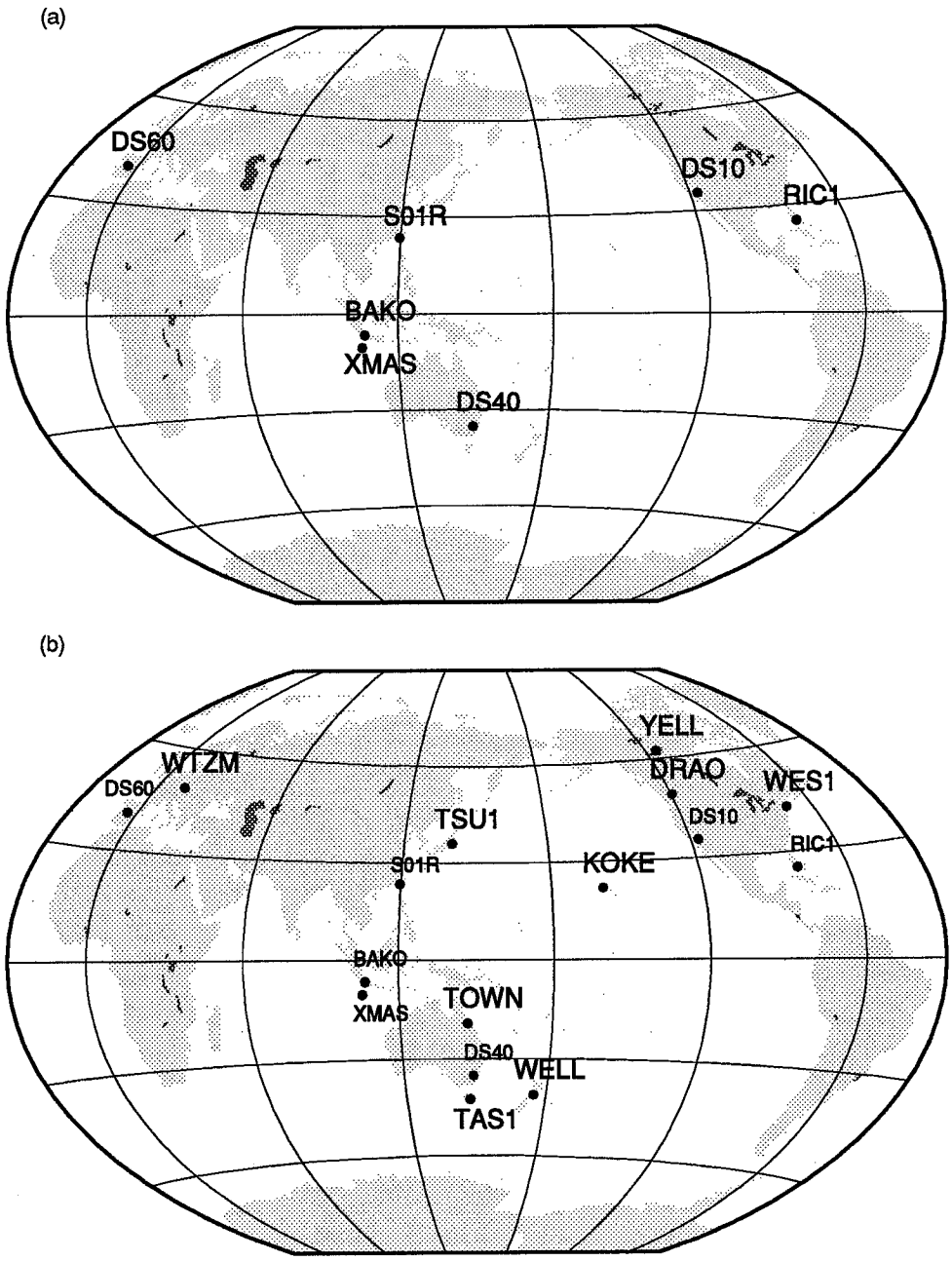

Figure 3.8 Fiducial tracking stations in the 1991 Indonesian campaign: (a) Days of year 170-174; (b) days of year 175-181. Additional fiducial stations in (b) are shown in larger font.

Schwiderski [1980] computed a global 1° x 1° ocean tide model in which the deformation of the solid Earth under the weight of the ocean tide can be computed. However, due to local effects and the resolution of the model, the ocean loads in particular regions may not be correctly modelled.

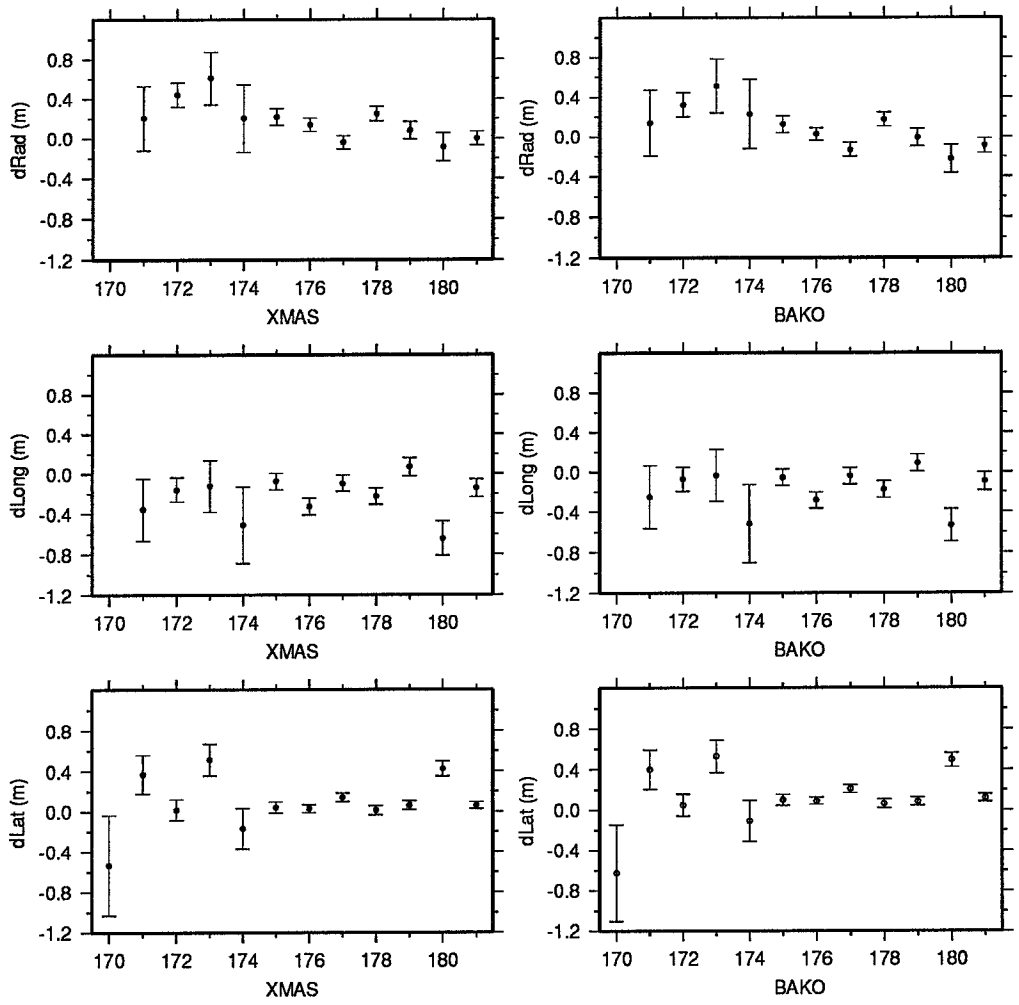

Figure 3.9 Daily corrections to a priori spherical coordinates of latitude, longitude and radius from GAMIT solutions of days 170-181, 1991 for BAKO and XMAS. Note that longitude and radius for day 170 are not plotted. Day 170 had only 3 fiducial tracking stations hence the solution is poorly constrained - the correction to a priori was 2.4±1.8 m and 1.8±0.8 m for longitude and radius, respectively.

Baker [1991] computed the ocean tide loading effects in the Australian region, using the global model of Schwiderski [1980] and a global elastic Earth model based on Green's function [Farrell, 1972]. For the M_2 tide, the maximum amplitude of vertical displacement occurs on the Northwest coast of Australia (30 mm). On the Southeast coast of Australia the amplitude is about 10-20 mm. There are also significant horizontal displacements which occur as a result of ocean loading. In the E-W direction, the displacement across Australia is about 5 mm, whilst the maximum N-S displacement of about 8 mm occurs on the Northwest coast of the continent [Baker, 1991].

The GAMIT software did not incorporate any ocean tide loading model until December 1993 (Peter Morgan, pers. comm, 1994). However, the displacements mentioned above are reduced to some extent by averaging the effect on GPS observations over a full cycle of the ocean loading (ie. 24 hours). The GPS observations from 1992 onwards span 24 hours but the 1989, 1990 and 1991 measurements span 7 hrs, 11 hrs and 19 hrs, respectively. Whilst it is recognised that this effect will introduce errors into the solutions, the effect on horizontal positions will probably be less than 5 mm (based on values from Baker [1991]).

CHAPTER 4

REFERENCE FRAMES

Reference frames are fundamental to the coordination of stations of large scale geodetic networks. The length of a vector between two points can be determined without a reference frame, but to obtain the orientation of vectors it is neccesary to define a reference frame in which all the points can be coordinated in a consistent manner. This section will look at the definition of two types of reference frames - Earth fixed (terrestrial) and space fixed (inertial). It will show how reference frames are defined in VBLI, SLR and GPS processing, how they are minimally constrained for each geodetic technique and how the problem of reference frame definition is generally approached operationally in the processing of geodetic data.

A three dimensional reference system can be defined by the location of an origin, a scale and the orientation of three axes defined by the unit vectors (1,0,0), (0,1,0) and (0,0,1). In order to make the system a useful and accessible entity, its basic structure and the actual coordinates of points within it must be linked. A number of parameters (e.g. star positions, station positions or pole coordinates) must be chosen to materialise the system and thus define a reference frame [Mueller, 1985]. Points can then be coordinated in the reference frame according to their location relative to the origin and the three axes. In the case of a terrestrial reference frame, the coordinates of points are tied to the surface of the Earth, whereas in an inertial frame the coordinates relate to the location of stellar objects or sources which are assumed to be fixed in space [Lambeck, 1988]. An inertial frame can also be defined dynamically. In this case the motion of a planet or satellite can be represented by Newton's equations of motion and relativistic effects, and all forces acting on the body are assumed to be modelled.

4.1 TYPES OF REFERENCE FRAMES

The following definitions of references frames have been adapted from Lambeck [1988]:

4.1.1 Inertial

In an inertial reference frame, the equations of motion of an object do not contain any rotational terms. Such a system is dynamic in nature and its realisation requires that all forces acting on the bodies are known and can be accurately modelled. Alternatively, the position of stars relative to each other, and the motion of the sun and planets relative to the stars can be used to coordinate these objects in an absolute frame (see e.g. Lambeck, [1988]). There are two types of inertial reference frames: a) stellar bodies and b) satellite systems.

In the case of a frame relating to stellar bodies the fundamental celestial plane of such an inertial frame is either the equatorial plane of the Earth or the ecliptic (the mean orbital plane of the Earth about the Sun). The line of intersection of these two planes is called the line of nodes. The principal axis is perpendicular to the fundamental plane. This is defined by the cross product of any two vectors in the fundamental plane. The vernal equinox, the point at which the Sun crosses the equatorial plane of the Earth in its apparent motion from South to North, is taken to be a secondary axis of the reference frame and the third axis completes a right handed system. The coordinates of bodies can be specified by the angular distance of the body from the fundamental plane (declination, δ) and the angle made on the fundamental plane between the vernal equinox and the projection of the plane containing the body and the pole of the fundamental plane (right ascension, RA) (Figure 4.1). The origin is implicitly defined once the stellar bodies are assigned coordinates.

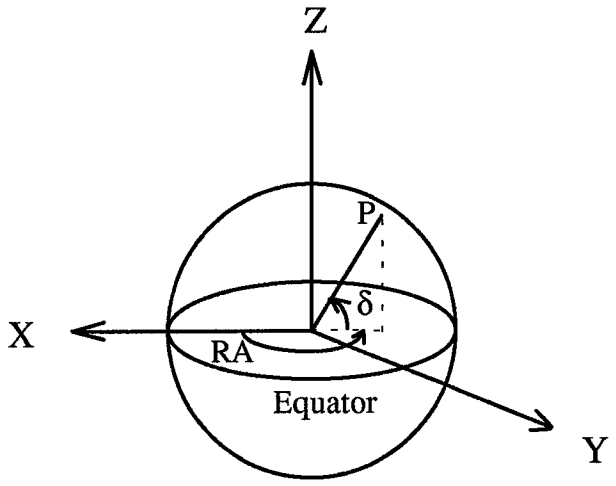

Figure 4.1 Right ascension (RA) and declination (δ) of a stellar body

The second type of inertial frame relates to a satellite system such as the moon or an artificial satellite orbiting the Earth. In this case, the defining planes are the orbit of the body and the equator of the Earth. The intersection of the two planes is the line of nodes and the secondary axis of the reference frame is again taken to be where the orbiting body appears to cross the equator from South to North. The position of an orbiting body can again be described by its declination and right ascension, although it is more common to describe its position and velocity in the terrestrial frame. Here the origin is the centre of mass of the Earth.

4.1.2 Terrestrial

A terrestrial reference frame can be thought of as one which is fixed to and moves with the Earth. The fundamental plane of the reference frame is the Equator and it is conventional to adopt the direction perpendicular to the equatorial plane, the mean position of the Earth's rotational axis, as the principal axis of the reference frame. The instantaneous location of the rotational axis of the Earth is related to the mean position by small rotational angles representing the motion of the pole with time (see Figure 4.2). By definition, the remaining two axes lie in the equatorial plane.

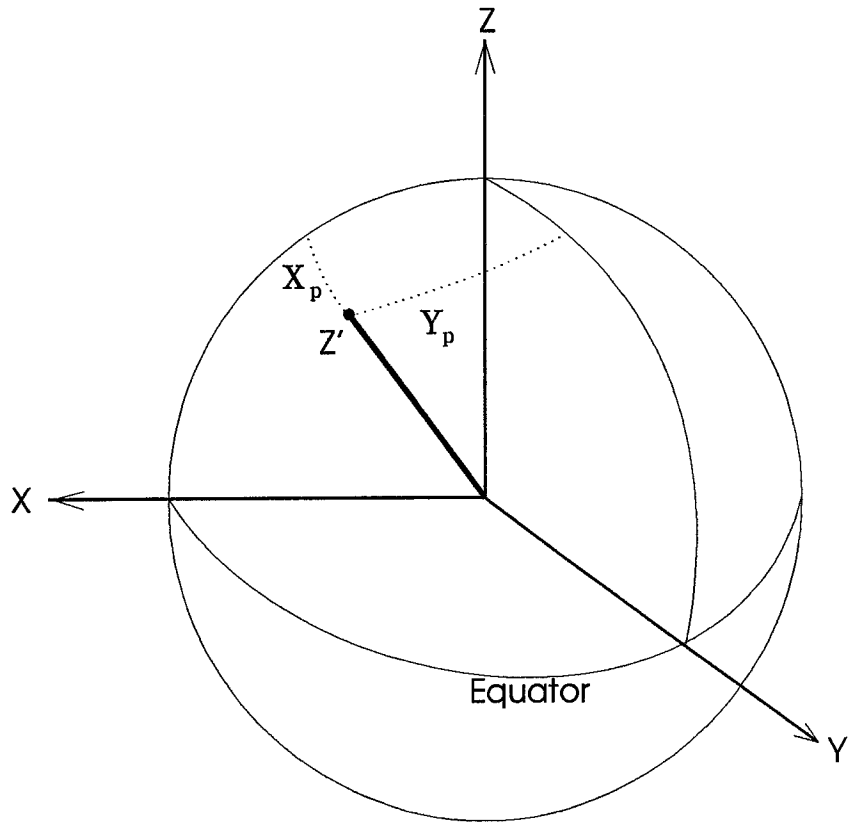

Figure 4.2 Instantaneous rotational axis, Z', is related to mean rotational axis, Z, by two rotations about the X and Y axes - X_p and Y_p.

The coordinates of objects are described by latitude, ϕ (analagous to δ), and longitude, λ (analagous to RA)(Figure 4.3). In a terrestrial system, the origin of longitude is arbitrarily defined. The origin of the reference frame is also arbitrary but can be chosen as the centre of mass of the Earth. This can be estimated by analysis of observations of satellites orbitting the Earth, or from observations of gravity. The scale of the reference frame must be defined, either by defining the velocity of light or by adopting values of GM where G is the gravitational constant and M is the mass of the Earth.

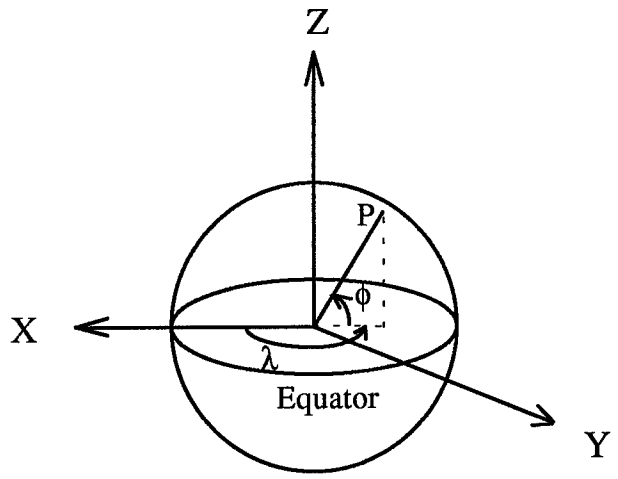

Figure 4.3 Spherical coordinates in a terrestrial reference frame.

The above will define a terrestrial reference frame. The realisation of this frame are the three dimensional coordinates of points on the surface of the Earth. Such coordinates must be derived from observations and hence the accuracy of the reference frame is subject to the accuracy of these observations. In addition, it is known that the crust of the Earth undergoes tectonic motion relative to the axes of a terrestrial reference frame as described above. Therefore, a terrestrial reference frame must be, in some respects, a dynamic system if the reference frame is to remain fixed to the Earth.

4.1.3 Relation of Terrestrial and Inertial Systems

Terrestrial and inertial coordinate systems are linked through the motion of the angular velocity vector of the Earth, which is represented in the terrestrial frame by polar motion and UT1 parameters. UT1 is a time system which is based on the actual daily rotation rate of the Earth. Terrestrial measurements are based on a mean time system (UTC) so it is neccesary to link UTC and UT1 in order to connect the terrestrial and inertial systems. This is achieved by measuring the daily rotation rate of the Earth using GPS, SLR or VLBI. There are two other effects which link the two systems - precession and nutation. Precession is the secular motion of the vernal equinox in the ecliptic, and

nutation is the periodic oscillations of the Earth in its orbit about the Sun [Lambeck, 1988]. Terrestrial and inertial frames can be made coincident by a system of rotations which will remove the time dependent effects of precession, nutation and polar motion. The coordinates of a point X in an inertial system can be transformed into terrestrial coordinates x by:-

$$x = SNPX \tag{4.1}$$

where x = coordinates in a terrestrial frame
S = polar motion matrix
N = matrix to account for nutation
P = matrix to account for precessional motion
X = coordinates in an inertial frame

4.2 RELATION OF REFERENCE FRAMES TO SPACE GEODESY

VLBI

VLBI observations are interferometric measurements of stellar radio sources usually made from points on the surface of the Earth. It is a geometric technique that has been in use since the 1970s. VLBI measurements are computed in an inertial system but, since the definition of a terrestrial system is arbitrary in some of its parameters (e.g. origin of coordinates, and one of the principal axes), it is not possible to directly link the two reference frames. For example, a change in the declination of a radio source can be compensated for by a change in the latitude of a vector baseline in the terrestrial system, and a common arbitrary constant can be added to both the right ascension of the radio source and the longitude of a vector baseline without affecting the interferometric analysis [Cannon, 1978].

The approach to VLBI analyses has changed with time. Cannon [1978] explains the early approach as follows: the degrees of freedom in the solution can be removed by fixing a number of parameters. The degree of freedom inherent in the declination can be removed by fixing either the latitude of one site in the terrestrial frame or the declination of at least one radio source. To remove the degree of freedom inherent in the right ascension and to separate the longitude of the terrestrial baselines from the right ascension of the sources, the arbitrary additive constants of both these quantities must be independently fixed. The definition of right ascension on the celestial sphere fixes the right ascension of the sources. This can be achieved by fixing the right ascension of a

single source at some predetermined value. Fixing the same value of the additive constant for the right ascension in the terrestrial system requires apparent sidereal time to be defined. Apparent sidereal time at a point is the sum of apparent sidereal time at Greenwich (GAST) plus the longitude of the point relative to Greenwich. Fixing either GAST or the longitude of a point will remove the remaining degree of freedom. The scale of the system is defined by adopting a value for the velocity of light in vacuum.

An alternative approach to defining the inertial frame is to consider the coordinates of all the radio sources as weighted observations rather than fixing the values of a single source and estimating the remainder as parameters. This removes the rank deficiencies associated with the inertial frame and reduces the rank deficiency of the system from nine to six [Dermanis and Mueller, 1978]. The terrestrial reference frame can be defined using a free-net adjustment of all station coordinates. Dermanis and Mueller [1978] define the origin of the Earth-fixed system by minimising the corrections to apriori coordinates, and define the orientation of the system as the average rotation needed to align all station coordinates with the mean origin.

SLR

SLR observations are processed using dynamic satellite geodesy, whereby all ranges to a satellite are combined with equations of motion describing the orbit of the satellite. The motion of the satellite is described in an inertial frame defined by the orbital plane of the satellite and the equator of the Earth, whilst the coordinates of the tracking stations are required in a terrestrial frame. Dynamic satellite geodesy provides three dimensional station positioning relative to the centre of mass of the Earth, with the horizontal and vertical components of station positions being strongly separated [Christodoulidis et al., 1985]. To achieve this, all forces acting on the satellite must be accurately modelled, and the relationship between the Earth's position and rotation relative to the satellite's orbital plane known.

The origin of the inertial frame is taken to be the centre of mass of the Earth, one principal axis is the pole of the orbital plane of the satellite, another being the ascending node of the body and the third orthogonal to both. The equations of motion of the satellite essentially define the inertial frame. The origin of the terrestrial frame is fixed as the centre of mass of the Earth by setting to zero the first three coefficients of the spherical harmonic expansion of the geopotential model [Boucher, 1989]. There is then only one remaining degree of freedom which must be accounted for to align the right ascension of the position of the satellite and the longitude of stations in the terrestrial

frame. This can be achieved by fixing the longitude of a single station in the terrestrial frame [Christodoulidis et al., 1985] or by defining UT1 from some predetermined values. With the reference frames linked in this manner, SLR has the capability to simultaneously estimate all remaining station positions and Earth rotation parameters.

GPS

The definition of the reference frames for GPS is similar to SLR, with the orbit of the satellite being inertial, and the coordinates of tracking stations being in a terrestrial frame. Again, the longitude of a single station must be fixed or UT1 defined in order to link the inertial and terrestrial frames. GPS solutions are capable of solving for Earth rotation parameters in a minimally constrained solution [Herring et al., 1991b].

4.3 EXAMPLES OF REFERENCE FRAME DEFINITIONS IN SOLUTIONS

The above has described how to minimally constrain the terrestrial and inertial reference frames in VLBI, SLR and GPS solutions. Examples of geodetic solutions available in the literature will now be given to demonstrate how analysts actually constrain their geodetic solutions.

VLBI

The VLBI solution by Ryan et al. [1993a] used a North America fixed frame. They fixed the position of Westford and the direction of Westford to Richmond, and did not use any external plate motion model. It is not directly stated that Westford was given a zero velocity but that would be required in order to "fix" the North American plate.

Shapiro [1983] defined the VLBI inertial frame in the following manner: "The basic inertial frame is chosen with origin at the barycentre of the solar system and with axis directions fixed with respect to the (assumed stationary) extragalactic sources in accord with the mean equinox and equator of 1950.0". He also fixed the origin of right ascension of one radio source. He defined the terrestrial frame as follows: "We also use a geocentric Earth-fixed cartesian frame in the analysis with the Z axis parallel to the mean pole of rotation of 1900-1905, as defined by the International Latitude Service and maintained by the Bureau International de l'Heure (BIH). The X axis is defined to be perpendicular to the Z axis and in the direction of the Greenwich meridian. The Y axis completes the right-handed triad. Operationally, the origin of this system is defined by the co-ordinates used for the intersection of the azimuth and elevation axes of one of the

'reference' radio telescopes in the interferometer array; these are obtained from a combination of spacecraft-tracking and VLBI observations made at various sites, chosen to be as consistent as feasible with the defined geocentre."

The Goddard Space Flight Centre (GSFC) has produced a number of different VLBI solutions. Ma et al. [1993] described how the celestial reference frame is defined, and how VLBI is more precise than the precession and nutation models currently available. They suggest that using the direction to a strong radio star to define the X axis is more logical than using the vernal equinox. Their GLB792, GLB795 and GLB803 solutions were defined as follows: source 0420-014 was fixed, the X, Y, Z coordinates of Westford were fixed, the velocity of Westford and the rate of change of direction of Westford-Richmond was fixed to some apriori value (they do not indicate what the source of the value was), the vertical rate of KAUAI (Hawaii) was fixed at zero. The GLB792 and GLB795 solutions fix the same parameters as above but use NNR NUVEL-1 velocities for the fixed stations, whilst their GLB803 solution is a North American fixed frame, that is, the velocity of Westford is fixed to zero and there is no rate of change of direction between Westford and Richmond. The GLB886a Solution is defined by fixing the position of Westford and the direction of the Westford-Richmond baseline which moves according to the NNR NUVEL-1 model [Watkins et al., 1994]. It is not stated that all solutions have a source fixed, but all must have the right ascension of at least one source fixed in order to remove a rank deficiency in the solution.

Feigl et al. [1993] minimised the horizontal velocities of 10 North American VLBI stations in their realisation of a North American fixed reference frame. They then minimised the differences in horizontal position of the same 10 stations between their solution and the ITRF 1991 reference frame to align the VLBI system with ITRF.

SLR

GSFC have also produced a number of SLR coordinate solutions. Smith et al. [1990] defined the terrestrial frame by adopting apriori the conventional international origin (CIO) for polar motion, and by fixing the latitude and longitude of Greenbelt (Maryland) and latitude of Maui (Hawaii). They also fixed the respective velocities to the AM0-2 values for these sites. A similar procedure was adopted by Smith et al. [1994], but velocities were fixed at NNR NUVEL-1 values instead of the AM0-2 model values.

The University of Texas Centre for Space Research solution 93L01 was derived from nearly 17 years of ranging to the Lageos satellite. The coordinate system was

constrained by fixing the latitude, longitude and latitude and longitude rates of the site at Haleakala, and the latitude and latitude rate of the site at GSFC (California). Velocities were held at NNR NUVEL-1 values [Watkins et al., 1994]. It is not stated whether Earth rotation parameters are estimated or fixed in the solution.

GPS

Herring et al. [1991b] used a GPS dataset observed during GIG'91 to estimate pole position variations. They used a free-net adjustment of the reference frame, constraining all station coordinates to 10 m, and define the orientation of the coordinate system by holding fixed the pole position and UT1 on the first day at the interpolated IERS Bulletin B value. The results were within 0.5 milliarc seconds (mas) of VLBI estimates of pole position, indicating that a minimally constrained GPS solution was both stable and accurate.

Freymueller et al. [1993] analysed GPS data from 1989-1991 in determining plate motion in the North Andean Region. They used a global fiducial network, and fixed the coordinates of three stations in the U.S.A. (Westford, Massechusetts; Owens Valley, California; and either Richmond, Florida or Fort Davis, Texas) and fixed the velocities of these stations to the AMO-2 plate motion model values. The coordinates for these stations were taken from GSFC VLBI solution GLB223 plus local ties.

Schutz et al. [1993b] used a global fiducial network of 20 stations in computing a GPS campaign in the Southwest Pacific. The reference frame was based on GSFC VLBI solution GLB718 with Lageos SLR analyses and local ties used to adjust the VLBI coordinates into a centre of mass reference frame. Local ties from SLR and VLBI stations to GPS stations were then applied in order to provide fiducial coordinates for the GPS tracking stations. The actual GPS solutions were processed with the coordinates of five stations fixed (Hobart, Mojave, Richmond, Westford, Wettzell). They experimented holding other fiducial stations fixed but found that this did not significantly affect the solutions of stations in the Pacific region.

Heflin et al. [1992] used a "no fiducial sites" approach to determine baseline lengths and geocentric radii of the 21 Rogue stations observed during GIG'91. They used the satellite force model to imply an origin at the Earth's centre of mass, and scale was implied by the force models, radio propagation model and GPS data. Earth rotation parameters and UT1 were fixed at values obtained from IERS Bulletin B. The absolute orientation of the polyhedron of stations was poorly determined with apriori constraints

of all station coordinates being 10 km. They compared estimates with GSFC VLBI solution GLB659 and found agreement of 2.1 ppb and 3.8 cm for length and radius, respectively. They found that the daily repeatability of the length of baselines in the Southern hemisphere was 8 times larger than baselines in the Northern hemisphere. They attribute this to poorer common satellite visibility due to there being only four stations in the Southern hemisphere compared with 17 stations in the Northern hemisphere. They conclude that fiducial networks are not necessary to provide an origin and scale for global GPS measurements. They suggest that fixing fiducial stations will lead to systematic errors unless the accuracy of the fixed coordinates are consistent with the inherent definitions implied by the force model, radio propagation model and GPS data.

4.4 THE IMPORTANCE OF CONSTRAINTS IN THE SOLUTIONS

As shown in Chapter 3, the network of global fiducial stations changed considerably between the Indonesian GPS campaigns. As a result, it is very difficult to constrain the coordinates of a set of fiducial stations and still maintain a consistent terrestrial reference frame definition for all campaigns. Changes in the terrestrial reference frame (TRF) definition can propagate as biases in the solution of the coordinates of the regional stations (see e.g. Larson et al., [1991]). Such biases will corrupt the estimates of station velocities, which rely principally on the assumption that every campaign solution is both accurate and bias free. In this section I show how to define the TRF such that distortions in the reference frame have minimal effect on the estimation of coordinates in the Australian region.

Consider the hypothetical situation of a station which is stationary relative to the mantle of the Earth (i.e. has a zero velocity relative to the TRF). If, due to a particular fiducial network, the estimate of the East coordinate of the station was in error by -10 mm in a 1990 solution and a different fiducial network in 1991 introduced a bias of +10 mm in the East component then the East velocity estimate for that station would be +20 mm/year when in fact the true velocity was zero. Thus, estimations of station velocities are very sensitive to the stability and accuracy of each campaign solution. It is therefore important to quantify the effect of changes in the fiducial network in the Indonesian campaigns in order to assess the accuracy of the velocity estimates.

There are a number of rank deficiencies to be considered in order to obtain a solution, and a number of options as to how they can be removed. A TRF can be defined as follows: the Z axis can be defined by adopting a mean equatorial plane and a conventional rotation axis of the Earth perpendicular to the equatorial plane. This is

realized by defining polar motion (i.e. the coordinates of the actual location of the rotational axis of the Earth relative to the theoretical Z axis). Adopting values for UT1 defines the location of the X axis in the mean equatorial plane, and the Y axis is orthogonal to both. Alternatively, the frame can be defined by the coordinates of a number of terrestrial stations [Mueller, 1985].

It has been shown that GPS measurements can be used to estimate Earth rotation parameters (ERP's) (e.g. Herring et al., [1991b]; Lichten et al., [1992]). There is a rank deficiency which must be considered if a free net adjustment of station coordinates is performed in conjunction with an estimation of UT1. Lichten et al. [1992] overcome this by fixing the ERP's for the first 12 hours of each day, and use the GPS observations to estimate the changes in the parameters in the following 12 hours. In order to determine the ability of the dataset of this thesis to estimate ERP's, I constrained all core stations to 5 mm horizontally and 10 mm vertically and estimated ERP's. I used values of polar motion and UT1 from a VLBI solution computed at MIT (Tom Herring, pers. comm., 1994). The solution (hereafter called TAH) is an adjustment of ten years of VLBI observations. I treated the ERP's stochastically in a back filter solution, using TAH values as apriori information. Figure 4.4 shows the difference between the resulting GPS estimates and the VLBI estimates for Xp, Yp and UT1. The estimates for polar wobble are within 5 mas. The difference in UT1 estimates prior to the introduction of IGS are between 10 and 20 mas - this amounts to a rotation of about 0.3 m in longitude at the Equator and is an unacceptable level of error. Thus the GPS data (in particular prior to July 1992) are not capable of accurately estimating ERP's. Hence, it was decided not to estimate ERP's, but to adopt values for polar motion and UT1 from an external source (i.e. the TAH solution)

Using GLOBK and minimally constraining the solution I experimented with different constraint levels on the remaining core IGS stations. I defined the Z and X axes of the TRF by adopting TAH Earth rotation parameters and UT1, respectively. Assuming that the core stations are accurately coordinated in ITRF 92, it should be possible to apply tight constraints without significantly affecting the solutions. On the other hand, if there are distortions in ITRF 92 then tight constraints will strain the solutions and affect the results. I performed solutions with four different levels of constraints which are shown in table 4.1

Comparison of results of solutions A to D revealed some interesting issues. Firstly, the level of constraint had little effect on the final coordinate estimates of the core stations. Secondly, the North, East and UP adjustments to apriori ITRF 92 coordinates were

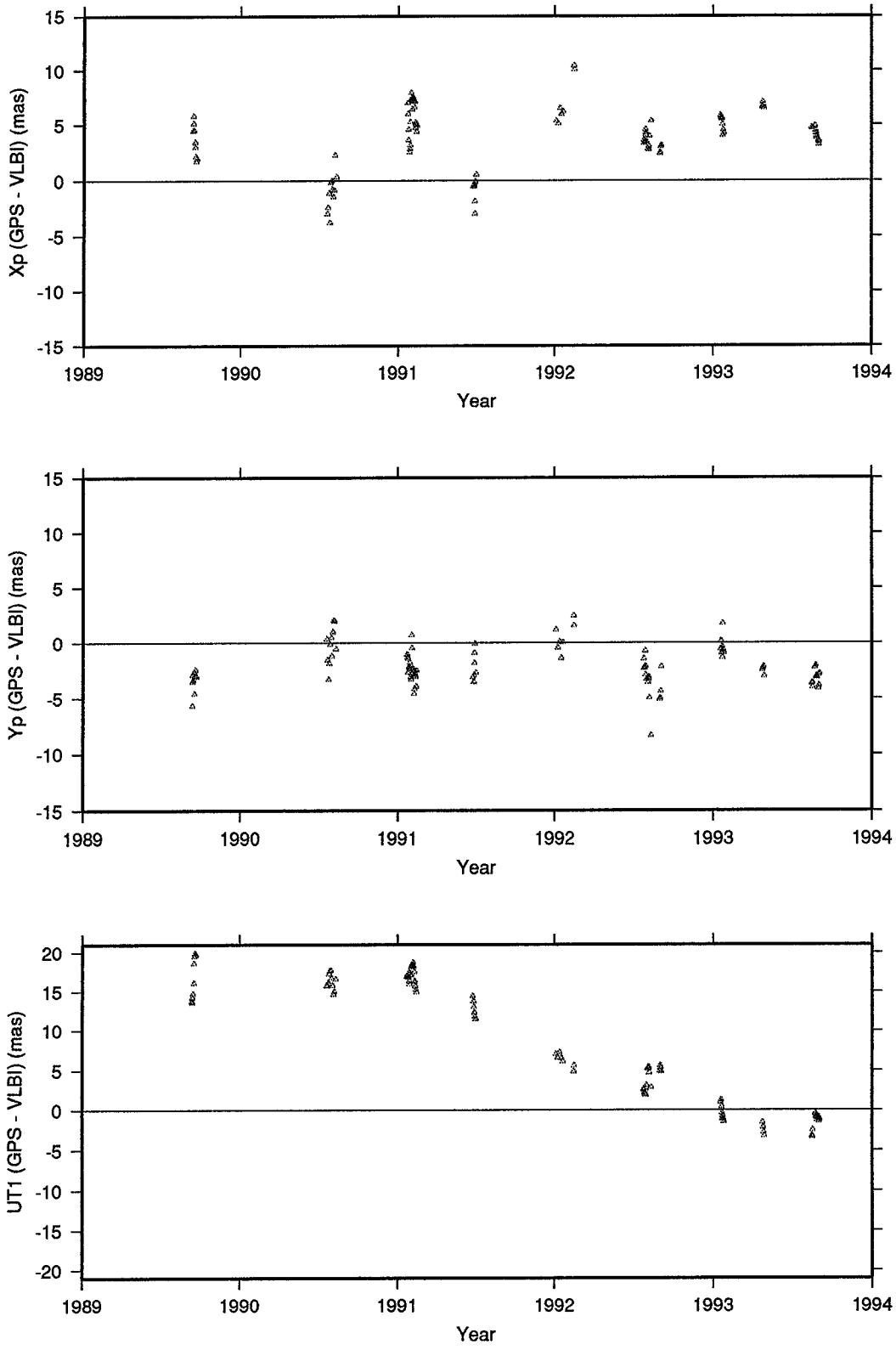

Figure 4.4 Difference between GPS and VLBI estimates of polar motion and UT1. VLBI estimates from Tom Herring (pers. comm., 1994).

Table 4.1 Levels of constraints applied in solutions (A) - (D).

Solution	Constraints Applied		
	N (m)	E (m)	U (m)
A	0.500	0.500	0.500
B	0.200	0.200	0.200
C	0.100	0.100	0.100
D	0.050	0.050	0.050

larger than expected - often up to 0.2 m. Thirdly, the adjustments to latitude appear to be geographically dependent rather than random with positive adjustments to latitude in North America and negative in Europe and the Southern hemisphere. Adjustments to longitude and height do not display any geographical pattern.

The adjustments to apriori coordinates indicate that the GPS dataset is not consistent with the ITRF 92 values for the core stations. Similar results have been determined at UC and MIT which show inconsistencies between global GPS solutions and ITRF 92. Statistically, at the 95% confidence level, a postfit residual should not be greater than two times the standard deviation of the parameter if the solution has been correctly weighted and the solution is stable. The formal sigmas for solutions A to D are unrealistically small for latitude and height so a rule of thumb test can be applied that the adjustment cannot exceed the apriori sigma. In this case, the preferred solution is B, with constraints of 0.2 m applied to the core stations.

The adjustments to the longitude of the stations in solutions B to D show a random pattern geographically with a mean adjustment that is not significantly different from zero. This indicates that the ITRF 92 definition of zero longitude as realized by the longitude of the core IGS stations is consistent with the definition of UT1 used in solutions B to D. Hence, the data is consistent with the definition of the TRF as outlined above. There is a significant longitudinal shift in solution A, indicating that the network in this solution is no longer aligned in longitude with ITRF 92. Hence, there is either insufficient power in the UT1 definition or there is a need for constraints to overcome the rank deficiency.

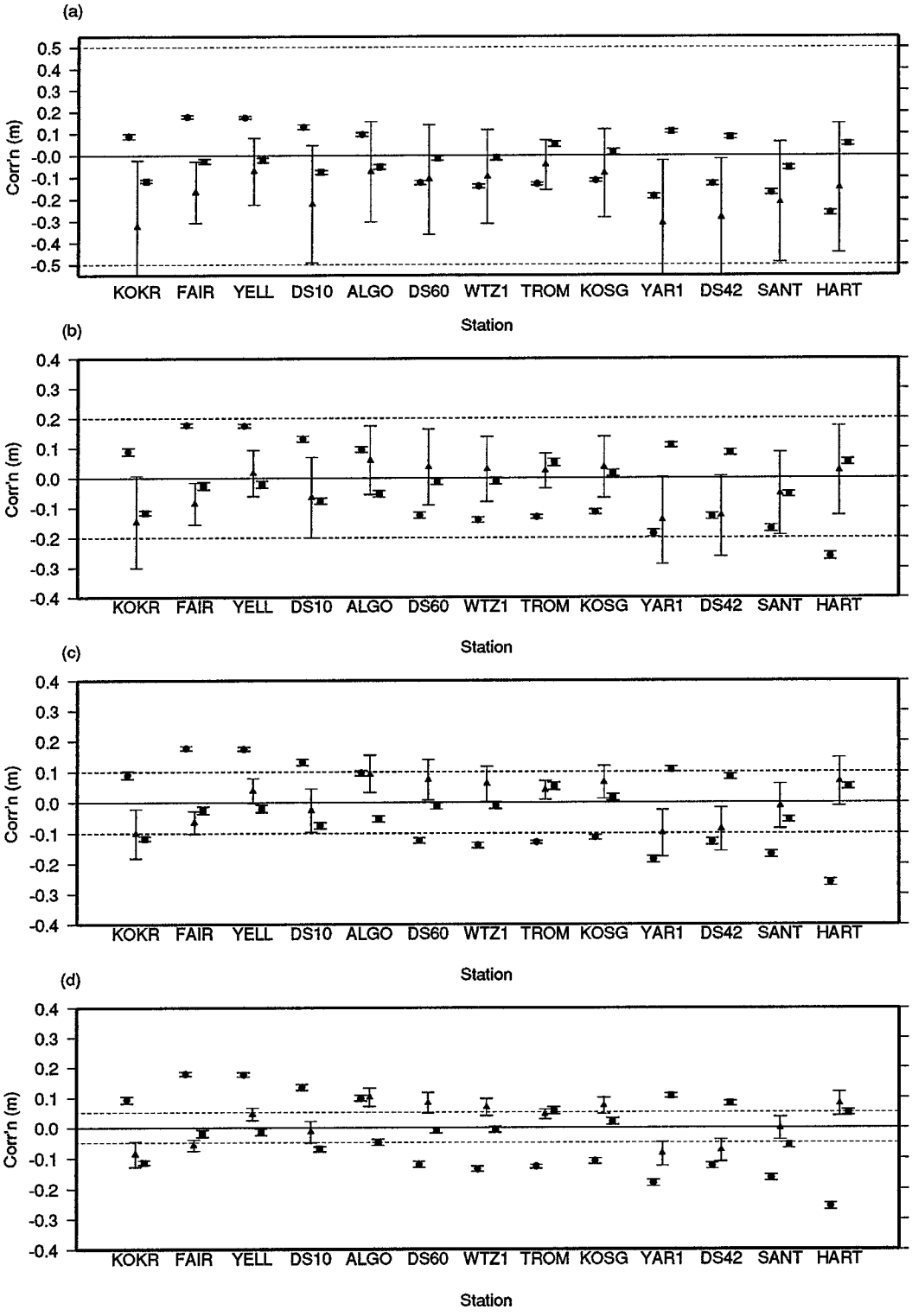

Figure 4.5 Corrections to apriori coordinates for core IGS stations with different constraint levels: (a) 0.5 m; (b) 0.2 m; (c) 0.1 m; (d) 0.05 m. North coordinate shown as •, East as Δ, Up as ■. Formal one sigma error bars are plotted.

In most cases, the level of constraint had little effect on the actual value for the coordinates of the core station in latitude and height - 90% of ϕ and h coordinates changed by less than 30 mm in all five solutions. This indicates stability in the data - the solutions are robust enough to produce the same results irrespective of apriori

constraints which try to hold a parameter away from its preferred value. However, it is concerning that the parameters are consistently shifting from the ITRF 92 values. This shows that there is a distinct difference between the minimally constrained GPS data solutions of this project and the ITRF 92 reference frame as defined by Boucher et al. [1993]. Possible explanations for this are:

- the Earth rotation parameters held fixed in solutions A to D are not connecting the terrestrial and inertial reference frames in a similar manner to the ITRF 92 connection; or

- the addition of a significant amount of GPS data in the Southern hemisphere has shown that there are distortions in ITRF 92.

Thus, the solutions are not strictly in the ITRF 92 reference frame. The core stations must be constrained to less than 1 mm to prevent any adjustment from the ITRF92 value. It is not important in this analysis that the results are relative to ITRF 92 - it is more critical that the TRF be defined such that distortions due to constraints are not introduced between different fiducial network configurations.

The decision as to how to constrain the fiducial tracking network stations must consider that the fiducial network did change considerably throughout the project. Constraints should be applied so as to maintain a reference frame definition which is as consistent as possible for all campaigns. This is investigated in section 4.4.1.1.

4.4.1 GPS Data Simulation

Experimenting with simulated GPS data allows comparisons with "true" values to be made - something that is never known with real data. I simulated GPS data and performed many tests in order to determine how the solutions could be minimally constrained whilst maintaining a consistent reference frame definition. I have shown above that the ITRF 92 coordinates for the core stations are not consistent with the GPS data. A stable solution will be achieved by constraining just enough station coordinates to define the reference frame consistently throughout all the campaigns. Section 4.4.1.1 investigates which constraints need to be applied to achieve such a solution.

Code and phase data for the stations shown in Figure 4.4 were simulated using Bernese V3.4 software [Rothacher et al., 1994]. The simulation program calculates ranges and phase observations between an orbit and specified coordinates of the stations whose data is to be simulated. Atmospheric and ionospheric path delays can be simulated, as can the

required precision of the code and phase measurements. The simulations were run with random noise of 10 mm on both the L1 and L2 phase observations, random noise of 10 m on C/A code observations, tropospheric delay as predicted by the Saastamoinen formula and no ionospheric delay (the processing is to be done using the Lc observable which removes the ionospheric delay anyway). An orbit from the global solution of day 054 of 1994 available from SIO data analysis centre and UC was used in the simulation, and 24 hour data was created using a sampling interval of 2 minutes with a cutoff elevation of 15°. Day 054 of 1994 had 27 operational satellites for which data was simulated. This day was selected as the global solution contained 39 GPS stations with perhaps the best global distribution currently available. Hence, the estimation of the GPS orbits should be as accurate as is currently possible.

The simulated data was converted to RINEX format and then processed in GAMIT. A number of different solutions were then computed and will be described below. In all cases, the apriori orbit was a broadcast ephemeris and orbital parameters were estimated in the solution. For the purpose of this simulation, the geographical distribution of the fiducial sites is very important. I consider the situation of two stations within a few hundred kilometres of each other as one site (e.g. Tsukuba and Usuda). There are only five sites that are observed in all Indonesian campaigns - Hawaii (KOKE/KOKR), West Java (BAKO), Usuda (TSU1/USUD/USU2/USU3), Wettzell (WTZM/WTZ1) and Southern California (DS10/MOJ1). YELL was observed in all but the 1990 campaign and TAS1 was observed from 1990 onwards, giving a total of seven stations that can be used to test the stability of the reference frame definition. The station at DS10 is substituted for Mojave (California) in the 1989 and 1990 solutions whilst WTZ1 is substituted for another tracking station at the same site in solutions prior to July 1992. Constraints were only applied to these stations if it was the actual core IGS station that was observed in the campaign.

4.4.1.1 Constraints for a nominal solution

A minimally constrained solution of GPS data can be attained by defining the inertial frame using dynamic modelling of the motions of the satellites, and by defining UT1 to separate the right ascension of the satellites from the longitude of stations in the terrestrial system. Adopting this procedure, and using simulated data, the actual fiducial networks and numbers of satellites were reproduced for each of the campaigns. Section 4.4 showed that with constraints of 0.2 m applied to all core stations, GLOBK estimates of the coordinates of the core IGS stations are typically within 0.2 m of the ITRF 92

Table 4.2 Stations observed in all of the GPS campaigns.

STATION	CAMPAIGN					
	1989	1990	GIG'91	1991	1992	1993
			** Regional Stations **			
AUSA	•	•				
BAKO	•	•	•	•	•	•
CAVE	•			•	•	•
COCO					•	•
DARW					•	•
DS42			•	•	•	•
KARR					•	•
TAS1		•	•	•	•	•
TOWN			•	•	•	•
XMAS	•	•		•	•	•
YAR1			•		•	•
			** Global Stations **			
ALGO			•		•	•
BAHA	•	•				
DRAO			•	•	•	•
DS10	•	•	•	•	•	•
DS60			•	•	•	•
ENGA	•	•				
FAIR			•		•	•
HART			•		•	•
KOKR	•	•	•	•	•	•
KOSG			•		•	•
KOUR					•	•
KWAJ	•	•				
MASP					•	•
MATE			•		•	•
MCM1					•	•
ONSA	•	•			•	•
PAMA					•	•
RIC1	•	•		•	•	•
SANT			•		•	•
TROM	•		•		•	•
TSU1	•	•	•	•	•	•
WES1	•	•		•	•	•
WTZ1	•	•	•	•	•	•
YELL	•		•	•	•	•

values. That is, the coordinates of the core stations are most probably accurate at this level.

Table 4.2 lists the regional and fiducial stations that were observed in all of the Indonesian campaigns. Table 4.3 lists the satellites that were observed during each campaign:

Table 4.3 Satellite PRN's observed during Indonesian campaigns. The satellites in the simulated data are also shown.

Campaign	Satellite PRN observed	Total # Satellites Observed
1989	2 3 6 9 11 12 13 14	8
1990	2 3 6 9 11 12 13 14 16 17 18 20	12
GIG'91	2 3 6 11 12 13 14 15 16 17 18 19 20 21 23	15
1991	2 3 11 12 13 14 15 16 17 18 19 20 21 23	14
1992	2 3 11 12 13 14 15 16 17 18 19 20 21 23 24 25 26 28	18
1993	1 2 3 7 9 12 13 14 15 16 17 18 19 20 21 22 23 24 25 26 27 28 29 31	24
Simulation	1 2 3 4 5 7 9 12 13 14 15 16 17 18 19 20 21 22 23 24 25 26 27 28 29 31	27

The adjustments to apriori coordinates of a number of stations from each campaign were compared. If the reference frame is strongly defined there would not be any significant adjustments to station coordinates from apriori values. If the fiducial tracking networks

introduce biases into the solutions through either a hemispherical imbalance or poor satellite-station intervisibility, then significant shifts to station coordinates would occur. In this case, additional constraints would be required in order to stabilize the reference frame in all campaigns.

Results

The adjustments to the true values of longitude of the seven test stations (KOKR, YELL, DS10, WTZ1, USU3, TAS1, BAKO) from the minimally constrained simulated GAMIT solutions of 1989-1992 are shown in Figure 4.6. These adjustments are not significant, hence there is no apparent bias being introduced into the solutions. This indicates that the data in all campaigns are still consistent with the longitude definition of the adopted UT1 values. Hence, no additional constraints are required to stabilize the definition of zero longitude of the reference frame. Figure 4.7 shows the adjustments to latitude for the same stations. There appears to be a pattern in that the adjustment to latitude is the same for all stations (with the exception of YELL), with significant changes occurring between some campaigns. This indicates that a bias of up to 0.2 m in latitude could be introduced between campaigns using the constraints as applied to these solutions. Thus, additional constraints are required in order to consistently define latitude of the stations in all campaigns.

The tracking site at Hawaii is the only site where a core IGS station has been operational during all the campaigns. It is also the closest core IGS station to the region (excluding those located on the Australian plate). I experimented with the constraints of this station in order to determine the most appropriate constraints for defining a stable reference frame. The mean adjustment to the true values of latitude and longitude of the seven stations were computed using the adjustments from all campaigns. Since a perfect solution would result in zero adjustments, the adjustments that occurred to station coordinates in each campaign can be considered as residuals. The weighted sum of the squares of the residuals (V^tWV) for each campaign were computed for the seven stations. Table 4.4 shows the constraints applied to KOKR, the resulting mean values of ϕ, λ and V^tWV for each station. A variance factor is computed for each of the constraint methods.

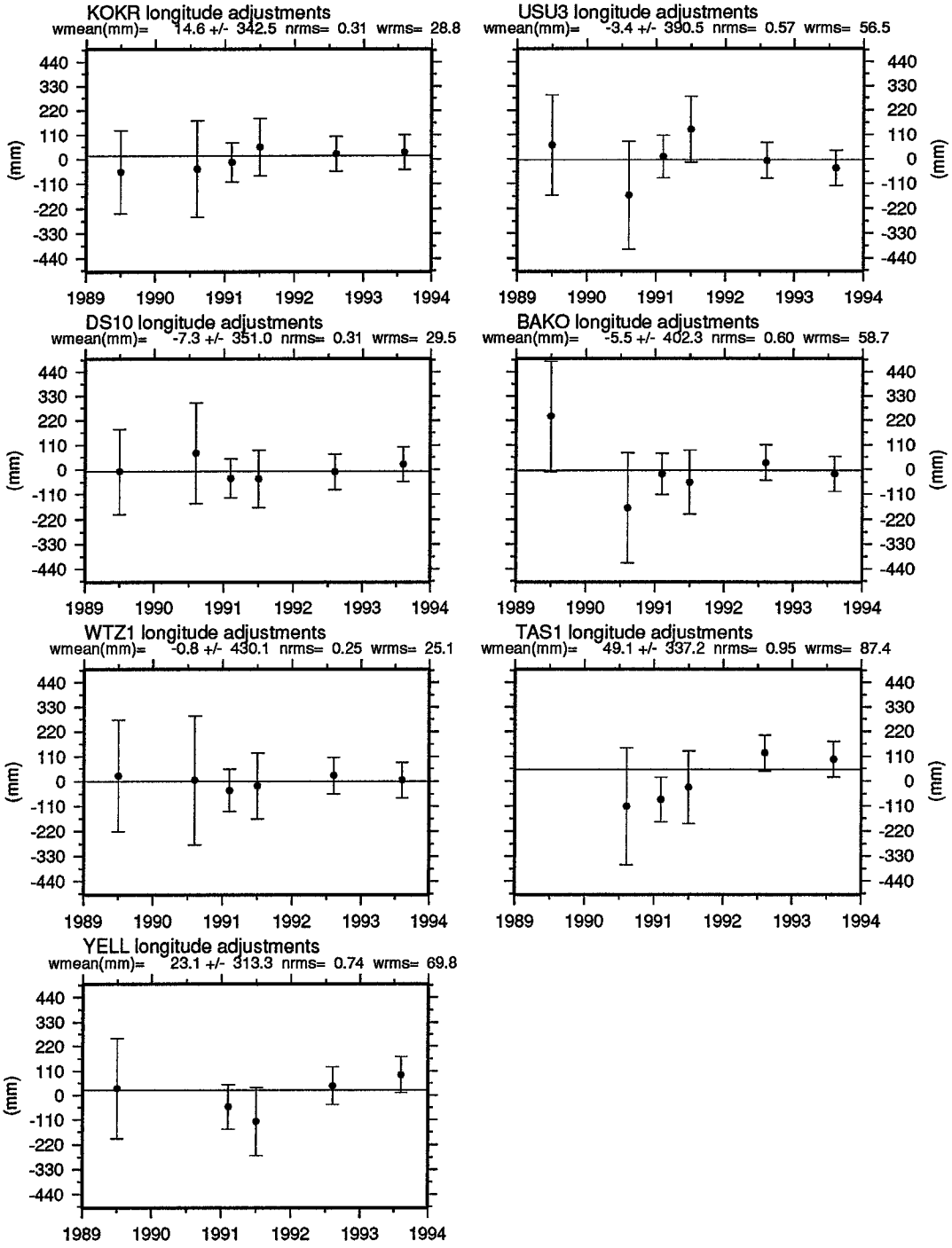

Figure 4.6 Adjustments to longitude of KOKR, BAKO, TAS1, DS10, WTZ1, USUD, YELL for campaigns 1989-1993. Mean estimate of longitude is plotted.

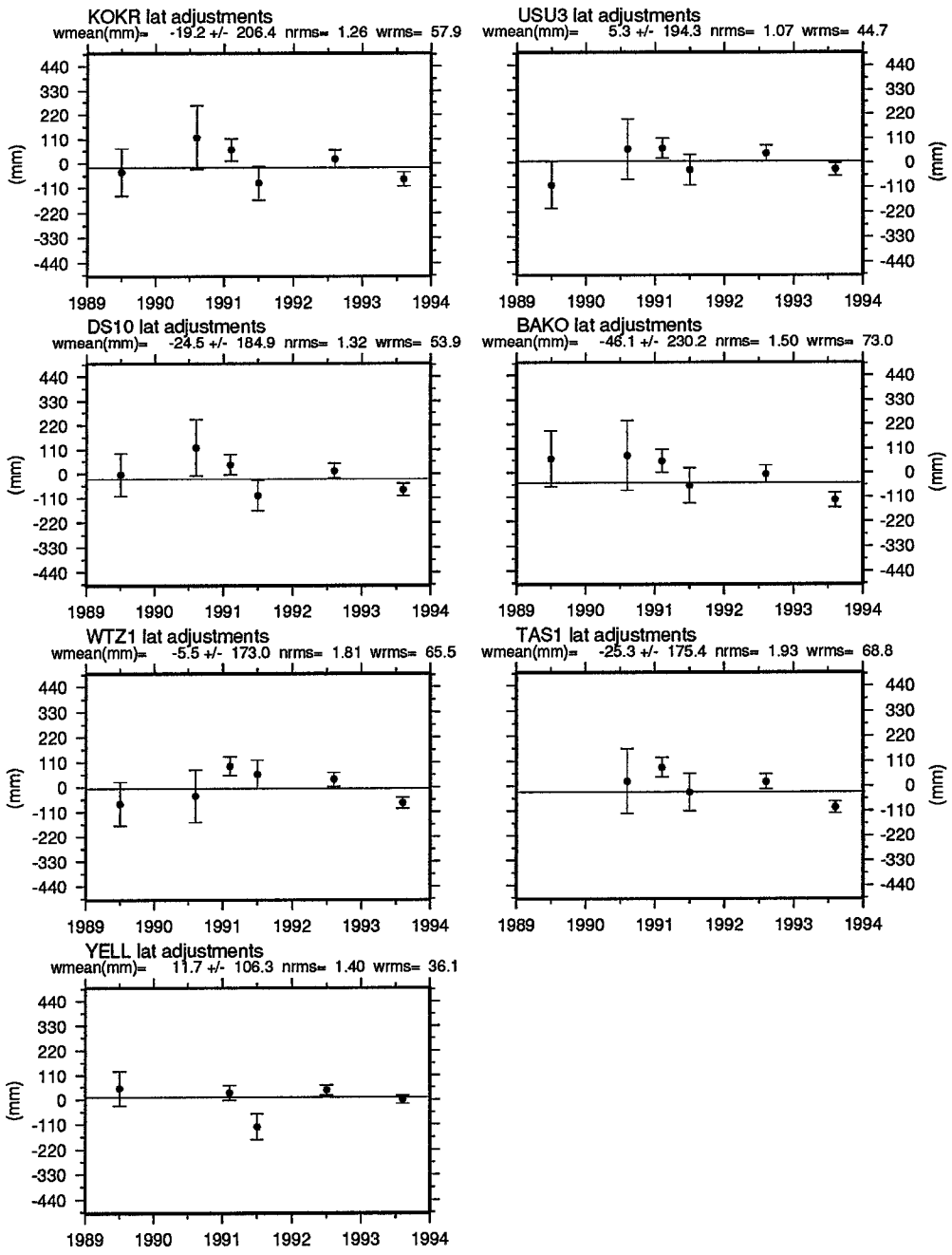

Figure 4.7 Adjustments to latitude of KOKR, BAKO, TAS1, DS10, WTZ1, USUD, YELL for campaigns 1989-1993. Mean estimate of latitude is plotted.

Table 4.4 Constraints applied to KOKR, resulting weighted mean coordinate shifts and V^tWV of TAS1, USUD, WTZ1, DS10, YELL, KOKR and BAKO. A free constraint was 0.2 m, fixed was 0.1 mm. Mean values are in mm. Variance factor is computed as $\Sigma V^tWV/\Sigma f$.

Constraints applied to KOKR		ϕ, λ free	ϕ fixed	λ fixed	ϕ, λ fixed	ϕ, λ free	ϕ fixed	λ fixed	ϕ, λ fixed
			LATITUDE				LONGITUDE		
YELL	Mean	-38	-24	-37	-23	137	138	77	80
(n[a]=4)	σ_{mean}	17	13	17	12	31	29	39	35
	V^tWV	16.6	7.9	15.9	6.8	10.7	11.1	4.8	4.8
DS10		-36	-17	-35	-17	68	67	13	14
(n=5)		25	7	42	6	19	19	35	32
		12.6	1.2	15.5	1.0	3	3.2	1.0	0.8
WTZ1		-62	-42	-62	-49	-109	-111	-161	-162
(n=5)		16	24	16	23	9	10	25	30
		31	16.3	31.4	16.3	6	6.6	13.5	13.9
USU3		20	38	19	37	-20	30	-87	-87
(n=5)		19	17	33	17	40	40	46	42
		7	5.6	9.0	5.3	2	1.9	5.6	5.6
BAKO		-27	-6	-26	-6	-67	-68	-121	-122
(n=5)		30	23	50	23	66	62	81	79
		12.8	2.3	15.4	2.3	4.2	4.1	10.6	10.7
TAS1		-72	-57	-71	-56	-54	-54	-115	-115
(n=4)		15	14	30	14	49	48	40	38
		31.3	13.8	32.2	13.5	5.0	4.8	9.0	8.8
KOKR		-21		-20		56	55		
(n=5)		26	-	47	-	19	24	-	-
		9.0		12.2		2.0	2.4		
ΣV^tWV		120.3	47.1	131.6	45.2	32.9	34.1	44.5	44.6
Σf[b]		26	22	26	22	26	26	22	22
$\Sigma V^tWV/\Sigma f$		4.6	2.14	5.06	2.05	1.26	1.31	2.02	2.03

[a] n = number of campaigns in which station was observed.

[b] f = degrees of freedom (equal to Σ(n-1) for all stations).

It is apparent that constraining the latitude of KOKR halves the variance factor for ϕ, whilst constraining the longitude of KOKR increases the variance factor for λ by about 50%. The mean adjustment and standard deviation of a longitude of a single station are unaffected by constraints applied to the latitude of KOKR. Similarly, the latitude means are unaffected by constraints to the longitude of KOKR. Therefore, it can be assumed that latitude and longitude estimates are uncorrelated. Thus, the ΣV^tWV of latitude and longitude can be added to compute an overall variance factor. Table 4.5 shows the combined ΣV^tWV and resulting combined variance factors.

Table 4.5 Calculation of combined variance factors.

Constraints applied to KOKR	ϕ, λ free	ϕ fixed	λ fixed	ϕ, λ fixed
ΣV^tWV	152.3	81.2	165.7	89.8
Σf	52	48	48	44
$\Sigma V^tWV/\Sigma f$	2.94	1.69	3.67	2.04

The solution with the smallest variance factor is the solution with the latitude of KOKR fixed. Therefore, this approach to constraining the reference frame is considered to provide the most consistent reference frame definition throughout all the Indonesian campaigns and will be adopted for all processing in this analysis.

4.4.2 Velocity field

Since the surface of the Earth is covered with a number of moving plates, the coordinates of any fixed station must include a velocity component. There are a number of different global velocity fields which have been estimated from SLR, VLBI, GPS, geophysical data and a combination of these techniques. When computing a solution of five years of GPS data, station velocities become crucial to the results. Obviously if a station is fixed then it must also have a fixed velocity. This requires information from an external source to provide the velocity of the station. The estimation of station velocities requires that the data be consistent and free of systematic errors. This is not always the case - indeed it is very difficult to determine whether all systematic errors have been removed.

The estimates of station velocities from a GLOBK solution of the GPS data can be compared to velocities from plate motion models and those derived using VLBI and SLR. One of the objectives of this thesis was to estimate a velocity field for the Australian region from GPS observations. One method for obtaining site velocities on the Australian plate is to define the velocities of a set of global tracking sites and then loosely (i.e. 1 m/year) constrain the velocities of all points on the Australian plate. The resulting velocities would then represent the motion of the Australian plate relative to the reference frame as defined by stations on the other plates of the Earth. This requires that a particular velocity field is adopted for the stations not located on the Australian plate. In this thesis, the velocities as defined in ITRF 92 are adopted. The ITRF 92 velocity field is an adjustment of the velocity solutions of a number of processing centres. The no-net-rotation constraint of the NNR NUVEL-1 model was superimposed on the adjustment. Resulting GPS velocities can then be compared to the ITRF92 solution. However, since there are only three sites on the Australian plate whose velocities have been determined by space geodetic observations, most of the velocity comparisons will not be made to ITRF 92 estimates but rather to the NNR-NUVEL-1A plate motion model.

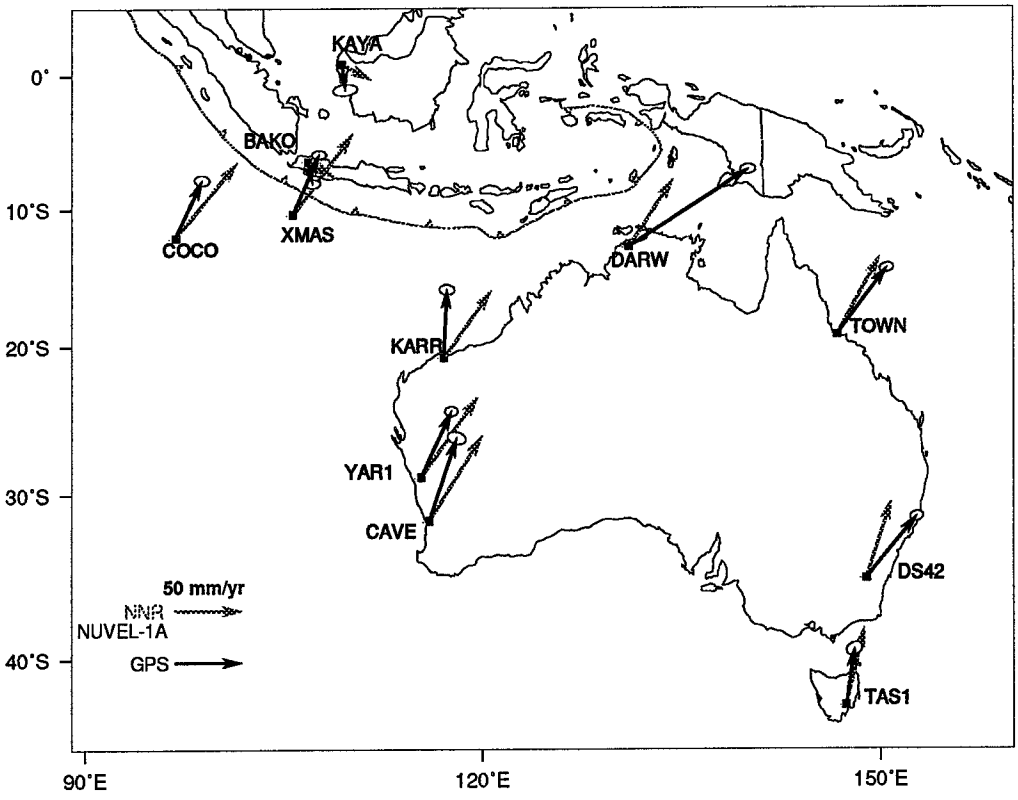

Figure 4.8 GPS determined station velocities compared with NNR-NUVEL-1A velocities. Formal 95% error ellipses plotted on GPS vectors.

Figure 4.8 shows NNR-NUVEL-1A and the resulting GPS velocities for all stations located on the Australian plate when all station velocities are estimated. There is poor agreement between the two velocity fields. The velocities in Figure 4.8 cannot be geophysically correct without the Australian plate showing large internal deformation. Such deformation is not apparent within the Australian plate (see Section 5.2.1 for a full discussion of station velocities).

Other geodetic studies have determined the velocities of Yaragadee, Tidbinbilla and Hobart using VLBI and SLR observations (e.g. Smith et al., [1990]; Larson and Freymueller, [1994]; Ryan et al., [1993b]). The principal difference between the data used in this analysis and other studies is that the data in this analysis is campaign based spanning only a few years and is very sporadic (i.e. often only two weeks per year) whereas other datasets have longer time spans and are more evenly sampled. Table 4.6 shows the most recent estimates of station velocities from geodetic measurements.

Table 4.6 Estimates of site velocities for Yaragadee, Canberra and Hobart. Azimuth in degress and magnitude of velocity in mm/yr given. GPS results are the estimates from this analysis, SLR results from Smith et al. [1990], VLBI results from Ryan et al. [1993], GPS-1 results from Larson and Freymueller [1994], NNR-NUVEL-1A values (called NNR-A in table) from DeMets et al. [1994a], ITRF92 velocities from Boucher et al. [1993].

Station	GPS		SLR		VLBI		GPS-1		NNR-A		ITRF92	
	°	mm/yr	°	mm/yr	°	mm/yr	°	mm/yr	°	mm/yr	°	mm/yr
YAR1	26	54	33	69	-	-	36	73	36	70	32	70
DS42	40	46	14	57	14	53	16	58	18	57	17	57
TAS1	8	42	-	-	16	52	26	58	13	56	11	60

It is apparent that the estimation of all station velocities on the Australian plate yields results which conflict with velocity estimates from other geodetic techniques and from plate motion models. Therefore, it is concluded that with the dataset of this analysis, GLOBK cannot reliably estimate *all* station velocities on the Australian plate. Thus, it is necessary to impose additional constraints in order to stabilize the solution. A velocity field was estimated with an additional constraint that the velocity of YAR1 was fixed. The velocity of CAVE was also fixed, allowing the constraint to be effective in the 1989 solution when YAR1 was not operational. The velocities were fixed to NNR-NUVEL-1A velocities, since the comparisons of the other stations on the Australian plate will be

made to this velocity field. This may introduce a small inconsistency since the velocities of the global stations are in the ITRF 92 frame. The difference between ITRF 92 and NNR-NUVEL-1A velocities for the Australian stations is only a few millimetres/year. This discrepancy will introduce a small inconsistency which is assumed to be negligible in this analysis.

A solution with the velocity of YAR1 and CAVE fixed showed a significant difference between the GPS estimate and the SLR estimate of the velocity of Canberra - clearly an additional constraint was required on the East coast of Australia. Another velocity field was estimated with the additional constraint of the velocity of DS42 fixed at the NNR-A value (see Figure 5.2). This solution generally shows a better fit to the NNR-NUVEL-1A values. Therefore, it is considered that fixing the velocity of YAR1, DS42 and CAVE is sufficient to stabilize the GLOBK solution of station velocities.

4.4.3 Summary

The terrestrial reference frame can be defined with an emphasis on Northern or Southern hemisphere stations, or a global approach can be used. The earliest Indonesian campaigns have a strong bias of Northern hemisphere tracking stations. This diminishes with time as the number of Southern hemisphere tracking stations increased. Overconstraining the reference frame definition can lead to distortions if the constrained parameters are not consistent [Heflin et al., 1992], and the absence of a station in one particular campaign could affect the level of distortion. This will introduce campaign dependent biases. I chose a global approach to defining the terrestrial reference frame, and applied the least number of constraints whilst still maintaining a stable reference frame definition.

A nominal solution of the GPS data can be obtained with the following constraints:

i) The station at Hawaii (KOKE/KOKR) constrained to 0.1 mm in latitude, 0.2 m in longitude and 0.2 m in height;

ii) All other core IGS stations constrained to 0.2 m in all components;

iii) The velocities of all core stations not located on the Australian plate fixed at the ITRF 92 values; and

iv) The velocities of YAR1, DS42 and CAVE fixed at the NNR-NUVEL-1A value.

The results presented in Chapters 5 and 6 are processed using such an approach. Such a terrestrial reference frame differs from ITRF 92 as the coordinates of the core stations have been allowed to change. However, the mean definition of zero longitude is consistent with ITRF 92. It is more important in this analysis that the results be related to a consistent reference frame than to ITRF 92. The above constraints define a terrestrial reference frame that is precise to about 30 mm in all campaigns.

CHAPTER 5

RESULTS

5.1 LONG TERM PRECISIONS

An estimate of the accuracy of the GPS measurements is essential in order to determine what results may have significance to the geophysical interpretation of the Indonesian and Australian region. A measure of "accuracy" is an unattainable quantity since the true value is not known. Precision of measurements from repeatability studies is generally adopted as being a measure of the accuracy of the results. The total dataset was processed using the constraints for a nominal solution as defined in section 4.4.4, and precision estimates are discussed below.

Davis et al. [1989] indicate that a number of the errors likely to affect GPS observations will be highly correlated over short experiments, thereby failing to affect the precision of surveys with a duration of only one or two weeks. This becomes a very important issue when looking at repeat occupations of stations over a number of years where the accuracy of the observations is particularly important. Undetectable systematic biases could be introduced into campaigns due to sources such as orbital errors, unbalanced satellite configurations, poor but constant fiducial tracking networks, satellite clock behaviour or propagation effects. It therefore becomes important to determine both the short and long term precision of GPS measurements. Long term precision provides a better indicator of the accuracy of the measurements, as campaign dependent biases which will affect the accuracy of the measurements will degrade the long term precision.

Davis et al. [1989] computed the short and long term stability of GPS from 4 campaigns observed in California between 1986 and 1989 and found that the long term precision was somewhere near 3-5 parts in 10^8 horizontally and about 40 mm vertically. Larson and Agnew [1991] performed a similar study (from 11 experiments in California between 1986 and 1989), and describe the long term precision of baseline components as 3.4 mm

+ 1.2 parts in 10^8, 5.2 mm + 2.8 parts in 10^8 and 11.7 mm + 13 parts in 10^8 in East, North and vertical, respectively. The values from both studies are very similar.

Both these studies were performed on datasets observed in North America where the fiducial tracking network has been quite strong from 1986 onwards, and also where a terrestrial reference frame can be well defined from VLBI observations. The baseline lengths of the studies were up to 230 km and 450 km, respectively. The dataset for this thesis is observed in the Southern hemisphere where there is significantly less fiducial tracking stations and a weaker definition of the reference frame - especially prior to 1992. The networks processed in this analysis consist of stations up to 5500 km apart, and typical baseline lengths are around 2000 km - significantly larger than the baselines used in the above studies. In addition, many factors were changed between campaigns such as receiver types, number of GPS satellites and regional tracking sites, which may have affected the accuracy of each campaign differently.

Section 4.3 showed that it is essential to tightly constrain or fix the velocities of two stations on the Australian plate in order to tie the regional network into the global reference frame. To compute the long term repeatability of this dataset the velocities of YAR1, DS42 and CAVE were fixed to NNR-NUVEL-1A values. The long term precision of the components of a baseline were computed as follows:-

$$S = \sqrt{\frac{\frac{n}{n-1}\sum_{i=1}^{n}\frac{(y_i-(a+bt_i))^2}{\sigma_i^2}}{\sum_{i=1}^{n}\frac{1}{\sigma_i^2}}} \qquad (5.1)$$

where
- S = long term precision estimate
- a, b = the intercept and slope of the best fitting line, respectively
- t_i = time of the ith measurement
- y_i = residual of the ith measurement
- n = number of measurements
- σ_i = formal error of baseline component estimate

The above formula is based on that of Larson and Agnew [1991] - the formulation given in Larson and Agnew [1991] is typographically incorrect (K. Larson, pers. comm, 1994). Long term precisions were computed from a back solution where all stations in the Australian/Indonesian region were estimated stochastically in a GLOBK back filter solution. This nullifies the constraints imposed on the velocities of YAR1, DS42 and

CAVE since these stations become free to randomly move from day to day. As a result, the long term precisions may be slightly degraded. The precision of North (N), East (E), Up (U) components and baseline length (L) are plotted against baseline length in Figure 5.1.

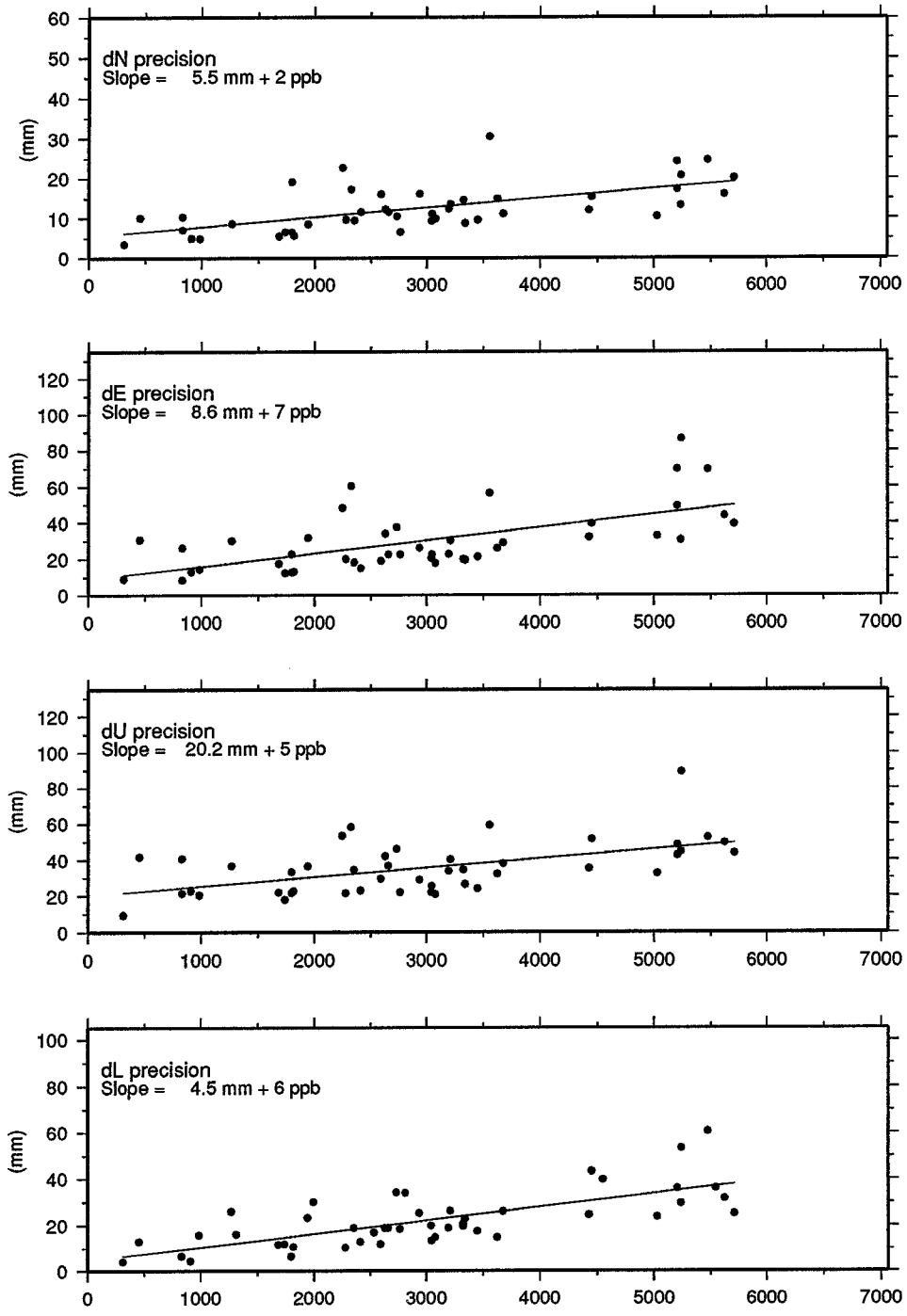

Figure 5.1 Long term precision estimates of N,E,U and baseline length with all regional stations estimated stochastically. Weighted L.S. estimates of line of best fit are shown for each component.

Weighted least squares estimates of lines of best fit yield 5.5 mm + 2 parts per billion (ppb), 8.6 mm + 7 ppb, 20.2 mm + 5 ppb and 4.5 + 6 ppb for N, E, U and L ,respectively. The few baselines on the Australian plate which were observed prior to 1992 have significantly worse long term precisions than those observed since 1992. This is due to systematic errors being introduced as a result of the reduced fiducial tracking networks in the earlier solutions, and such errors influence the overall precision estimates. If the long term precisions of all baselines are computed with YAR1, DS42 and CAVE estimated deterministically then the long term precisions are 4.7 mm + 1 ppb, 16.4 mm + 3 ppb, 21.9 mm + 3 ppb and 6.9 mm + 4 ppb for N, E, U and L, respectively. In all cases the constant term has increased slightly but the length dependent component decreases. These values indicate that the long term precision of baselines between 300 km and 6000 km have only a small dependence on baseline length - the major proportion of the error estimate is the constant term.

5.2 MOTION OF THE AUSTRALIAN PLATE

Motion of the Australian plate can be predicted by plate motion models, and has also been measured by geodetic observations. There are two SLR and two VLBI stations located in Australia, and the number of permanently tracking GPS stations is steadily increasing. In this analysis, an overall velocity field of sites on the Australian plate and the differential motion at two of the boundaries of the plate have been determined.

It is usual in such continental studies to compare the geodetic results with a plate motion model in order to determine whether the motion estimated agrees with geological predictions. Geodetic measurements usually span less than 20 years (or about 5 years in the case of GPS in Australia) whilst the plate motion models are based on geological events which have occurred over millions of years. Hence, the geodetic observations can be likened to an instantaneous snapshot in geological time. Thus, agreement between a current (or short term) and a geological estimate of plate motion indicates that the "instantaneous" motion of the plates is behaving in accordance with a long term average estimate of its motion.

If the geodetic and geological results are consistent then it is usually assumed that the geodetic results confirm the accuracy of the rigid plate motion model. If there are differences then either the geodetic results or the rigid plate motion model are in error. Since the "true" answer is not known, agreement between the two different methods is a reasonable indication that the geodetic results are accurate. As the number of cases where geodetic results agree with plate motion models increases, the faith in the

accuracy of the plate motion models also increases. However, disagreement with a model does not automatically indicate tectonic motion, as the "accuracy" of the geodetic results must still be proven.

5.2.1 Estimates of Station velocities

The velocities of all GPS stations located in the Australian and Indonesian regions were estimated in a GLOBK solution (with the exception of YAR1, DS42 and CAVE). The terrestrial reference frame was defined by fixing Earth rotation parameters and UT1 at TAH values (Tom Herring, pers. comm., 1994), fixing the latitude of KOKE/KOKR, constraining all other coordinates of the core IGS stations to 0.2 m and fixing the core site velocities to ITRF 92 values. The velocities of YAR1, DS42 and CAVE were fixed at the NNR-NUVEL-1A values. Figure 5.2 shows the resulting GPS velocities of stations relative to the terrestrial reference frame compared with the NNR-NUVEL-1A velocities. The velocities of stations located in Indonesia are discussed in 5.3.2.

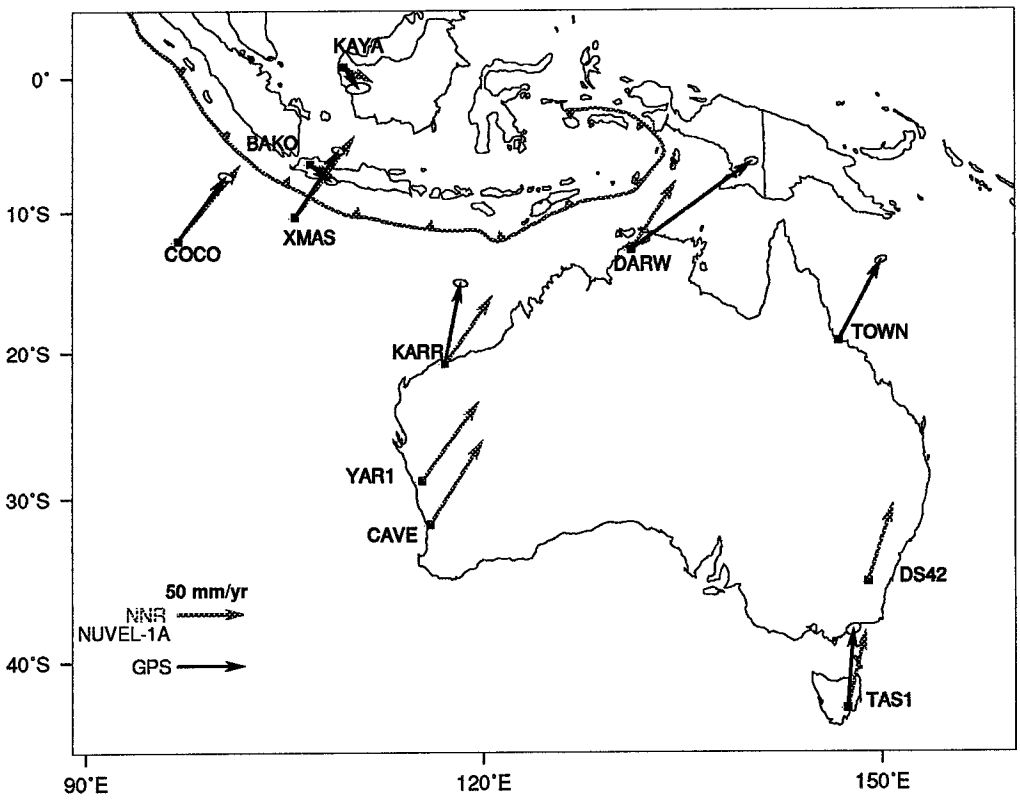

Figure 5.2 GPS determined velocities for stations located on the Australian Plate. NNR-NUVEL-1A velocities are also plotted. Formal 95% error ellipses are shown on GPS vectors. Formal errors are not available for NNR-NUVEL-1A vectors. Note that the velocities of YAR1, DS42 and CAVE are not estimated in this solution but are fixed at ITRF92 values for YAR1 and DS42, and NNR-NUVEL-1A value for CAVE.

In general, there is good agreement between the GPS and NNR-NUVEL-1A velocities. However, the GPS velocities at DARW and KARR are significantly different. The velocity of DARW is about 60 mm/year greater in the East component than NNR-NUVEL-1A, and KARR has a similar magnitude to the model but the direction of motion is rotated about 15° anticlockwise. There are three possible explanations for these apparent outliers in the estimated velocity field:

i) the results are tectonic signals;
ii) there is localised deformation occurring at DARW and KARR; or
iii) the velocity estimates are in error.

If these velocities are tectonic signals then this indicates major deformation in the Northwestern region of the Australian plate. A compression of 40 mm/year between Darwin and Townsville should cause large stresses and buckling in the lithosphere. This is not evident in the geology of Australia. If the motion at KARR is correct then there must be a block of the Australian plate which is moving away from the centre of Australia. Again, there is no geophysical evidence of this. In addition, the velocities of XMAS and COCO seem to agree with NNR-NUVEL-1A so if such a block existed, it must terminate somewhere in the Wharton Basin where it would again meet with the stable Australian plate. This is a very complicated and highly unlikely scenario. Thus, at this stage the possibility of the results being tectonic signals of intraplate deformation is questionable and is not supported by geophysical observations.

Local surveys connecting the GPS pillars at DARW and KARR to reference marks up to a distance of 100 m away show that there is no detectable local motion of the pillars at the millimetre level. Both DARW and KARR are pillars connected to bedrock located on hilltops. If the velocities estimated represent localised deformation then the hills on which they are located must be deforming relative to the surrounding region. This possibility is unlikely but has not yet been tested and so cannot be completely discounted. Larger local networks need to be observed in order to determine the stability of the hills on which the marks are located.

The third and most likely explanation is that the velocity estimates are in error. The observations at both DARW and KARR commenced in July 1992 hence there is only a small timespan from which to estimate a velocity for the stations. KARR was only occupied in the 1992 and 1993 campaigns, whilst DARW was also observed during the Jan'93 campaign. It is possible that two or three occupations of a station over only a one year period is not sufficient to accurately determine a station velocity. However, the

number and spacing of observations at COCO were very similar to those at DARW and the velocity estimate at COCO appears to agree with the NNR-NUVEL-1A prediction.

Is it just a coincidence that some velocity estimates agree with the model whilst others are quite different? It is difficult to prove an argument either way. How can the accuracy of a velocity estimate be checked? In the case of a station position, the long term precision of the position estimates is assumed to represent the accuracy of the position. However, there is only one velocity estimate for each station, so an analysis of repeatability is not possible. The formal errors of the velocity estimates are fairly small (ie about 5-10 mm for North and East components) and may not represent the accuracy of the estimates. If the NNR-NUVEL-1A predicted velocities at DARW and KARR are assumed to be correct then the velocities at DARW and KARR are in error and the formal errors underestimate the uncertainty by a large amount. This suggests that the formal errors are not reliable indicators of accuracy of the velocity measurements.

In order to investigate the accuracy of the velocity estimates, a number of solutions were performed with different amounts of data included in each. Starting with the earliest campaigns, each campaign was added in turn and velocities of stations with multiple occupancies were estimated. Figure 5.3 shows the resulting velocities for the stations in this analysis. The velocities of YAR1 and DS42 are fixed to NNR-NUVEL-1A values in all solutions.

It is immediately clear that the formal error ellipses do not represent the accuracy of the measurements. In many cases the first GPS estimate of a station velocity is very different from the NNR-NUVEL-1A vector and also differs from the final GPS estimate yet the error ellipse on the first estimate is about the same size as the final error ellipse. Hence, if only the first estimate of the velocity is available then it would appear that there is a significant difference between the GPS and the NNR-NUVEL-1A velocities when in fact it is only an artefact of the processing in that there is insufficient data to compute a reliable estimate of the velocity.

There is a pattern in how the velocities change with the addition of extra data. In general, the first estimate of a station velocity has a direction which is more Westward than the final estimate of the velocity (see e.g. XMAS, TOWN, TAS1 in Figure 5.3). As additional data is added to the solution the direction of the velocity swings towards the NNR-NUVEL-1A estimate. This may provide an explanation for the apparent Westward velocity estimated at KARR. Differences in the reference frame definitions from campaign to campaign will corrupt station velocity estimates, and the effect of such

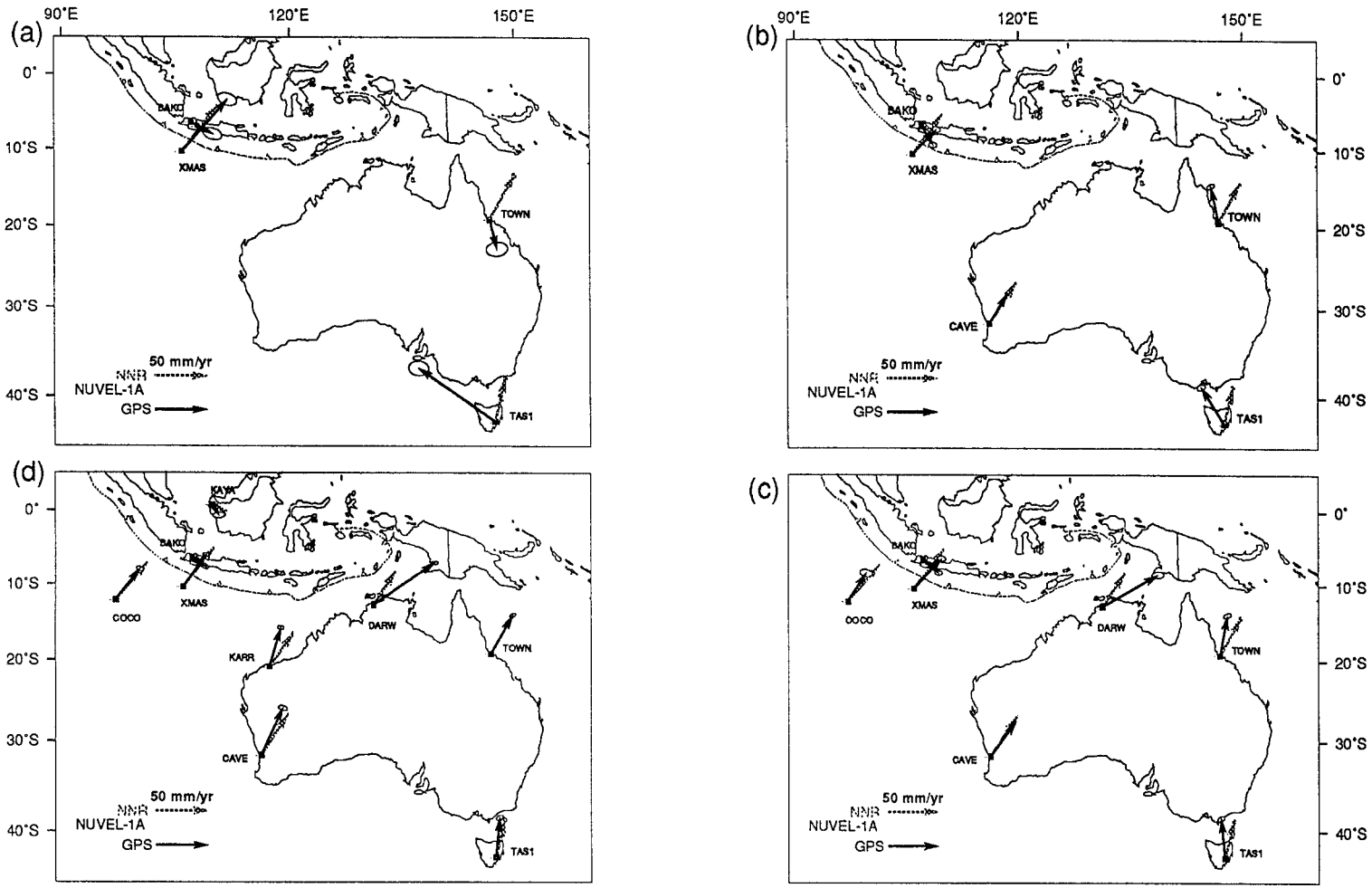

Figure 5.4 GPS velocity estimates for solutions using data from different campaigns: a) data to July 1991 b) data to September 1992; c) data to January 1993 and d) data to September 1993. NNR-NUVEL-1A velocities plotted for comparison. Formal 95% error ellipses plotted on GPS velocities. Note that the estimates of TOWN and TAS1 in (a) are based on two occupations only 6 months apart and hence are very unreliable.

biases will be reduced by having more data and a longer time scale over which to estimate a velocity.

There are two exceptions to this pattern - COCO and DARW. In the case of COCO, the first velocity estimate is only a few degrees from the final estimate, although the magnitude of the vector is 15% less. This is possibly due to the close proximity of COCO to XMAS and BAKO - two stations whose velocity estimates by September 1992 had stabilised to values very close to their final values. In the case of DARW, the velocity estimate after only six months (August 1992 - January 1993) is almost identical to the estimate after twelve months (August 1992 - September 1993). This is not understood, and the large East component in the velocity estimate at DARW needs further investigation.

5.2.1.1 Summary

The analysis of the velocity estimates of stations on the Australian plate yielded the following results:

- The velocities of COCO, XMAS, TAS1 and TOWN are not significantly different to the NNR-NUVEL-1A predicted values. This supports the notion that the Australian plate is behaving as a rigid mass, as assumed in the derivations of global plate motion models. The velocities of YAR1, DS42 and CAVE were held fixed in the solution to stabilise the solution such that geophysically meaningful results could be obtained.

- The velocity of KARR is 15° different in azimuth but agrees in magnitude with the NNR-NUVEL-1A prediction. The azimuthal difference is believed to be as a result of the short time span and small quantity of GPS data with at KARR. There was a mixture of receiver/antenna types used at KARR which was not accounted for with phase centre modelling in the processing of the data. This may have introduced small position errors. In addition, the site at Karratha has one of the largest ocean tide loading signals of Australia which was also not considered in the analysis. The modelling of these effects and the addition of future data should remove the azimuthal difference between the GPS and the plate moption model vectors.

- The magnitude and azimuth of DARW is significantly different to NNR-NUVEL-1A. In particular, the East component is 60 mm/year greater than the model prediction. This is not understood and requires further research and observations. The station at DARW is a concrete pillar which is locally stable (see Section 2.4.4) and only an Ashtech LMXII

antenna has been used so there should not be large phase centre variation effects at the site. Auslig installed a permanently operating Rogue SNR-8000 on the pillar in April 1994. The analysis of this data should resolve the apparent anomaly of the velocity estimate at DARW.

- Formal errors of the velocity parameters are not reliable indicators of the accuracy of the velocity estimates from the GLOBK solutions. Systematic errors introduced into a campaign (e.g. a bias in the reference frame definition, an error in the Earth rotation parameters) will corrupt the vecity estimate without affecting the formal errors of the solution. Such systematic baises dominate the velocity estiamtes of stations with short time spans between occupations and only few days of GPS observations.

- The GPS estimated velocities are shown in Table 5.1

Table 5.1 GPS estimates of station velocities compared to NNR-NUVEL-1A plate motion model values.

STATION	GPS		NNR-NUVEL-1A		GPS - NNR	
	N (mm/yr)	E (mm/yr)	N (mm/yr)	E (mm/yr)	ΔN (mm/yr)	ΔE (mm/yr)
COCO	48	36	54	44	-6	-8
XMAS	49	33	57	43	-6	-10
KARR	60	12	50	35	10	-23
DARW	64	91	50	33	14	58
TOWN	58	31	57	31	1	0
TAS1	58	4	57	13	1	-8

5.2.2 Measurement of Subduction at the Northern Plate Boundary

This project has determined geodetically that convergence of 64±2 mm/yr in a direction of 15°±4° is occurring between Christmas Island and West Java. This has been computed by subtracting the cartesian components of the velocities of both stations, and then converting these cartesian components into local N,E,U velocities at XMAS. This estimate is not significantly different to the initial estimate by Tregoning et al. [1994] of 67±7 mm/yr in a direction of 11°±4° and is in close agreement with the convergence predicted by NUVEL-1. This indicates that the global relative plate motion model used

in many geophysical studies of the Indonesian region does accurately represent the subduction process occurring beneath Java.

Since the relative velocity vector of XMAS to BAKO is nearly parallel to its relative position vector, I computed as a comparison the rate of change of baseline length of XMAS to BAKO from a weighted least squares slope through all daily GLOBK back filtered solutions (Figure 5.4) The weighted least squares slope of 62±2 mm/yr agrees with the rate obtained from a deterministic forward solution.

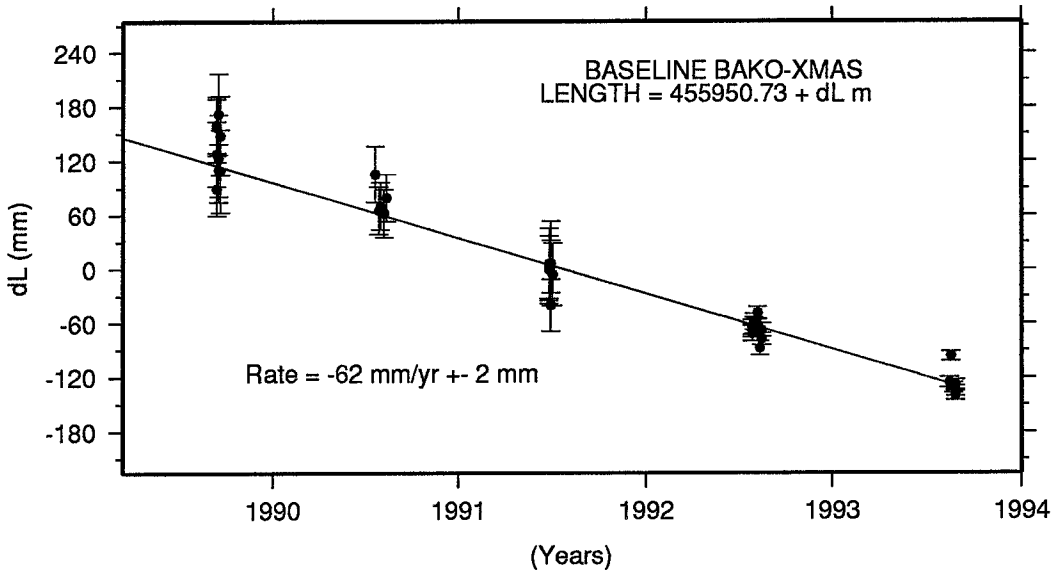

Figure 5.4 Convergence computed from changes in the magnitude of the vector between BAKO and XMAS between September 1989 and September 1993. Weighted least squares estimate of convergence is -62±2 mm/yr.

The direction of convergence is slightly Westward of the NUVEL-1 prediction but lies midway between the NUVEL-1 prediction (20°) and convergence direction estimated from slip vectors (11°±9°). However, the directions of all three estimates are not significantly different at the 95% confidence level.

This result provides a measure of the convergence across the plate boundary. This is a sum of the convergence of the two plates plus any elastic strain due to a locked plate boundary. It is not possible to separate these two quantities without independent knowledge of the true convergence between Australia and Java. XMAS and BAKO are at a sufficient distance from the plate boundary that the effect of elastic strain due to a locked interface (if present) will be small - probably less than 10 mm/year[1].

[1] Calculation performed using a program written by Rob McCaffrey using the algorithms of Okada [1985].

The fact that the measured convergence agrees with a long term geological average suggests that the GPS vector is mostly comprised of plate convergence, with very little elastic strain. There is little seismic activity on this section of the Java Trench which led Newcomb and McCann [1987] to suggest that the subduction is occurring aseismically. Reobserving this baseline immediately after a major thrust earthquake has occurred on the trench may provide further insight into this issue. However, the agreement between the GPS derived convergence and the geologically based plate motion model shows that the NUVEL-1 model accurately represents the motion across the Java Trench.

5.2.3 Measurement of Spreading at Southern Plate Boundary

If the Australian plate is subducting beneath Java and new sea-floor is being created at the Australian-Antarctic plate boundary then the distance from Australia to Antarctica should be increasing. GPS observations made at MAWS and MAW1 have been used to estimate such spreading. The NUVEL-1 model predicts that Mawson and Yaragadee are diverging at a rate of 66 mm/year. MAWS and MAW1 were observed simultaneously in February 1992 (days of year 046, 047) enabling a local tie in X, Y, Z to be computed. Figure 5.5 shows the baseline length from MAW1 to YAR1 for GIG'91 (days 030-039), SCAR'92 (days 004, 008, 012, 016, 020 - data processed at UC), Jan'93(days 017-023) and July'94 (days 187-190). MAWS coordinates in GIG'91 and SCAR'92 are corrected to MAW1 by a local cartesian coordinate tie (see table 3.3). I computed the rate of change of baseline length of MAW1 to YAR1 from a weighted least squares slope through all daily GLOBK back filtered solutions (Figure 5.6). The weighted least squares line of best fit yields a slope of 58±8 mm/year.

This rate is slightly slower than the NUVEL-1 prediction. However, the result is being significantly biased by the distance measurements during GIG'91 - a period where MAWS was the only station operating in Antarctica. Nonetheless, the result is not significantly different to the plate motion model prediction at a 95% confidence level Larson and Freymueller [1994] found agreement in spreading rates between GPS and NUVEL-1 for baselines between McMurdo (Antarctica) and stations in Australia. Thus, the motion at the Southern edge of the Australian plate does not appear to significantly differ from the plate motion model. The agreement of subduction and spreading rates from both geodetic measurements and geological models shows that the geodetic results presented are accurate and provide a consistent geophysical picture in the Australian region.

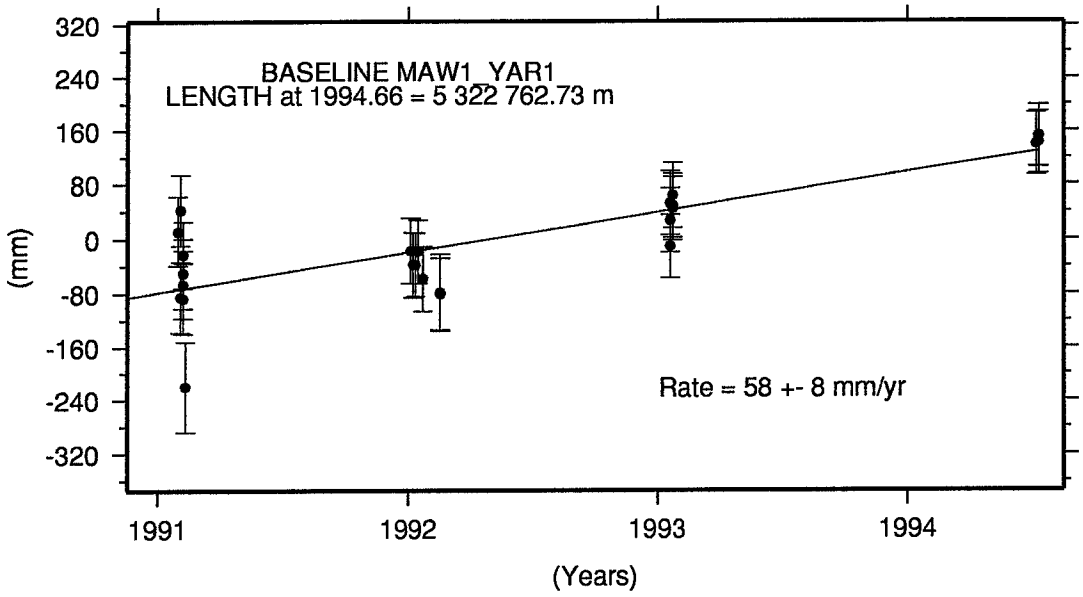

Figure 5.5 Spreading rate computed from changes in the magnitude of the vector between MAW1 and YAR1. Weighted least squares estimate of spreading is 58±8 mm/yr.

5.3 MOTIONS OF STATIONS IN INDONESIA

5.3.1 Velocities of Indonesian stations

The stations of BAKO, DEMP, KAYA and BPIL had sufficient data to estimate station velocities relative to the terrestrial reference frame (KRUI and CINA were only observed for 2 days in 1992, thus rendering a velocity estimate unreliable). Table 5.2 shows the estimated GPS velocities for these stations relative to NNR-NUVEL-1A velocities. Figure 5.2 shows the velocity estimates of BAKO and KAYA (for clarity, DEMP and BPIL were omitted).

Table 5.2 GPS determined velocities for stations located in Indonesia.

STATION	GPS		NNR-NUVEL-1A		GPS - NNR	
	N (mm/yr)	E (mm/yr)	N (mm/yr)	E (mm/yr)	dN (mm/yr)	dE (mm/yr)
BAKO	-13	16	-11	19	-2	-3
DEMP	-4	5	-10	18	6	-13
BPIL	-6	30	-10	18	4	12
KAYA	-16	11	-11	21	5	-10

The GPS estimate for BAKO is in close agreement with the NNR-NUVEL-1A value. The velocities of the other stations differ to some extent, with the East component of DEMP and KAYA about 10 mm less than the model, and BPIL 12 mm higher than the model. There is significantly more data observed at BAKO included in the solution hence it is not surprising that the velocity estimate of BAKO shows the closest agreement to NNR-NUVEL-1A. However, it has not been proven that the NNR-NUVEL-1A model is appropriate for the Indonesian region so there is no necessity for the GPS results to agree with the model. With the exception of BAKO, the velocity estimates of these Indonesian stations are not considered reliable. Section 5.2.1.1 showed that the accuracy of velocity estimates of stations with few reoccupations is questionable.

Tregoning et al. [1994] indicated that there was a significant difference between the GPS and NNR-NUVEL-1A velocity at BAKO but suggested that this may have been due to inconsistencies in the reference frame definitions. Now, I suggest that the constraints they applied to the terrestrial reference frame introduced distortions in the results which are no longer present in the estimates shown in Table 5.2. This does not discount the idea that there is a distinct Southeast Asian plate which is separate from the Eurasian plate but such distinction is not evident in these GPS results at these stations. Further investigation is required with a much larger distribution of stations if the motion of a Southeast Asian plate is to be determined using GPS velocity estimates.

5.3.2 Sunda Strait Surveys

The Sunda Strait is the transitional region where convergence of the Australian and Southeast Asian plates changes from frontal subduction beneath Java to oblique subduction beneath Sumatra. This section will give a summary of the current geophysical understanding of this area, describe the results of the GPS observations across the Sunda Strait and will make a geophysical interpretation of the geodetic results.

5.3.2.1 Geodetic Observations

In 1992 and 1993 a number of stations in the Sunda Strait area were observed using GPS as part of a larger field campaign spanning most of Indonesia. The locations of the stations are shown in Figure 3.1. Table 5.3 shows the observation pattern for the Sunda Strait stations.

Table 5.3 GPS observations on Sunda Strait stations. Data is a subset of a larger Indonesian dataset. Days of year for 1992 and 1993 shown. Observations were made in 24 hour sessions commencing at 0000 UT. Observations at BAKO not made simultaneously with Sunda Strait sites are omitted from the table.

Site	'92							'93					
	224	225	226	227	231	232	233	230	231	232	233	234	235
BAKO	x	x	x	x	x	x	x	-	-	-	-	-	x
CINA	-	-	-	-	x	x	x	-	x	x	x	x	-
BPIL	-	x	x	x	x	x	-	x	x	x	x	x	-
DEMP	x	x	x	x	x	-	-	-	x	x	x	x	-
KRUI	-	-	-	-	x	x	x	x	x	x	x	x	-
KAYA	x	x	-	-	-	-	-	-	x	x	x	x	x
KRAK	-	-	-	-	x	x	x	-	-	-	-	-	-

The GPS data were processed using GAMIT (see Section 2.3.1). As can be seen in Table 5.3, the collection of data was sporadic in 1992, resulting in few days of simultaneous observations between all sites. AS was switched on during days 228-230 of 1992. This resulted in poor quality global tracking data, as receiver hardware at the time was not sufficiently developed to maintain tracking of satellites under AS. Hence, the accuracy of the global orbit available on AS days is degraded, thereby introducing a bias into the processing of regional data. I decided not to process any regional data collected on days when AS was switched on. Unfortunately, this decimates the available 1992 Sunda Strait data by about 30%. In 1993, receiver problems at the BAKO site resulted in the station not operating at all during the Sunda Strait survey. This is regrettable, as BAKO was designed to be the principal station in the Sunda Strait project.

Owing to the small and fragmented nature of the GPS dataset, estimating station velocities in GLOBK yields questionable results (see section 5.2.1). The network is relatively small, with the longest baseline across the Strait being about 260 km. The closest global fiducial stations to the Sunda Strait are YAR1 (about 2 600 km to the Southeast) and TAIW (about 3 700 km to the Northeast). If only the core IGS sites (Table 3.2) are tightly constrained, then the relatively small network of the Sunda Strait is related to the reference frame only by the definition of the orbit from distant fiducial stations. The actual observations from the Sunda Strait network do not have enough

power to significantly improve the global orbit. The expected motion between the station on Java and Sumatra will probably not exceed 20 mm/yr, and the motion on the Central Sumatra fault may be in the range of 0-36 mm/yr. Therefore, without a close fiducial station the resolution of station velocities from as little as 2 days observations in 1992 followed by 4 days in 1993 is questionable. I decided to investigate this region by analysing changes in baseline lengths between the stations.

I intended to obtain coordinates and velocities for XMAS, COCO and BAKO from an analysis of the total Indonesian dataset, and then constrain these sites in the GAMIT solutions of the Sunda Strait data. This would effectively create a fiducial station at BAKO, and another two within 1000 km of the Strait. However, observations had ceased at COCO and XMAS before the completion of the 1992 Sunda Strait survey, and BAKO was not operating during the 1993 survey. Therefore, it is not possible to apply tight constraints consistently for both surveys - the addition or omission of BAKO, XMAS or COCO would change the regional orbit and possibly introduce a bias into the solution (Section 3.4.5 showed how the regional solutions are drastically affected by changes in the fiducial network - see also Larson et al., [1991]).

The Sunda Strait data was incorporated into the processing of all data in this analysis. The velocities of BAKO, XMAS, and COCO were fixed to NNR-NUVEL-1A values to add strength to the regional reference frame definition. The positions of the Sunda Strait stations were stochastically estimated (with the exception of BAKO), and the positions of all other regional stations were deterministically estimated. Baseline lengths were computed between simultaneously observed stations. BAKO was not operational during the 1993 Sunda Strait survey, but coordinates for the station were estimated in the days of the 1993 campaign when BAKO was operational. Since the coords of BAKO were deterministically determined, such estimates can be adopted as representing the coordinates of BAKO during the five days of the 1993 Sunda Strait survey.

5.3.2.2 GPS Results

GAMIT solutions were estimated with the terrestrial reference frame defined as in 4.4.3. Baseline lengths were computed where stations were observed simultaneously and mean distances computed from daily values. The stations of KRUI, CINA, DEMP, BPIL and KAYA were estimated stochastically whilst BAKO was estimated deterministically. Since the velocities of COCO, XMAS and BAKO have been found to agree with NNR-NUVEL-1A values (section 5.2.1.1 and 5.3.1), the velocities of these stations were also

fixed at NNR-NUVEL-1A values in order to add regional strength to the solutions. The results are shown in Table 5.4.

Table 5.4 Changes in baseline lengths between 1992 and 1993 GPS surveys. Standard deviation of change in length, Δ, computed from daily repeatability estimates of individual years. An asterisk indicates that the standard deviation is computed from one year only. Only sub-ten metre part of the length shown for 1993 dstances.

FROM	TO	Length in 1992 (m)	SIGMA (mm)	Length in 1993 (m)	SIGMA (mm)	Δ (mm)	SIGMA (mm)
BAKO	BPIL	133 953.506	9	3.489	13	-17	16
	DEMP	261 633.217	8	3.223	8	5	11
	CINA	261 497.701	25	7.704	4	3	25
	KRUI	353 427.403	16	7.436	10	33	19
BPIL	DEMP	175 420.446	3	0.457	6	11	7
	CINA	137 842.414	3	2.439	14	25	14
	KRUI	240 191.731	8	1.760	13	29	15
DEMP	CINA	97 268.081	*	8.073	5	-8	5
	KRUI	110 429.941	*	9.964	7	23	7
CINA	KRUI	105 744.970	5	4.961	7	-9	9

* only one day of simultaneous observation therefore sigma from repeatability not available

5.3.2.3 Interpretation of Results

An increase of about 25±10 mm/yr between BPIL and CINA, KRUI indicates that there is extension occurring at the Southern end of the Sunda Strait. Motion between DEMP and BPIL is much smaller and barely significant statistically. Motion is not significant between CINA and KRUI. Owing to the lack of simultaneous observations between DEMP, CINA and KRUI, we cannot state conclusively that strike slip motion is occurring between these sites. A 25 mm lateral slip on the fault would result in changes in the distances between DEMP-CINA and DEMP-KRUI of -10 mm and +15 mm, respectively. The geodetic measurements show changes in the baseline lengths of -8±5

mm and 23±7 mm, respectively, which are compatible with a 25 mm lateral motion. on the fault. Measurements between DEMP-BAKO and CINA-BAKO show no significant motion, although there may be extension between BAKO and KRUI

It appears that the fore-arc sliver is moving Northwestward away from Java as suggested by many geophysical papers (e.g. Huchon and Le Pichon, [1984]; Harjono et al., [1991]). It is not clear whether the region to the North of the fault is moving away from Java but it is certainly not moving at the same rate as the fore-arc, indicating that there is right lateral slip occurring on the fault. The GPS results are not conclusive and the addition of the 1994 observations may improve the understanding of this region. In addition, an M_W=6.8 right lateral earthquake occurred on the Central Sumatra fault on 15th February, 1994. The slip due to this earthquake (if any) could be determined by a comparison of the 1993 and 1994 solutions for the stations. This will be reported elsewhere.

5.4 COMPARISON WITH PREVIOUS GEODETIC STUDIES

The first geodetic measurement of convergence across the Java Trench subduction zone was by Tregoning et al. [1994]. The results in their paper are preliminary results of the analysis contained in this thesis. Their absolute velocity vectors for BAKO, XMAS and COCO are significantly different to those presented in Tables 5.1 and 5.2. Table 5.5 shows the preliminary estimates, the final estimates and the differences in the two values.

Table 5.5 Velocity estimates of BAKO, XMAS and COCO by Tregoning et al. [1994] (Prelim) and the final estimates of my analysis (Final). Differences between estimates are also shown.

STATION	MAGNITUDE		AZIMUTH		Δ	
	Prelim	Final	Prelim	Final	Mag (mm)	Az (°)
BAKO	30±2 mm	21±2 mm	140°±4°	129°±5°	9±3	-11±6
XMAS	53±2 mm	59±2 mm	37°±2°	34°±2°	6±3	-3±3
COCO	44±2 mm	60±2 mm	41°±5°	37°±2°	16±3	-4±5

There are a number of important differences between the two velocity solutions :-

- The absolute vector for XMAS in both solutions is similar, but the magnitude of the COCO vector has significantly increased in my final solution. The preliminary results

showed a 9 mm difference in magnitude between COCO and XMAS. This is not present in the final results, indicating that there is no relative motion between COCO and XMAS.

- The preliminary results showed that the motion of BAKO was significantly different to the NNR-NUVEL-1A prediction. This was tentatively interpreted as evidence for a block movement of the Southeast Asian region, although it was acknowledged that there may be some inconsistency in the reference frame definition. My final velocity estimate for BAKO is much closer to the NNR-NUVEL-1A value, and it could no longer be strongly stated that the motion of BAKO is significantly different to that of stable Eurasia. Whilst this does not discount that there is a distinct Southeast Asia block, it shows that BAKO appears to move as part of stable Eurasia.

- The relative motions between BAKO-XMAS and BAKO-COCO have not changed by as much as the absolute velocities of the three stations. This indicates that the preliminary absolute velocities were biased by some systematic effect which was reduced when the relative vectors were computed. The final absolute velocities agree more closely with the NNR-NUVEL-1A predictions, and provide a more realistic geophysical interpretation of the region (e.g. no significant relative motion between XMAS and COCO).

The fundamental difference in the preliminary and final solutions lies in the constraints applied to station coordinates and the estimation of Earth rotation parameters. In the preliminary solution, all core IGS stations were constrained to 5 mm horizontally and 10 mm vertically, with all velocities fixed to ITRF92 values. Polar motion and UT1 values were also estimated. Section 4.4 showed how this approach affected the solution. My final solution is more loosely constrained, with Earth rotation parameters fixed at values derived from VLBI analysis (Tom Herring, pers. comm., 1994), core stations constrained to 0.2 m in all components with the latitude of KOKE/KOKR constrained to 0.1 mm, and core velocities fixed at ITRF92 values. This approach removed the systematic biases in the absolute velocities at BAKO, XMAS and COCO. It also highlighted how sensitive the estimation of absolute velocities was to the constraints which defined the reference frame of the solution.

CHAPTER 6

CONCLUSIONS AND RECOMMENDATIONS

There are two main areas addressed by this thesis - the means to obtain and the quality of geodetic GPS measurements in the Australian region, and the geophysical interpretation of such measurements. The GPS measurements span 1989 to 1993 plus four days of 1994 data. During this period, the GPS system developed with many more satellites and fiducial tracking stations being available in the later campaigns. The geophysical interpretation can only be made once the geodetic data has been processed, analysed and proven to have the required accuracy. Providing evidence of accuracy of a continental network is very difficult, especially when the measurements are campaign based and in general repeated annually leaving little redundancy in the design of the surveys.

Reference Frame

A fundamental issue to this thesis is the determination and realisation of a terrestrial reference frame. This was important due to the changes in the fiducial tracking networks during this research. The better the fiducial network, the better will be the determination of the satellite orbits and hence the GPS solutions. In addition, having more stations in the region of interest which are also used in a global computation of the orbits leads to having a better regional orbit, and a better connection to the global reference frame.

Many investigators have different approaches to defining the terrestrial reference frame, and the thrust of the research influences how this issue is considered. In the case of this thesis, one major issue was to determine a velocity field for the Australian plate. This requires that all campaigns must refer to the same reference frame so that any differences in campaign networks can be interpreted as motion of the Earth relative to the reference frame. The

difficulties that this creates is that a bias in the realisation of the reference frame is interpreted as a deformation of the network and will propagate into the station velocity estimates. To this end, an analysis was undertaken to determine the most appropriate method of defining a reference frame that was as consistent as possible throughout all campaigns. Such analysis concluded that fixing Earth rotation parameters and UT1 at values derived from VLBI analysis, and fixing the latitude of KOKE/KOKR provided the most stable average reference frame.

Such a frame is quite loosely defined and this will have increased the scatter of the resulting measurements, but it is believed that the biases due to different fiducial networks have been minimised using this method. It is acknowledged that with the introduction of more permanent global tracking stations a different approach could be taken with a more recent dataset.

The precisions of the measurements of this project were found to be 4.7 mm + 1 ppb, 16.4 mm + 3 ppb, 21.9 mm + 3 ppb and 6.9 mm + 4 ppb in N, E, U and L, respectively. This was computed using all stations and baselines that have at least two simultaneous occupations. The results are at similar level as the results of other continental campaigns. There appears to be only a small dependence on baseline length, with most of the error being in the constant component. This indicates that a station can be positioned relative to the reference frame with a precision of a few centimetres, even when the station may be thousands of kilometres from the nearest global fiducial tracking station.

Tectonic Results

Subduction was measured at the Java Trench where the Australian and Southeast Asian plates collide. We found convergence of 64±2 mm/year in a direction of 15°±4°. This is not significantly different to the motion predicted by the NNR-NUVEL-1A model, and the azimuth also agrees with that predicted by local earthquake slip vectors. The convergence appears to be constant over the period of this project, although we acknowledge that it cannot be determined whether the plate boundary is locked or freely subducting. Newcomb and McCann [1987] suggested that the subduction occurs aseismically but an MW=7.5 earthquake in June 1994 very close to this region puts this interpretation in question.

A spreading rate of 58±8 mm/year was measured between Mawson, Antarctica and Yaragadee between January 1992 and July 1994. This agrees with the NNR-NUVEL-1A

prediction of 68 mm/year. Larson and Freymueller [1994] also report agreement between GPS and NNR-NUVEL-1A in an analysis of measurements between McMurdo, Antarctica and GPS stations in Australia. This spreading rate is also very close to the subduction rate measured at the Northern edge of the plate indicating that oceanic lithosphere is being created at the Southern boundary as quickly as it is being destroyed at the Northern edge. This provides support for the accuracy of the geodetic measurements presented in this thesis.

GPS velocities were estimated at a number of stations in the Australian region. It was found that the velocities of two station must be fixed at some predetermined values before the velocity solutions were realistic. With the velocity of YAR1 and DS42 fixed, the velocities of COCO, XMAS, BAKO, TOWN and TAS1 were found to agree with the NNR-NUVEL-1A values (the velocity of CAVE was also fixed in place of YAR1 in the 1989 solutions). Thus, the NNR-NUVEL-1A model seems to represent the motion of the Australian plate to within the uncertainties of these geodetic estimates.

Velocity estimates of KARR and DARW significantly differ to the general apparent motion of the Australian plate. The discrepancy at KARR is most likely due to the short time span of the available data. Other stations have shown a similar Westward azimuthal bias after only two occupations. It is not understood why the velocity of DARW differs so drastically from the general motion of the Australian plate. The estimated East component is 60 mm/year greater than the NNR-NUVEL-1A value. The analysis of DARW data also spans just one year, and light may be cast on this problem with the additional processing of more data from the station.

The apparent inconsistencies of two velocities do not cast doubt upon the velocity estimates of the other stations. The GPS campaigns were performed on a shoestring budget and no redundancy was built into the network design due to lack of funding. As for any measurements, it can be expected that there will be outliers and errors. The errors could be due to a particular receiver firmware, mulitpathing effects at a particular station or any number of reasons beyond the control of the analysts. Multiple occupations at a station, densification of the network and future observations will help to identify such errors.

The geodetic results were essentially inconclusive in determining motion between Java and Sumatra. The errors in the measurements were larger than any strongly detectable tectonic signal. However, this indicates that there is no tectonic motion detectable at the 10-20 mm

level. The stations used in the Sunda Strait network have only been occupied twice and both occupations were only for short periods (ie about five days). Further occupations will improve the precision of the geodetic results and hence the understanding of the tectonics in this area. A right lateral earthquake occurred on the Central Sumatra Fault on 15th February, 1994. It will be of great interest to compare the solutions of the 1994 Sunda Strait survey with the results presented here as this will indicate any deformation that may have occurred as a result of the earthquake.

The station velocities presented here for BAKO, XMAS and COCO are significantly different to those of Tregoning et al. [1994] and agree more closely with the NNR-NUVEL-1A model. The fundamental difference in the processing approach between that used by Tregoning et al. [1994] and that used in this analysis is that here I have held Earth rotation parameters and UT1 values fixed at estimates derived from VLBI experiments (Tom Herring, pers. comm., 1994). This made a significant change in the station velocities estimated in GLOBK.

Network Design

Observing annual GPS campaigns is the least expensive approach to crustal deformation studies, and it is possible to detect tectonic motion using such an approach. However, uncertainty in the measurements and the possible change in some important parameters (such as the number of satellites, the fiducial network configuration or the state of the ionosphere) make it difficult to determine whether a difference between campaigns is a tectonic signal or whether it is simply just noise within the long term precision estimate of the network. If GPS is to be used in Australia and elsewhere to determine discrepancies between geodetic measurements and plate motion models then the analysis needs to be done on a continual basis rather than sporadic campaigns. This would improve situations such as the Sunda Strait experiment of this project where uncertainties due to non simultaneous observations and equipment failure at crucial stations swamp the tectonic signals.

Suggested Future Developments and Studies

An interesting side issue that resulted from looking at the reference frame definition was that there appear to be inconsistencies between the GPS dataset used in this analysis and the ITRF 92 - in particular in the Southern Hemisphere. The ITRF is based on VLBI, SLR and GPS solutions with the velocity field incorporating the NNR NUVEL-1 model. There could

be a Northern hemisphere bias in any SLR and VLBI solutions due to the lack of stations in the Southern Hemisphere. However, at this stage of the history of GPS solutions of Southern hemisphere stations, the available SLR and VLBI coordinates are probably more accurate than the GPS coordinates. Future GPS solutions should be monitored to determine whether the discrepancies are due to the infancy of global GPS solutions, local tie errors between GPS and SLR/VLBI stations or whether there are distortions in ITRF 92.

It is possible to determine the relative motion across a plate boundary with only two annual measurements since the rate of motion of the Australian plate is greater than the current noise level of GPS solution. However, in order to determine the motion of a station relative to the reference frame, one cannot really be sure of the accuracy of a velocity estimate from two measurements. It was shown in this analysis that the formal errors of a velocity estimate are not necessarily reliable indicators of the accuracy of a velocity estimate. Another approach which can provide some indication of the accuracy of a velocity estimate is to monitor how the velocity of a station changes as more data from the station is processed. When the estimate stabilises to a constant value, it is probably a believable estimate. However, this approach requires many occupations of the stations, and many years before reliable estimates of velocities can be achieved. This is an area which needs further research. Ideally, the velocities of stations on the Australian plate should be estimated without fixing any station velocity as this will then provide information about the motion of the plate relative to the reference frame defined only by the velocities of stations on other plates.

The network of this project was reobserved in September 1994. Data from this has not been included in this thesis. In addition, AUSLIG has installed permanently operating Rogue SNR-8000 receivers at DARW, KARR, COCO and MAW1 as well as a number of other sites in Australia and Antarctica. The inclusion of the 1994 data would improve the velocity estimates at some stations which have short observations spans, and future processing of MAW1 data will improve the understanding of the motion of Australia relative to Antarctica.

APPENDIX 1

STATION OCCUPATIONS

STATION	YEAR	DAYS OF YEAR OBSERVED
ALGO	1991	030-039
	1992	207-213, 217-220, 224-227, 231-233, 244-247
	1993	017-024, 227-239, 242-245
	1994	187-190
ARE1	1994	187-190
AUSA	1989	254-263
	1990	200-223
BAHA	1989	254-263
	1990	200-223
BAKO	1989	254-263
	1990	200-223
	1991	030-039, 175-181
	1992	207-213, 217-220, 224-227, 231-233, 244-247
	1993	017-024, 227-229, 236-239, 242-245
BPIL	1992	225-227, 231-232
	1993	230-234

STATION	YEAR	DAYS OF YEAR OBSERVED
BRMU	1994	187-190
CAS1	1994	187-190
CAVE	1989	260-263
	1992	244-247
	1993	242-245
CINA	1992	231-233
	1993	231-234
COCO	1992	207-213, 217-220, 224-227
	1993	017-022, 227-239, 242-245
DARW	1992	207-213, 217-219
	1993	017-024, 227-239, 242-245
DEMP	1992	224-227, 231
	1993	231-234
DRAO	1991	175-181
	1992	207-213, 217-220, 224-227, 231-233, 244-247
	1993	017-024, 227-239, 242-245
	1994	187-190
DS10	1991	030-039, 175-181
	1992	046-047, 207-213, 217-220, 224-227, 231-233, 244-247
	1993	017-024, 227-239, 242-245
	1994	187-190
DS40	1991	030-039, 175-181
	1992	004, 008, 012, 016, 020
DS41	1992	046-047

STATION	YEAR	DAYS OF YEAR OBSERVED
DS42	1992	207-213, 217-220, 224-227, 231-233, 244-247
	1993	017-024, 227-239, 242-245
	1994	187-190
DS60	1991	030-039, 175-181
	1992	046-047, 207-213, 217-220, 224-227, 231-233, 244-247
	1993	017-024, 227-239, 242-245
	1994	187-190
ENGA	1989	254-263
	1990	200-220
FAIR	1991	030-039
	1992	046-047, 207-213, 217-220, 224-227, 231-233, 244-247
	1993	017-024, 227-239, 242-245
	1994	187-190
HART	1991	030-036, 038-039
	1992	207-213, 217-220, 224-227, 231-233, 244-247
	1993	017-024, 227-239, 242-245
	1994	187-190
HERS	1992	046-047
HOB1	1993	227-239, 242-245
	1994	187-190
HONE	1991	030-033, 038-039
HUAH	1990	200-223

STATION	YEAR	DAYS OF YEAR OBSERVED
JPL1	1991	030-039
	1992	207-213, 217-220, 224-227, 231-233, 244-247
	1993	017-024, 227-239, 242-245
	1994	187-190
KARR	1992	207-213, 217-220, 224-227, 231-233, 244-247
	1993	017-024, 227-239, 242-245
KOKE	1989	254-263
	1990	200-223
	1991	030-039, 175-181
KOKR	1991	030-039
	1992	046, 207-213, 217-220, 224-227, 231-233, 244-247
	1993	017-024, 227-239, 242-245
	1994	187-190
KOSG	1991	030-039
	1992	046-407, 207-213, 217-220, 224-227, 231-233, 244-247
	1993	017-024, 227-239, 242-245
	1994	187-190
KOUR	1993	017-024, 227-239, 242-245
	1994	187-190
MAC1	1994	187-190
MASP	1992	207-213, 217-220, 224-227, 231-233, 244-247
	1993	017-024, 227-239, 242-245
	1994	187-190
MATE	1992	207-213, 217-220, 224-227, 231-233, 244-247
	1993	017-024, 227-239, 242-245

STATION	YEAR	DAYS OF YEAR OBSERVED
MAW1	1992	046-047
	1993	017-021, 023
	1994	187-190
MAWS	1991	030-039
	1992	004, 008, 012, 016, 020, 046-047
MCMU	1992	209-213, 217-220, 224-227, 231-233, 244-245, 247
MCM1	1993	227-239, 242-245
	1994	187-190
METS	1992	207-213, 217-220, 224-227, 231-233, 244-247
MOJ1	1989	254-259, 261-263
	1990	200-223
NALL	1992	046-047, 207-213, 217-220, 224-227, 231-233, 244-247
ONSA	1989	254-261
	1990	200-201, 204-233
	1992	046-407, 207-213, 217-220, 224-227, 232-233, 244-247
	1993	017-024, 227-239, 242-245
	1994	188-190
ORRO	1990	200-233
PAMA	1992	207-213, 217-220, 224, 226-227, 231-233, 244-247
	1993	017-024, 227-232, 239, 242
	1994	187-190
PERT	1993	238-239, 242-245

STATION	YEAR	DAYS OF YEAR OBSERVED
RIC1	1989	254-259, 261-263
	1990	200-223
	1991	175-181
RCM2	1992	211-213, 217-220, 224-227, 231
	1993	023, 227-234
S01R	1990	200-223
	1991	175-181
SANG	1991	030-039
SANT	1992	207-208, 210-213, 217-220, 224-227, 231-233, 244-247
	1993	017-024, 227-239, 242-245
	1994	187-190
STJO	1992	207, 209-213, 217-220, 224-227, 231-233, 244-247
	1993	017-024, 227-239, 242-245
	1994	187-190
TAIW	1992	207-213, 217-220, 224-227, 231-233, 244-247
	1993	018-024, 227-239, 242-245
	1994	187-190
TAS1	1990	200-223
	1991	030-039, 175, 177-181
	1992	046-047, 207-210, 244-247
	1993	017-024
TOWN	1991	030-039, 175-181
	1992	046-047, 207-213, 217-220, 224-227, 231-233, 244-247
	1993	227-239, 242-245

STATION	YEAR	DAYS OF YEAR OBSERVED
TROM	1991	033-039
	1992	046-407, 207-213, 217-220, 224-227, 231-233, 244-247
	1993	017-024, 227-239, 242-245
	1994	187-190
TSU1	1989	254-263
	1990	200-223
	1991	030-039, 175-181
USUD	1991	031-033, 035, 037
USU2	1992	046-047, 208, 212, 217, 233
USU3	1993	017-024, 227-239, 242-245
	1994	187-190
WELL	1990	200-223
	1991	030-039, 175-181
	1992	046-047
WES1	1989	254-263
	1990	200-223
	1991	175-181
WTZM	1989	254-263
	1990	200-223
	1991	030-039
WETT	1991	175-181
WTZ1	1992	046-407, 207-213, 217-220, 224-227, 231-233, 244-247
	1993	017-024, 227-235
	1994	187-190

STATION	YEAR	DAYS OF YEAR OBSERVED
XMAS	1989	254-263
	1990	200-223
	1991	175-181
	1992	208-213, 217-220, 224-227
	1993	227-239
YAR1	1991	030-039
	1992	046-407, 207-213, 217-220, 224-227, 231-233, 244-247
	1993	017-024, 227-239, 242-245
	1994	187-190
YELL	1989	254-263
	1991	030-039, 175-181
	1992	046-407, 207-213, 217-220, 224-227, 231-233, 244-247
	1993	017-024, 227-239, 242-245
	1994	187-190

APPENDIX 2

A2.1 STATION COORDINATES

Core and regional station coordinates from a solution with core station coordinates constrained to 0.2 m in all components, latitude of KOKE/KOKR constrained to 0.1 mm and all core station velocities fixed at ITRF92 values are shown in table A.1. Formal one sigma standard deviations are also shown. Coordinates are as at 2nd September, 1993 (1993.6694).

Table A.1 Cartesian coordinates of stations.

Station	Cartesian Coordinates (in metres) X	Y	Z
		** Core Stations **	
ALGO	918 129.647 ± 0.043	-4 346 071.129 ± 0.009	4 561 977.750 ± 0.001
DS10	-2 353 614.052 ± 0.046	-4 641 385.277 ± 0.024	3 676 976.440 ± 0.002
DS42	-4 460 995.986 ± 0.027	2 682 557.210 ± 0.044	-3 674 444.153 ± 0.001
DS60	4 849 202.600 ± 0.004	-360 329.142 ± 0.048	4 114 912.856 ± 0.001
FAIR	-2 281 621.216 ± 0.015	-1 453 595.632 ± 0.023	5 756 961.895 ± 0.001
HART	5 084 625.381 ± 0.027	2 670 366.502 ± 0.051	-2 768 494.371 ± 0.001
KOKE	-5 543 817.886 ± 0.021	-2 054 582.681 ± 0.055	2 387 858.367 ± 0.001
KOKR	-5 543 837.968 ± 0.021	-2 054 587.304 ± 0.055	2 387 809.539 ± 0.001
KOSG	3 899 225.426 ± 0.004	396 731.813 ± 0.039	5 015 078.139 ± 0.001
SANT	1 769 693.161 ± 0.050	-5 044 573.982 ± 0.018	-3 468 321.329 ± 0.001
TROM	2 102 940.560 ± 0.007	721 569.423 ± 0.021	5 958 191.978 ± 0.002
WTZ1	4 075 578.761 ± 0.010	931 852.676 ± 0.041	4 801 569.816 ± 0.001
YAR1	-2 389 025.258 ± 0.050	5 043 316.874 ± 0.024	-3 078 531.199 ± 0.001
YELL	-1 224 452.298 ± 0.027	-2 689 215.957 ± 0.012	5 633 638.232 ± 0.001
		** Regional Stations **	
AUSA	-3 942 242.116 ± 0.081	3 468 859.311 ± 0.119	-3 608 197.420 ± 0.058
BAHA	3 633 911.154 ± 0.051	4 425 277.847 ± 0.041	2 799 862.404 ± 0.014
BAKO	-1 836 968.688 ± 0.061	6 065 617.233 ± 0.019	-716 258.052 ± 0.001
BPIL	-1 708 327.972 ± 0.061	6 102 695.225 ± 0.018	-720 766.379 ± 0.001
CAVE	-2 375 390.447 ± 0.048	4 875 553.893 ± 0.024	-3 345 387.550 ± 0.002
CINA	-1 594 719.555 ± 0.062	6 140 752.566 ± 0.019	-652 609.891 ± 0.006
COCO	-741 949.685 ± 0.062	6 190 961.634 ± 0.008	-1 337 769.082 ± 0.001

Station	Cartesian Coordinates (in metres)		
	X	Y	Z
DARW	-4 091 358.570 ± 0.047	4 684 606.858 ± 0.041	-1 408 580.911 ± 0.001
DEMP	-1 636 587.786 ± 0.061	6 138 897.891 ± 0.017	-564 833.536 ± 0.001
DS40	-4 460 987.947 ± 0.027	2 682 362.370 ± 0.045	-3 674 626.639 ± 0.003
KARR	-2 713 831.983 ± 0.053	5 303 935.188 ± 0.027	-2 269 515.509 ± 0.001
KAYA	-2 119 512.687 ± 0.060	6 015 103.282 ± 0.022	89 809.708 ± 0.001
KRUI	-1 529 657.048 ± 0.062	6 165 260.274 ± 0.017	-572 934.056 ± 0.004
MAWS	1 111 246.991 ± 0.023	2 169 171.202 ± 0.014	-5 874 393.976 ± 0.011
MAW1	1 111 287.156 ± 0.022	2 168 911.338 ± 0.012	-5 874 493.946 ± 0.005
MCM1	-1 310 696.249 ± 0.004	310 469.156 ± 0.013	-6 213 368.625 ± 0.002
SING	-1 52 073.482 ± 0.062	6 192 742.050 ± 0.016	143 324.609 ± 0.001
TAIW	-3 024 781.680 ± 0.049	4 928 937.000 ± 0.030	2 681 234.308 ± 0.001
TAS1	-3 950 184.086 ± 0.026	2 522 364.655 ± 0.040	-4 311 588.796 ± 0.004
TOWN	-5 041 024.834 ± 0.033	3 296 980.396 ± 0.050	-2 090 553.535 ± 0.001
TSU1	-3 957 193.757 ± 0.034	3 310 191.436 ± 0.039	3 737 733.301 ± 0.005
USUD	-3 855 262.462 ± 0.035	3 427 432.542 ± 0.039	3 741 020.682 ± 0.004
USU3	-3 855 262.835 ± 0.034	3 427 432.666 ± 0.039	3 741 020.278 ± 0.001
WELL	-4 780 649.012 ± 0.049	436 507.092 ± 0.057	-4 185 440.604 ± 0.041
XMAS	-1 696 462.924 ± 0.060	6 039 563.059 ± 0.017	-1 149 236.411 ± 0.001

A2.2 CORE STATION VELOCITIES

Velocities of core stations were fixed at ITRF 92 values as listed in Table A.2.

Table A.2 Cartesian velocities of core stations.

Station	X Velocity (m)	Y Velocity (m)	Z Velocity (m)
ALGO	-0.015	-0.006	0.004
DS10	-0.014	0.004	-0.006
DS42	-.039	0.004	0.042
DS60	-0.007	0.020	0.015
FAIR	-0.021	-0.004	0.042
HART	-0.003	0.019	0.015
KOKR	-0.008	0.063	0.031
KOSG	-0.014	0.017	0.007
SANT	0.001	-0.005	0.008
TROM	-0.017	0.013	0.005
WTZ1	-0.017	0.016	0.009
YAR1	-0.045	0.008	0.053
YELL	-0.022	-0.001	-0.005

REFERENCES

Allègre, C., The Behavior of the Earth, *Harvard University Press*, Cambridge, Massachusetts and London, England, 1988.

Argus, D. F., and R. G. Gordon, No-Net-Rotation Model of Current Plate Velocities Incorporating Plate Motion Model NUVEL-1, *Geophys. Res. Lett.*, 18, 2039-2042, 1991.

Baker, T., Perturbations of Survey Procedures in the Coastal Zone, in *The 2nd Australasian Hydrographic Symposium, 9th-12th December,* University of NSW, 1991.

Baksi, A. K., Concordant sea-floor spreading rates obtained from geochronology, astrochronology and space geodesy, *Geophys. Res. Lett.*, 21, 133-136, 1994.

Blewitt, G., An automatic editing algorithm for GPS data, *Geophys. Res. Lett.*, 17, 199-202, 1990.

Blewitt, G., Advances in Global Positioning System Technology for Geodynamics Investigations: 1978-1992, in *Contributions of Space Geodesy to Geodynamics: Technology, AGU Geodynamics Series*, 25, 195-213, 1993.

Bock, Y., Fang, P., Stark, K., Zhang, J., Genrich, J., Wdowinski, S. and S. Marquez, SCRIPPS Orbit and Permanent Array Center: Report to '93 IGS Bern Workshop, in *Proceedings of the 1993 IGS Workshop, 25-26 March, 1993*, 101-110, Astronomical Institute University of Berne, G. Beutler and E. Brockman Eds., Druckerei der Universität Bern, 1993a.

Bock, Y., Agnew, D. C., Fang, P., Genrich, J. F., Hager, B. H., Herring, T. A., Hudnut, K. W., King, R. W., Larsen, S., Minster, J. B., Stark, K., Wdowinski, S. and F. K. Watt, Detection of crustal motion from the Landers earthquake sequence using continuous geodetic measurements, *Nature,* 361, 337-340, 1993b.

Bonatti, E. and K. Crane, Oceanic Fracture Zones, *Sci. Amer.*, 250, 36-47, 1984.

Boucher, C., Current Intercomparisons between CTS's, in *Reference Frames*, Kovalevsky, J. and I. Mueller Eds., 327-348, 1989.

Boucher, C., Altamimi, Z. and L. Duhem, ITRF 92 and its associated velocity field. *IERS Technical Note 15*, 1993.

Brunner, F. K. and P. Tregoning, Investigation of Height Repeatability from GPS Measurements, *Aust. J. Geod. Photogram. Surv.*, 60, 33-48, 1994.

Oral, M. Burc, Global Positioning System (GPS) Measurements in Turkey (1988-1992): Kinematics of the Africa-Arabia-Eurasia Plate Collision Zone, *PhD Thesis*, MIT, 1994.

Burchfiel, B. C., The Continental Crust, *Sci. Amer.*, 249, 86-98, 1983.

Calais, E., Bock, Y., FGenrich, G. J., McCaffrey, R., Stevens, C., Fauzi, Zwick, P., Beavan, J., Tregoning, P., Brunner, F. K., Puntodewo, S. S. O., Subarya, C. and J. Rais, Plate Kinematics and Crustal Deformation in Southeast Asia from the Global Positioning System, in preparation, 1994.

Cannon, W. H., The Classical Analysis of the Response of a Long Baseline Radio Interferometer, *Geophys. J. Roy. Astr. Soc.*, 53, 503-530, 1978.

Carlson, R. L., Plate Motions, Boundary Forces, and Horizontal Temperature Gradients: Implications for the Driving Mechanism, *Tectonophysics*, 99, 149-164, 1983.

Chase, C. G., Plate kinematics: The Americas, East Africa and the Rest of the World, *Earth Planet. Sci. Lett*, 37, 353-368, 1978.

Christodoulidis, D. C., Smith, D. E., Kolenkiewicz, R., Klosko, S. M., Torrence, M. H. and P. J. Dunn, Observing Tetonic Plate Motions and Deformations From Satellite Laser Ranging, *J. Geophys. Res.*, 90, 9249-9263, 1985.

CSTG (International Coordination of Space Techniques for Geodesy and Geodynamics) Bulletin, M. Chin, ed., *National Geodetic Survey*, Vol. 2, 1989.

Cox, A., Doell, R.R. and G. B. Dalrymple, Radiometric time scale for Geomagnetic Reversals, *Quart. Jour. Geol. Soc. London*, 124, 53-66, 1968.

Cox, A. and R. B. Hart, Plate Tectonics: How it Works, *Blackwell Scientific Publications*, 391pp, 1986.

Davis, J. L., Prescott, W. H., Svarc, J. L. and K. J. Wendt, Assesssment of Global Positioning System Measurements for Studies of Crustal Deformation, *J. Geophys. Res.*, 94, 13635-13650, 1989.

DeMets, C., Gordon, R. G., D. F. Argus, and S. Stein, Current plate motions, *Geophys. J. Int.*, 101, 425-478, 1990.

DeMets, C., Earthquake Slip Vectors and Estimates of Present-Day Plate Motions, *J. Geophys. Res.*, 98, 6703-6714, 1993.

DeMets, C., R. G. Gordon, D. F. Argus, and S. Stein, Effects of recent revisions to the geomagnetic reversal time scale on estimates of current plate motions, *Geophys. Res. Lett.*, 21, 2191-2194, 1994a.

DeMets, C., Gordon, R. G. and P. Vogt, Location of the Africa-Australia-India Triple Junction and Motion between the Australian and Indian Plates: Results from an Aeromagnetic Investigation of the Central Indian and Carlsberg Ridges, *Geophys. Jour. Int.*, in press, 1994b.

Dermanis, A. and I. I. Mueller, Earth Rotation and Network Geometry Optimization for Very Long Baseline Interferometers, *Bull. Géod.*, 52, 131-158, 1978.

Dietz, R. S., Continent and Ocean Basin Evolution by Spreading of the Sea Floor, *Nature,* 190, 854-857, 1961.

Dixon, T. H., An Introduction to the Global Postioning System and some Geological Applications, *Review of Geophysics,* 29, 249-276, 1991.

Dong, D., N. and Y. Bock, Global Positioning System Network Analysis with Phase Ambiguity Resolution Applied to Crustal Deformation Studies in California, *J. Geophys. Res.*, 94, 3949-3966, 1989.

Dow, J. M., Martin Mur, T. J., Feltens, J. and C. Garcia Martinez, The ESOC GPS Facility: Report on the IGS 1992 Campaign and outlook, in *Proceedings of the 1993 IGS Workshop, 25-26 March, 1993*, 111-122, Astronomical Institute University of Berne, G. Beutler and E. Brockman Eds., Druckerei der Universität Bern, 1993.

Du Toit, A. L., Our Wandering Continents, Edinburgh, Oliver and Boyd, 366pp, 1937.

Fang, P., Bock, Y., Genrich, J. F., Otero, V., Stark, K., Wdowinski, S., Herring, T. A. and R. W. King, Determination of Precise Satellite Ephemerides, High Frequency Earth Rotation, and Crustal Deformation before and during the IGS Campaign, *EOS Trans. AGU,* 73, 134, 1992.

Farrell, W. E., Deformation of the Earth by Surface Loads, *Reviews of Geophys. Space Physics,* 10, 761-797, 1972.

Feigl, K., L., King, R., W., and T. A. Herring, A Scheme for Reducing the Effect of Selective Avalability on Precise Geodetic Measurements from the Global Positioning System, *Geophys. Res. Lett,* 18, 1289-1292, 1991.

Feigl, K. L., Agnew, C.A., Bock, Y., Dong, D., Donnellan, A., Hager, B. H., Herring, T. A., Jackson, D. D., Jordan, T. H., King, R. W., Larsen, S., Larson, K. M., Murray, M. H., Shen, Z. and F. H. Webb, Space Geodetic Measurement of Crustal Deformation in Central and Southern California, 1984-1992, *J. Geophys. Res,* 98, 21677-21712, 1993.

Forsyth, D. and S. Uyeda, On the Relative Importance of Driving Forces of Plate Motion, *Geophys. J. R. Astron. Soc.*, 43, 163-200, 1975.

Freymueller, J. T., Kellog, J. N. and V. Vega, Plate Motions in the North Andean Region, *J. Geophys. Res.*, 98, 21853-21863, 1993.

Gelb, A. ed., Applied Optimal Estimation, *MIT Press*, Cambridge, Mass., 374pp, 1974.

Genrich, J., Bock, Y., McCaffrey, R., Calais, E., Stevens, C. and C. Subarya, Accretion of the Aouthern Banda Arc to the Australian Plate Margin Determined by Global Positioning System Measurements, submitted to *Science*, 1994.

Ghose, R., Yoshioka, S. and K. Oike, Three-dimensional Numerical Simulation of the Subduction Dynamics in the Sunda Arc Region, Southeast Asia, *Tectonophysics*, 181, 223-255, 1990.

Gripp A. E., and R. G. Gordan, Curent Plate Velocities Relative to the Hotspots incorporating the NUVEL-1 Global Plate Motion Model, *Geophys. Res. Lett,* 17, 1109-1112, 1990.

Gurtner, W., Beutler, G., Botton, S., Rothacher, M., Geiger, A., Khle, H. -G., Schneider, D and A. Wiget, The use of the Global Positioning System in Mountainous Areas, *Man. Geod.*, 14, 53-60, 1989.

Hamilton, W., Tectonics of the Indonesian region, *U.S. Geol. Survey Prof. Paper 1078*, 345 pp, 1979.

Harjono, H., Diament, M., Dubois, J. and M. Larue, Seismicity of the Sunda Srait: Evidence for crustal extension and volcanological implications, *Tectonics*, 10, 17-30, 1991.

Heflin, M., Bertiger, W., Blewitt, G., Freedman, A., Hurst, K., Lichten, S., Lindqwister, U., Vigue, Y., Webb, F., Yunck, T. and J. Zumberge, Global Geodesy using GPS Without Fiducial Sites, *Geophys. Res. Lett.*, 19, 131-134, 1992.

Herring, T. A., Davis, J. L. and I. I. Shapiro, Geodesy by Radio Interferometry: The Application of Kalman Filtering to the Analysis of Very Long Baseline Interferometry Data, *J. Geophys. Res.*, 95, 12561-12581, 1991a.

Herring, T. A., Dong, D. and R. W. King, Sub-milliarcsecond Determination of Pole Position using Global Positioning System Data, *Geophys. Res. Lett.*, 18, 1893-1896, 1991b.

Herring, T. A., Documentation for the Global Kalman filter VLBI and GPS analysis program (GLOBK), Version 3.0. Massachusetts Institute of Technology, unpublished, 1992.

Hess, H. H., History of Ocean Basins, in *Petrologic Studies: A Volume to honour A. F. Buddington*, eds. A. E. J. Engle, H. L. James and B. L. Leonard, 599-620, 1962.

Holmes, A., Principles of Physical Geology, London and Edinburgh, Thomas Nelson and Sons, 1945.

Huchon, P. and X, Le Pichon, Sunda Strait and Central Sumatra fault, *Geology*, 12, 668-672, 1984.

Isacks, B. and P. Molnar, Distribution of Stresses in the Descending Lithosphere from a Global Survey of Focal Mechanisms of Mantle Earthquakes, *Rev. Geophys.*, 9, 103-174, 1971.

Jarrard, R. D. and S. Sassajima, Palaeomagnetic Synthesis for Southeast Asia: Constraints on Plate Motions, *in* Hayes, D. E. ed., The Tectonic and Geologic Evolution of southeast Asian seas and islands: *AGU Geophysical Monograph,* 23, 293-316, 1980.

Jarrard, R. D., Relations among Subduction Parameters, *Rev. Geophys.*, 24(2), 217-284, 1986.

Katili, J. A. and Hehuwat, On the Occurrence of Large Transcurrent Faults in Sumatra, Indonesia, *Osaka City Univ. J. Geosciences,* 10, 5-17, 1967.

King, R. W., Collins, J., Masters, E. G., Rizos, C. and A. Stoltz, Surveying with GPS, *Monograph No. 9*, School of Surveying, The University of New South Wales, Sydney, 1985.

King, R. W. and Y. Bock, Documentation for the GAMIT GPS Analysis Software, Massachusetts Institute of Technology and Scripps Institution of Oceanography, Release 9.1, unpublished, 1993.

Kouba, J., Tétrealt, P., Ferland, R. amd F. Lahaye, IGS data Processing at the EMR Master Active Control System Centre, in *Proceedings of the 1993 IGS Workshop, 25-26 March, 1993*, 123-132, Astronomical Institute University of Berne, G. Beutler and E. Brockman Eds., Druckerei der Universität Bern, 1993.

Lambeck, K., Geophysical Geodesy - The Slow Deformation of the Earth, *Clarendon Press,* Oxford, 718pp, 1988.

Larson, K. M. and D. C. Agnew, Application of the Global Positioning System to Crustal Deformation Measurement: 1. Precision and Accuracy, *J. Geophys. Res.*, 96, 16547-16565, 1991.

Larson, K. M., Webb, F. H. and D. C. Agnew, Applications of the Global Positioning System to Crustal Deformation Measurements, 2, The Infuence of Orbit Determination Errors, *J. Geophys. Res.*, 96, 16567-16584, 1991.

Larson, K. M. and J. Freymueller, Relative Motions of the Australian, Pacific and Antarctic paltes estimated by the Global Positioning System, *Geophys. Res. Lett.* in press, 1994.

Lassal, O., Huchon, P. and H. Harjono, Extension crustale dans le détroit de la Sonde (Indonésie). Données de la sismique réflexion (campagne KRAKATAU), *C. R. Acad. Sci. Paris,* t. 309, Série II, 205-212, 1989.

Le Pichon, X., Sea Floor Spreading and Continental Drift, *J. Geophys. Res.,* Vol. 73, No 12, 3663-3697, 1968.

Le Pichon, X., Angelier, J. and J. C. Sibuet, Subsidence and Stretching, in *Continental Margin Geology: American Association of Petroleum Geologists Memoir,* 34, 731-741, 1982.

Lichten, S. M., Marcus, S. L. and J. O. Dickey, Sub-daily Resolution of Earth Rotation Variations with Global Positioning System Measurements, *Geophys. Res. Lett.,* 19, 537-540, 1992.

Ma , C., Ryan, J. W., Gordon, D., Caprette, D. S. and W. E. Himwich, Reference Frames from CDP VLBI Data, in *Contributions of Space Geodesy to Geodynamics: Earth Dynamics, AGU Geodynamics Series,* 24, 121-145, 1993.

Manning, J. and B. Harvey, A National Geodetic Fiducial Network, *The Aust. Surveyor, Vol.* 37, No. 2, 87-90, 1992.

McCaffrey, R., Slip Vectors and Stretching of the Sumatran fore arc, *Geology,* 19, 881-884, 1991.

McCaffrey, R., Oblique Plate Convergence, Slip Vectors and Forearc Deformations, *J. Geophys. Res.,* 97, 8905-8915, 1992.

McCaffrey, R., Global Variability in Subduction Thrust Zone - Forearc Systems, *Pure Appl. Geophys.,* 141, 173-224, 1994.

Melbourne, W. G., Fichser, S. S., Neilan, R. E., Yunck, T. P., Engen, B., Reigber, Ch. and S Tatevjan, The First GPS IERS and Geodynamics Experiment -- 1991, in *Permanent Satellite Tracking Networks for Geodesy and Geodynamics,* International Association of Geodesy Symposium No. 109, G. Mader, Ed., Vienna, Austria, August 11-24, 1991.

Menard, H. W., The Deep-Ocean Floor, *Sci. Amer.,* 221, 127-136, 1969.

Milliken, R. J. and C. J. Zoller, Principle of Operation of NAVSTAR and System Characteristics, in Global Positioning System, Papers published in Navigation, The Institute of Navigation, 3-14, 1980.

Minster, J. B., Jordan, T. H., Molnar, P. and E. Haines, Numerical Modelling of Instantaneous plate tectonics, *Geophys J. Roy. Astron. Soc.,* 36, 541-576, 1974.

Minster, J. B., and T. H. Jordan, Present-Day Plate Motions, *J. Geophys. Res.,* Vol. 83, 5331-5354, 1978.

Molnar, P. and P. Tapponnier, Cenozoic Tectonics of Asia: Effects of Continental Collisions, *Science,* 189, 419-426, 1975.

Molnar, P. and P. Tapponier, The Collision Between India and Eurasia, *Sci. Amer.*, 236, 30-41, 1977.

Morgan, P. and J. Manning, What is IGS and why is it important to Australia, *Aust. Surv.*, 37, 91-100, 1992.

Morgan, P., Rizos, C. and R. Coleman, Network Solutions from Epoch 92, *Aust. J. Geod. Photogram. Surv.*, 59, 97, 1993.

Morgan, W. J, Rises, Trenches, Great Faults and Crustal Blocks, *J. Geophys. Res.*, 73, 1959-1982, 1968.

Mueller, I. I., Reference Coordinate Systems and Frames: Concepts and Realization, *Bull. Geod.*, 59, 181-188, 1985.

Mueller, I. I. and G. Beutler, The International GPS Service for Geodynamics - Development and Current Status, in *Proceedings of the Sixth International Geodetic Symposium on Satellite Positioning,* Columbus, Ohio, March 1992.

Newcomb, K. R., and W. R. McCann, Seismic History and Seismotectonics of the Sunda Arc, *J. Geophys. Res.*, 92, 421-439, 1987.

Nierenberg, W. A., The DSDP after ten years, *Amer. Scientist*, 66, 20-27, 1978.

Ninkovich, D., Late Cenozoic Clockwise Rotation of Sumatra, *Earth Planet. Sci. Lett.*, 29, 269-275, 1976.

Nishimura, S., Nishida, J., Yokoyama, T. and F. Hehuwat, Neo-tectonics of the Strait of Sunda, Indonesia, *J. Southeast Asian Earth Sci.*, 1,81-91, 1986.

Okada, Y. , Surface Deformation due to Shear and Tensile Faults in a Half Space, *Bull. Seis. Soc. Amer.*, 75, 1135-1154, 1985.

Parkinson, B. W. and S. W. Gilbert, NAVSTAR: Global Positioning System - Ten Years Later, *Proceedings of the IEEE,* Vol. 71, No 10, 1983.

Pramumijoyo S. and M. Sebrier, Neogene and Quaternary Fault Kinematics around the Sunda Strait area, Indonesia, *Jour. Southeast Asian Ear. Sci.,* 6(2), 137-145, 1991.

Puntodewo, S. S. O., Analysis of Plate Movements and Crustal Deformation in Indonesia through deduction from Space Geodetic Measurements by Global Positioning System. *PhD Thesis* (in preparation), Bandung Institute of Technology, 1994.

Puntodewo, S. S. O., McCaffrey, R.,. Calais, E, Bock, Y., Rais, J., Subarya, C., Poewariardi, R., Stevens, C., Genrich, J., Fauzi, Zwick, P. and S. Wdowinski,

GPS Measurements of Crustal Deformation within the Pacific-Australia Plate Boundary Zone in Irian Jaya, Indonesia, *Tectonophysics*, 237, 141-153, 1994.

Reid, H. F., Sudden Earth-movements in Sumatra in 1892, *Seis. Soc. Amer. Bull.*, 3, 72-79, 1913.

Renard, V., Dubois, J., Larue, M., Huchon, P., Diament, M., Deplus, C., Harjono, H. and I. Suhardi, Krakatau '85 Cruise Report, *IFREMER,* Brest, France, 132pp, 1985.

Rocken, C., GPS Antenna Mixing Problems, *UNAVCO Memo*, November 12, 1992.

Rothacher, M., Becker, M., Beutler, G., Brockman, E., Friedli, F., Groten, E., Hou, Z. W., Mervart, L. and K. Sauermann, Location of ESA Tracking Sites by GPS, *ESOC Contract 9166/90/D/IM(SC) - Final Report*, December 7, 1992.

Rothacher, M., Beutler, G., Gurtner, W., Botton, S. and C. Boucher, Results of the IGS Data Processing at the "Centre for Orbit Determination in Europe" (CODE), in *Proceedings of the 1993 IGS Workshop, 25-26 March, 1993*, 133-143, Astronomical Institute University of Berne, G. Beutler and E. Brockman Eds., Druckerei der Universität Bern, 1993.

Rothacher, M., Beutler, G., Gurtner, W., Brockman, E. and L. Mervart, Bernese GPS Software Version 3.4 Documentation, 1994.

Ryan, J. W., Clark, T. A., Ma, C., Gordan, D., Caprette, D. S. and W. E. Himwich, Global Scale Tectonic Plate Motions Measured with CDP VLBI Data, in *Contributions of Space Geodesy to Geodynamics: Crustal Dynamics, AGU Geodynamics Series, 23, 37-49,* 1993a.

Ryan, J. W., Ma, C. and D. S. Caprette, NASA Space Geodesy Program - GSFC Data Analysis 1992 Final Report of the Crustal Dynamics Project VLBI Geodetic Results 1979-1991, *NASA Technical Memorandun 104572*, 1993b.

Schutz, B., Abusali, P. and M. Watkins, CSR Results from IGS and EPOCH-92, in *Proceedings of the 1993 IGS Workshop, 25-26 March, 1993*, 145-147, Astronomical Institute University of Berne, G. Beutler and E. Brockman Eds., Druckerei der Universität Bern, 1993a.

Schutz, B., Bevis, M., Taylor, F., Kuang, D. Abusali, P., Watkins, M. Recy, J., Perin, B. and O. Peyroux, The Southwest Pacific GPS Project: Geodetic Results from Burst 1 of the 1990 Field Campaign, *Bull. Geod.*, 67, 224-240, 1993b.

Schwiderski, E. W., Ocean Tides, Part I: Global Ocean Tidal Equations; Part II: A Hydrodynamical Interpolation Model, *Marine Geodesy,* 3, 161-217 and 219-255, 1980.

Shapiro, I. I., Use of Space Techniques for Geodesy, in *Proceedings of the International School of Physics, Course LXXXV,* Italian Physical Society, 1983.

Shemenda, A. I., Horizontal Lithosphere Compression and Subduction: Constraints Provided by Physical Modeling, *J. Geophys. Res.*, 97, 11097-11161, 1992.

Small, C. and D. T. Sandwell, Imaging Mid-ocean Ridge Transitions with Satellite Gravity, *Geology*, 22, 123-126, 1994.

Smith, D. E., Kolenkiewicz, R., Dunn, P. J, Robbins, J. W., Torrence, M. H., Klosko, S. M., Williamson, R. G., Pavlis, E. C., Douglas, N. B. and S. K. Fricke, Tectonic Motion and Deformation From Satellite Laser Ranging to LAGEOS, *J. Geophys. Res.*, 95, 22013-22041, 1990.

Smith, D. E., Kolenkiewicz, R., Nerem, R. S, Dunn, P. J., Torrence, M. H., Robbins, J. W., Klosko, S. M., Williamson, R. G. and E. C. Pavlis, Contemporary Global Horizontal Crustal Motion, *Geophys. Jour.Int.*, in press, 1994.

Spence, W., Slab Pull and the Seismotectonics of Subducting Lithosphere, *Rev. Geophysics*, 25, 55-69, 1987.

Spilker, J. J. Jr, GPS Signal Structure and Performance Characteristics, in *Global Positioning System, Papers published in Navigation,* The Institute of Navigation, 29-54, 1980.

Tregoning, P., Brunner, F. K., Bock, Y., Puntodewo, S. S. O., McCaffrey, R., Genrich, J. F., Calais, E., Rais, J. and C. Subarya, First Geodetic Measurement of Convergence across the Java Trench, *Geophys. Res. Lett.*, 21, 2135-2138, 1994.

Vine, F. J. and D. H. Matthews, Magnetic anomalies over oceanic ridges, *Nature*, 199, 947-949, 1963.

Vine, F. J. and J. T. Wilson, Magnetic anomalies over a young oceanic ridge southwest of Vancouver Island, *Science*, 150, 485-489, 1965.

Watkins, M. M., Eanes, R. J. and C. Ma, Comparison of Terrestrial Reference Frame Velocities Determined from SLR and VLBI, *Geophys. Res. Lett.*, 21, 169-172, 1994.

Weins, D. A, DeMets, C. A., Gordon, R. G., Stein, S., Argus, D., Engeln, J. F., Lundgren P., Quible, D., Stein, C., Weinstein, S. and D. F. Woods, A Diffuse Plate Boundary Model for Indian Ocean Tectonics, *Geophys. Res. Lett.*, 12, 439-432, 1985.

Wessel, P., and W. H. F. Smith, Free software helps map and display data, *EOS. Trans. AGU*, 72, 441, 1991.

Wilson, J. T., A new class of faults and their bearing on Continental Drift, *Nature*, 207, 343-347, 1965.

Woodroffe, C. D., Vertical movement of isolated oceanic islands at plate margins: evidence from emergent reefs in Tonga (Pacific Ocean), Cayman Islands (Carribean Sea) and Christmas Island (Indian Ocean), 1988.

Woodroffe, C. D., McLean, R. and E. Wallensky, Darwin's Coral Atoll: Geomorphology and Recent Development of Cocos (Keeling Islands), Indian Ocean, *Nat. Geogr. Res.*, 6, 262-275, 1990a.

Woodroffe, C. D., McLean, R., Polach, H. and E. Wallensky, Sea level and coral atolls: Lte Holocene emergence in the Indian Ocean, *Geology*, 18, 62-66, 1990b.

Zhu, S. Y., Reigber, Ch., Angermann, D., Galas, R., Gendt, G., Sommerfeld, W. and T. Nischan, Global Geometric Parameters Determined from Multi-months GPS Data, in *Proceedings of the 1993 IGS Workshop, 25-26 March, 1993*, 148-153, Astronomical Institute University of Berne, G. Beutler and E. Brockman Eds., Druckerei der Universität Bern, 1993.

Zumberge, J. F., Jefferson, D. C., Blewitt, G., Heflin, M. B. and F. H. Webb, Jet Propulsion Laboratory IGS Analysis Center Report, 1992, in *Proceedings of the 1993 IGS Workshop, 25-26 March, 1993*, 154-163, Astronomical Institute University of Berne, G. Beutler and E. Brockman Eds., Druckerei der Universität Bern, 1993.

Publications from

THE SCHOOL OF GEOMATIC ENGINEERING

(Formerly School of Surveying)

THE UNIVERSITY OF NEW SOUTH WALES

All prices include postage by surface mail. Air mail rates on application.

To order, write to Publications Officer, School of Geomatic Engineering
The University of New South Wales, Sydney 2052, AUSTRALIA

NOTE: ALL ORDERS MUST BE PREPAID

UNISURV REPORTS - G SERIES

Price (including postage): $6.00

G14. A. Stolz, "The computation of three dimensional Cartesian coordinates of terrestrial networks by the use of local astronomic vector systems", Unisurv Rep. 18, 47 pp, 1970.

G16. R.S. Mather et al, "Communications from Australia to Section V, International Association of Geodesy, XV General Assembly, International Union of Geodesy and Geophysics, Moscow 1971", Unisurv Rep. 22, 72 pp, 1971.

G17. Papers by R.S. Mather, H.L. Mitchell & A. Stolz on the following topics:- Four-dimensional geodesy, Network adjustment and Sea surface topography, Unisurv G17, 73 pp, 1972.

G18. Papers by L. Berlin, G.J.F. Holden, P.V. Angus-Leppan, H.L. Mitchell & A.H. Campbell on the following topics:- Photogrammetry co-ordinate systems for surveying integration, Geopotential networks and Linear measurement, Unisurv G18, 80 pp, 1972.

G19. R.S. Mather, P.V. Angus-Leppan, A. Stolz & I. Lloyd, "Aspects of four-dimensional geodesy", Unisurv G19, 100 pp, 1973.

G20. Papers by J.S. Allman, R.C. Lister, J.C. Trinder & R.S. Mather on the following topics:- Network adjustments, Photogrammetry, and 4-Dimensional geodesy, Unisurv G20, 133 pp, 1974.

G21. Papers by E. Grafarend, R.S. Mather & P.V. Angus-Leppan on the following topics:- Mathematical geodesy, Coastal geodesy and Refraction, Unisurv G21, 100 pp, 1974.

G22. Papers by R.S. Mather, J.R. Gilliland, F.K. Brunner, J.C. Trinder, K. Bretreger & G. Halsey on the following topics:- Gravity, Levelling, Refraction, ERTS imagery, Tidal effects on satellite orbits and Photogrammetry, Unisurv G22, 96 pp, 1975.

G23. Papers by R.S. Mather, E.G. Anderson, C. Rizos, K. Bretreger, K. Leppert, B.V. Hamon & P.V. Angus-Leppan on the following topics:- Earth tides, Sea surface topography, Atmospheric effects in physical geodesy, Mean sea level and Systematic errors in levelling, Unisurv G23, 96 pp, 1975.

G24. Papers by R.C. Patterson, R.S. Mather, R. Coleman, O.L. Colombo, J.C. Trinder, S.U. Nasca, T.L. Duyet & K. Bretreger on the following topics:- Adjustment theory, Sea surface topography determinations, Applications of LANDSAT imagery, Ocean loading of Earth tides, Physical geodesy, Photogrammetry and Oceanographic applications of satellites, Unisurv G24, 151 pp, 1976.

G25. Papers by S.M. Nakiboglu, B. Ducarme, P. Melchior, R.S. Mather, B.C. Barlow, C. Rizos, B. Hirsch, K. Bretreger, F.K. Brunner & P.V. Angus-Leppan on the following topics:- Hydrostatic equilibrium figures of the Earth, Earth tides, Gravity anomaly data banks for Australia, Recovery of tidal signals from satellite altimetry, Meteorological parameters for modelling terrestrial refraction and Crustal motion studies in Australia, Unisurv G25, 124 pp, 1976.

G26. Papers by R.S. Mather, E.G. Masters, R. Coleman, C. Rizos, B. Hirsch, C.S. Fraser, F.K. Brunner, P.V. Angus-Leppan, A.J. McCarthy & C. Wardrop on the following topics:- Four-dimensional geodesy, GEOS-3 altimetry data analysis, analysis of meteorological measurements for microwave EDM and Meteorological data logging system for geodetic refraction research, Unisurv G26, 113 pp, 1977.

G27. Papers by F.K. Brunner, C.S. Fraser, S.U. Nasca, J.C. Trinder, L. Berlin, R.S. Mather, O.L. Colombo & P.V. Angus-Leppan on the following topics:- Micrometeorology in geodetic refraction, LANDSAT imagery in topographic mapping, adjustment of large systems, GEOS-3 data analysis, Kernel functions and EDM reductions over sea, Unisurv G27, 101 pp, 1977.

G29. Papers by F.L. Clarke, R.S. Mather, D.R. Larden & J.R. Gilliland on the following topics:- Three dimensional network adjustment incorporating ξ , η and N, Geoid determinations with satellite altimetry, Geodynamic information from secular gravity changes and Height and free-air anomaly correlation, Unisurv G29, 87 pp, 1978.

From June 1979 Unisurv G's name was changed to Australian Journal of Geodesy, Photogrammetry and Surveying. These can be ordered from The Managing Editor, Australian Journal of Geodesy, Photogrammetry and Surveying, Institution of Surveyors - Australia , Nos 27 - 29 Napier Close, Deakin, ACT 2600, AUSTRALIA.

UNISURV REPORTS - S SERIES

S8 - S20	Price (including postage) :		$10.00
S29 onwards	Price (including postage) :	Individuals	$25.00
		Institutions	$30.00

S8 A. Stolz, "Three-D Cartesian co-ordinates of part of the Australian geodetic network by the use of local astronomic vector systems", Unisurv Rep. S8, 182 pp, 1972.

S10 A.J. Robinson, "Study of zero error & ground swing of the model MRA101 tellurometer", Unisurv Rep. S10, 200 pp, 1973.

S12. G.J.F. Holden, "An evaluation of orthophotography in an integrated mapping system", Unisurv Rep. S12, 232 pp, 1974.

S14. Edward G. Anderson, "The Effect of Topography on Solutions of Stokes` Problem", Unisurv Rep. S14, 252 pp, 1976.

S16. K. Bretreger, "Earth Tide Effects on Geodetic Observations", Unisurv S16, 173 pp, 1978.

S17. C. Rizos, "The role of the gravity field in sea surface topography studies", Unisurv S17, 299 pp, 1980.

S18. B.C. Forster, "Some measures of urban residential quality from LANDSAT multi-spectral data", Unisurv S18, 223 pp, 1981.

S19. Richard Coleman, "A Geodetic Basis for recovering Ocean Dynamic Information from Satellite Altimetry", Unisurv S19,332 pp, 1981.

S20. Douglas R. Larden, "Monitoring the Earth's Rotation by Lunar Laser Ranging", Unisurv Report S20, 280 pp, 1982.

S29 Gary S Chisholm, "Integration of GPS into hydrographic survey operations", Unisurv S29, 190 pp, 1987.

S30. Gary Alan Jeffress, "An investigation of Doppler satellite positioning multi-station software", Unisurv S30, 118 pp, 1987.

S31. Jahja Soetandi, "A model for a cadastral land information system for Indonesia", Unisurv S31, 168 pp, 1988.

S32. D. B. Grant, "Combination of terrestrial and GPS data for earth deformation studies" Unisurv S32, 285 pp, 1990.

S33. R. D. Holloway, "The integration of GPS heights into the Australian Height Datum", Unisurv S33, 151 pp.,1988.

S34. Robin C. Mullin, "Data update in a Land Information Network", Unisurv S34, 168 pp. 1988.

S35. Bertrand Merminod, "The use of Kalman filters in GPS Navigation", Unisurv S35, 203 pp., 1989.

S36. Andrew R. Marshall, "Network design and optimisation in close range Photogrammetry", Unisurv S36, 249 pp., 1989.

S37. Wattana Jaroondhampinij, "A model of Computerised parcel-based Land Information System for the Department of Lands, Thailand," Unisurv S37, 281 pp., 1989.

S38. C. Rizos (Ed.), D.B. Grant, A. Stolz, B. Merminod, C.C. Mazur "Contributions to GPS Studies", Unisurv S38, 204 pp., 1990.

S39. C. Bosloper, "Multipath and GPS short periodic components of the time variation of the differential dispersive delay", Unisurv S39, 214 pp., 1990.

S40. John Michael Nolan, "Development of a Navigational System utilizing the Global Positioning System in a real time, differential mode", Unisurv S40, 163 pp., 1990.

S41. Roderick T. Macleod, "The resolution of Mean Sea Level anomalies along the NSW coastline using the Global Positioning System", 278 pp., 1990.

S42. Douglas A. Kinlyside, "Densification Surveys in New South Wales - coping with distortions", 209 pp., 1992.

S43. A. H. W. Kearsley (ed.), Z. Ahmad, B. R. Harvey and A. Kasenda, "Contributions to Geoid Evaluations and GPS Heighting", 209 pp., 1993.

S44 Paul Tregoning, "GPS Measurements in the Australian and Indonesian Regions (1989-1993)", 134 + xiii pp, 1996.

PROCEEDINGS

Prices include postage by surface mail

P1. P.V. Angus-Leppan (Editor), "Proceedings of conference on refraction effects in geodesy & electronic distance measurement", 264 pp., 1968. Price: $10.00

P2. R.S. Mather & P.V. Angus-Leppan (Eds), "Australian Academy of Science/International Association of Geodesy Symposium on Earth`s Gravitational Field & Secular Variations in Position", 740 pp., 1973. Price $15.00

MONOGRAPHS

Prices include postage by surface mail

M1.	R.S. Mather, "The theory and geodetic use of some common projections", (2nd edition), 125 pp., 1978.	Price	$15.00
M2.	R.S. Mather, "The analysis of the earth's gravity field", 172 pp., 1971.	Price	$8.00
M3.	G.G. Bennett, "Tables for prediction of daylight stars", 24 pp.,1974.	Price	$5.00
M4.	G.G. Bennett, J.G. Freislich & M. Maughan, "Star prediction tables for the fixing of position", 200 pp., 1974.	Price	$8.00
M8.	A.H.W. Kearsley, "Geodetic Surveying", 96 pp, (revised) 1988.	Price	$12.00
M10.	W. Faig, "Aerial Triangulation and Digital Mapping", 102 pp., 1986.	Price	$16.00
M11.	W.F. Caspary, "Concepts of Network and Deformation Analysis", 183 pp., 1988.	Price	$25.00
M12.	F.K. Brunner, "Atmospheric Effects on Geodetic Space Measurements", 110 pp., 1988.	Price	$16.00
M13.	Bruce R. Harvey, "Practical Least Squares and Statistics for Surveyors", (2nd edition), 319 pp., 1994.	Price	$30.00
M14.	Ewan G. Masters & John R. Pollard (Ed.), "Land Information Management", 269 pp., 1991. (Proceedings LIM Conference, July 1991).	Price	$20.00
M15/1	Ewan G. Masters & John R. Pollard (Ed.), "Land Information Management - Geographic Information Systems - Advance Remote Sensing Vol 1" 295 pp., 1993 (Proceedings of LIM & GIS Conference, July 1993).	Price	$30.00
M15/2	Ewan G. Masters & John R. Pollard (Ed.), "Land Information Management - Geographic Information Systems - Advance Remote Sensing Vol 2" 376 pp., 1993 (Proceedings of Advanced Remote Sensing Conference, July 1993).	Price	$30.00
M16.	A. Stolz, "An Introduction to Geodesy", 112 pp., 1994.	Price	$20.00